12-2012

BIOCHEMICAL CHARACTERIZATION OF BINDING PARTNERS OF TWO HSP70 CO-CHAPERONES IN SACCHAROMYCES CEREVISIAE

Jacob Verghese

BIOCHEMICAL CHARACTERIZATION OF BINDING PARTNERS OF TWO HSP70 CO-CHAPERONES IN *SACCHAROMYCES CEREVISIAE*

by

Jacob Verghese, B.Sc., M.S.

APPROVED:

Supervisory Professor, Kevin A. Morano, Ph.D.

Peter Christie, Ph.D.

Michael Lorenz, Ph.D.

Ambro van Hoof, Ph.D.

Eric Wagner, Ph.D.

APPROVED:

Dean, The University of Texas
Graduate School of Biomedical
Sciences at Houston

BIOCHEMICAL CHARACTERIZATION OF BINDING PARTNERS OF TWO HSP70 CO-CHAPERONES IN *SACCHAROMYCES CEREVISIAE*

A

DISSERTATION

Presented to the Faculty of

The University of Texas Health Science Center at Houston

and

The University of Texas M.D. Anderson Cancer Center

Graduate School of Biomedical Sciences

in Partial Fulfillment

of the Requirements

for the Degree of

DOCTOR OF PHILOSOPHY

by

Jacob Verghese, B.Sc., M.S.

Houston, Texas

December 2012

DEDICATION

I dedicate this thesis to my late aunt Omana who was instrumental in bringing me to the United States to pursue my Ph.D. She was like a mother to me and always encouraged me to be better than I was.

ACKNOWLEDGEMENTS

This thesis is the culmination of an incredible journey and would not have been possible without a number of individuals who have helped and supported me along this fulfilling path.

I would like to express my heartfelt gratitude to my mentor, Dr. Kevin Morano for giving me the wonderful opportunity to pursue my Ph.D. training in his laboratory. I am extremely grateful for his support and constant encouragement in every task I undertook in the lab and also in the graduate school. I am grateful for his continued persistence in improving my presentation and scientific writing skills. I could not have asked for a better role model and mentor and thank him for all his help during my graduate career.

I would especially like to acknowledge members of my supervisory committee consisting of Dr. Peter Christie, Dr. Michael Lorenz, Dr. Ambro van Hoof and Dr. Eric Wagner for their guidance and advice during this journey. They helped to shape and guide the direction of my work with thoughtful and detailed comments.

I would like to thank current and former members of the Morano lab for their help and support including Dr. Patrick Gibney, Dr. Hugo Tapia, Yanyu Wang, Jennifer Abrams, Kimberly Cope and Veronica Garcia. They were a pleasure to work with in the lab and I will always treasure the fun times we also shared outside the lab.

My sincere thanks go to the faculty, staff and students of the Department of Microbiology and Molecular Genetics for their support, encouragement and helpful scientific discussions. I thank Dr. Jesus Eraso for always being available to discuss my experiments. Special thanks to Dr. Jennifer Dale who mentored me during my second laboratory rotation and later became a close friend.

I would like to thank the administrators and staff of the Graduate School of Biomedical Sciences (GSBS). The GSBS team was very supportive of all my endeavors at the graduate school and was always available to answer questions. They helped to make graduate school a great learning experience. I will miss the friendly interactions with all the GSBS staff, especially Ms. Lily at the GSBS front desk.

I wish to thank the Schissler Foundation and the Tzu Chi Foundation for their funding support. I am grateful to the Graduate Student Education Committee (GSEC) and GSBS for providing travel awards to attend national and international conferences.

I would like to thank my wonderful wife, Stefanie Verghese whom I met while in graduate school. She has been my rock and ardent supporter and I am grateful that she agreed to relocate to Munich, Germany to pursue my research aspirations.

To all my friends, thank you. I got a chance to be part of a great tennis team (The Good Guys) in Houston, which went to the State Championships in summer of 2012. I thank the captain, Dave Patangia for giving me this wonderful opportunity.

Finally, I would like to thank my family. My parents, Ashok and Reena have been my biggest fans and constant supporters. To my sister, Amritha and her husband Rahul, thank you for your constant encouragement. I am indebted to my dad's siblings, aunt Omana and uncle Babu, who gave me the opportunity to come to the US. Their guidance and support made this journey a special experience. I also thank my uncle Reggie and aunt Rekha for their encouragement and support. My cousins have been a source of constant joy my entire life and for that I am extremely thankful. To my nephews, Christopher, Ethan and Luke and nieces Kate and Blake, I love you.

BIOCHEMICAL CHARACTERIZATION OF BINDING PARTNERS OF TWO HSP70 CO-CHAPERONES IN *SACCHAROMYCES CEREVISIAE*

Publication No. _____

Jacob Verghese

Advisor: Kevin A. Morano, Ph.D.

Abstract

Cells are exposed to a variety of environmental and physiological changes including temperature, pH and nutrient availability. These changes cause stress to cells, which results in protein misfolding and altered cellular protein homeostasis. How proteins fold into their three-dimensional functional structure is a fundamental biological process with important relevance to human health. Misfolded and aggregated proteins are linked to multiple neurodegenerative diseases, cardiovascular disease and cystic fibrosis. To combat proteotoxic stress, cells deploy an array of molecular chaperones that assist in the repair or removal of misfolded proteins.

Hsp70, an evolutionarily conserved molecular chaperone, promotes protein folding and helps maintain them in a functional state. Requisite co-chaperones, including nucleotide exchange factors (NEFs) strictly regulate and serve to recruit Hsp70 to distinct cellular processes or locations. In yeast and human cells, three structurally non-related cytosolic NEFs are present: Sse1 (Hsp110), Fes1 (HspBP1) and Snl1 (Bag-1). Snl1 is unique among the cytosolic NEFs as it is localized at the ER membrane with its Hsp70 binding (BAG) domain exposed to the cytosol. I discovered that Snl1 distinctly interacts with assembled

ribosomes and several lines of evidence indicate that this interaction is both independent of and concurrent with binding to Hsp70 and is not dependent on membrane localization. The ribosome-binding site is identified as a short lysine-rich motif within the amino terminus of the Snl1 BAG domain distinct from the Hsp70 interaction region. In addition, I demonstrate ribosome association with the Snl1 homolog in the pathogenic fungus, *Candida albicans* and localize this putative NEF to a perinuclear/ER membrane, suggesting functional conservation in fungal BAG domain-containing proteins. As a first step in determining specific domain architecture in fungal BAG proteins, I present the preliminary steps of protein purification and analysis of the minimal Hsp70 binding region in in both *S.cerevisiae* and *C. albicans* Snl1.

Contrary to previous *in vitro* evidence which showed the Fes1 NEF to interact with both cytosolic Hsp70s, Ssa and Ssb, Fes1 is shown to interact specifically with Ssa when expressed under normal cellular conditions in *S. cerevisiae*. This is the first reported evidence of Hsp70 binding selectivity for a cytosolic NEF, and suggests a possible mechanism to achieve specificity in Hsp70-dependent functions. Taken together, the work presented in this dissertation highlights the striking divergence among Hsp70 co-chaperones in selecting binding partners, which may correlate with their specific roles in the cell.

TABLE OF CONTENTS

LIST OF FIGURES

LIST OF TABLES

Chapter 1: Introduction to the cellular stress response and maintenance of proteostasis

The word ‘protein’ first appeared in scientific literature in 1838 and was derived from the Greek adjective *proteios*, meaning “of the first rank or position.” Proteins are the most abundant molecules in biology apart from water and form a versatile group of macromolecules in cells that play essential roles in almost all biological processes. For example, they work as enzymes, facilitate transport, maintain structural integrity of a cell and are key components in immune function, signal transduction and regulation.

The cellular stress response

The cellular environment where proteins reside is constantly in flux with regard to nutrient status, temperature, exposure to toxic molecules, pressure, pH, etc. The cellular stress response is an evolutionarily highly conserved mechanism that protects cells from detrimental effects caused by environmental fluctuations. For example, sudden changes in salt (NaCl) concentrations outside the cell can cause a dramatic loss in intracellular water content thereby damaging cellular proteins. To deal with this stress, cells respond by rapidly stimulating the expression of proteins involved in sodium transport systems to adjust the balance and to counteract the toxic effects of sodium ions. Continued exposure to stress also interferes with normal functions of the cell by altering the biochemical properties of proteins, which can facilitate their misfolding, unfolding or aggregation. Thus, the cellular stress response represents a mechanism to sense the stress and mount a response to negate or adapt to its toxic effects.

The stress response to temperature increase (heat stress) is conserved among all organisms and a prominent feature includes the induction of a gene expression program called the heat shock response (HSR) (110, 147). Much of the cellular response to stress is similar, regardless of the kind of stressor, and activation of HSR can often occur during other

stressors including pathophysiological states and oxidative damage. This adaptation mechanism is well studied and results in metabolic remodeling, transient reduction in growth and global transcriptional changes. One characteristic of HSR is the induction of a number of cytoprotective genes encoding heat shock proteins (HSPs). Many HSPs function as molecular chaperones that bind partially unfolded proteins and protect them from aggregation or degradation. Much of what we know about HSR in eukaryotic cells has been learned through studies using the budding yeast, *Saccharomyces cerevisiae* due to its facile genetics, biochemistry and cell biology as well as the numerous genome-wide and proteome-wide tools that have become available in the last few years. Yeast cells grow optimally within a narrow temperature range (25°C – 30°C) but a temperature change to 37°C, activates the yeast HSR (147).

Stress responses in *Saccharomyces cerevisiae*

In eukaryotes, the heat shock transcription factor (HSF) protein family is the main modulator of HSR (85). In evolutionary diverse organisms such as unicellular yeasts and metazoans such as nematodes and fruit flies, there exists a single essential heat shock factor (Hsf1) that activates the transcription of *hsp* genes. In contrast, vertebrates have evolved a family of four members, HSF1-4, of which HSF1 is the equivalent of the fungal and metazoan HSF1 (81). In mammals, while HSF1 is the ubiquitous heat stress response activator, HSF2 is developmentally regulated and important for neuronal specification. HSF3 has been characterized only in avian species while HSF4 is cell type-specific associated with expression of crystallines in the lens of the eye (93). Hsf1 recognizes a pentameric heat shock transcription element (HSE) consisting of repeating units of the sequence nGAAn, where “n” can be any nucleotide, in promoters of target genes and activates their transcription (12, 142).

Under normal conditions in mammalian cells, Hsf1 exists as a monomer but during stress, Hsf1 gets rapidly trimerized, accumulates in the nucleus and binds to HSEs. In contrast, yeast Hsf1 is constitutively trimerized, nuclear-associated and bound to high-affinity HSEs under normal and additional HSEs during stress conditions. The target genes of Hsf1 include components of the protein quality control machinery (ubiquitin proteasome system) and molecular chaperones.

In addition to Hsf1-mediated stress response, a parallel pathway in *S. cerevisiae* responds to a variety of cellular and environmental stresses including oxidative and osmotic stress and nitrogen starvation. This pathway referred to as "general stress response" is governed by two highly related transcription factors, Msn2 and Msn4 (77, 124). These factors bind to an invariant five base pair sequence element (CCCCT) called the "stress response element" (29). The response mediated by Msn2/4 is generally transient and the strength and duration of the response is dependent on the strength of the stresses. (42). Although many of the genes induced by Msn2/4 are distinct from those regulated by Hsf1, there are a few exceptions such as *HSP104*, which contains both HSE and STRE elements in their promoters. Hsp104 in yeast cells, a member of the Hsp100 family of chaperones helps to disassemble protein aggregates that accumulate in the cell due to stress (102). Transcriptional activation of *HSP104* is obtained through cooperation between both Msn2/4 and Hsf1 systems although either factor can activate the promoter alone. Thus, cells have evolved back-up measures for certain cytoprotective genes whose activity is essential for proper stress response and cannot be replaced or bypassed by another gene (117, 118).

At any given time in the cell, processes that involve proteins must be properly regulated to efficiently maintain cellular functions. This requires that all cellular protein

concentrations, conformations, binding interactions, localization and removal must be coordinately regulated, and the balance between them is required to maintain protein homeostasis or "proteostasis" (Figure1-1) (6). One of the major consequences of cellular stress is intracellular protein unfolding and misfolding, which can result in their accumulation in cells. Although it is still unclear how a cell senses stresses like temperature change and transduces this signal to Hsf1, protein unfolding caused by this stress is sufficient to activate HSR. However, it is not known if this is the main signal for HSR activation during other stresses.

Cellular proteostasis

"Proteostasis" is defined as the state of dynamic equilibrium in the cell where protein synthesis and folding is balanced with degradation (Figure 1-1). Genetic screens performed in model organisms such as *S. cerevisiae*, *C. elegans* and *D. melanogaster* identified factors that maintain proteostasis in the cell that either promote protein folding or protein degradation (136). The factors forming the proteostasis network (PN) include molecular chaperones, subunits of the proteasome, components of the autophagy system, and Hsf1. The PN coordinates molecular pathways including protein synthesis, folding, transport and clearance and thus has the task of surveying the cellular proteome for proteins that are unable to achieve their native conformation (6). This suggests that a set of factors function in response to imbalances in proteostasis and represent a core of the PN. Despite the robust regulation of the PN during stress conditions, chronic expression of aggregation-prone proteins escape its vigilance and causes accumulation of misfolded and damaged proteins that in turn overburdens the proteostasis machinery and can lead to cell death.

A challenge facing the PN is the high volume-occupied space in the cell. Non-specific influences of steric repulsions on intracellular reactions and processes, also known as 'macromolecular crowding' occur in this space. In the 'crowded' environment of a cell (total cytosolic protein concentrations reach 300-400 g/l) the free space that a protein molecule can move is limited and will affect its stability and reactions (33, 34) Although this may increase the interactions between macromolecules, crowding can also enhance the tendency of non-native and structurally flexible proteins to aggregate (34). In addition, the constant production of newly synthesized proteins provides a large protein-folding challenge in this crowded environment, as is the recognition of damaged and aggregated proteins that must be targeted for degradation. Thus, factors that can facilitate proper molecular interactions within a protein and between proteins are vital to maintain proteostasis. These include molecular chaperones (51).

Regulation of PN occurs through signaling pathways that directly control the concentration, activities and distribution of components of the PN. Signaling pathways regulate protein synthesis, folding, transport, aggregation, disaggregation and clearance. These include (i) the unfolded protein response (153), which senses the folding capacity of the ER, (ii) the HSR, (1) pathways that influence Ca^{2+} levels in the ER that in turn regulate the folding of N-linked glycoproteins in the ER via Ca^{2+}-sensitive chaperones (calnexin, calreticulin) and (iv) cell death pathways. These signaling pathways control the capacity of the cellular proteome through transcriptional, translational and post-translational processes by balancing the biogenesis and folding of proteins with protein degradation. When the PN is severely compromised in the case of early and late- onset genetic diseases (see below), signaling attempts to rebalance proteostasis fails and can activate cell death pathways,

FIGURE 1-1. Model of proteostasis. Shown are the various states of a protein after their synthesis. Maintenance of the balance between protein synthesis and folding with protein degradation is termed “proteostasis.”

FIGURE 1-1. Model of proteostasis

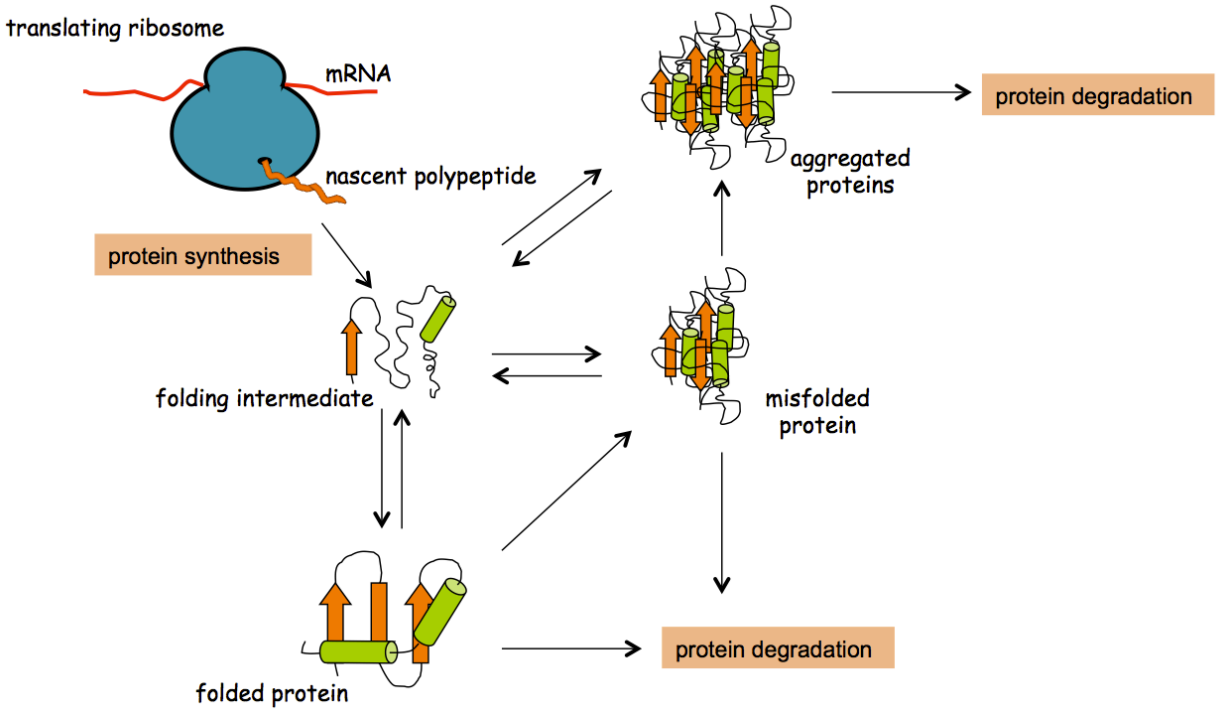

targeting the cell for destruction. Any imbalance in the PN is associated with diseases that cause metabolic disorders, neurodegeneration, cancer and cardiovascular disease.

Thus, understanding each component of the PN and how they function cooperatively within this network can aid in future manipulations of these components for therapeutic purposes.

Protein aggregation diseases

When a protein fails to fold properly due a change in its sequence and/or its concentration or if components of the PN are compromised, a breakdown in cellular protein homeostasis occurs. Conformational diseases associated with improper folding can be categorized as gain- or loss-of-function disorders. Gain-of-function diseases arise due to proteotoxicity caused by accumulation of protein aggregates in the cell. These include Parkinson's disease (PD), Huntington's disease, amyotrophic lateral sclerosis (ALS) and Alzheimer's disease (AD) (23, 57, 86, 87). Loss-of-function diseases on the other hand include cystic fibrosis and Gaucher disease and are caused by inherited mutations that lead to inefficient protein folding and excessive degradation (17, 112).

AD affects millions of older individuals worldwide and is a direct outcome of protein aggregation. AD is a result of neuron degeneration in the forebrain and hippocampus region, which is caused by the accumulation of β-amyloid plaques and neurofibrillary tangles. Plaques are composed of aggregated amyloid β (Aβ) peptides. Aβ monomers are soluble and largely helical in structure, however, at sufficiently high concentrations, they undergo dramatic conformational changes to form β-sheet structures. Amyloid aggregation and their deposition outside neurons is driven by the intrinsic aggregating property of the mutant Aβ form (111). Neurofibrillary tangles are composed of protein tau, a microtubule associated

protein. Hyperphosphorylation of tau results in its propensity to aggregate inside nerve cells and contributes to disease pathogenesis (133).

PD is also an outcome of protein aggregation. Two mutations (A53T and A30P) in the α-synuclein protein accelerates the formation of amyloid fibers, which self-associates and forms an oligomeric species (Lewy bodies) inside nerve cells resulting in proteotoxicity (71). α-synuclein exists in two structurally distinct populations in cells: an α-helical membrane-bound and disordered free cytosolic form. Membrane-bound forms have an increased tendency to aggregate, which act as seeds to accelerate the aggregation of the cytosolic form.

HD is caused by a mutation in a gene that results in an expansion of CAG repeats coding for polyglutamine (polyQ) at the amino-terminus of protein Huntington (Htt). Aggregation of Htt within neuronal cells (inclusion bodies) leads to their degeneration. Interestingly, HD occurs in individuals when there are 35 or more CAG repeats in the gene coding for the Htt protein. Below this number, individuals are unaffected, suggesting a correlation between polyQ length and disease progression (55).

ALS, also called Lou Gehrig's disease is caused by a mutation in a gene, TDP-43, which is expressed in the brain and spinal cord. It has been reported that 19 missense and one truncating mutation to this gene occurs in ALS patients and progressive accumulation and aggregation of this gene product contributes to the disease due to a failure of the proteasome to recycle damaged proteins (95).

In addition to protein misfolding diseases related to the nervous system, other diseases that are caused by protein aggregation include cystic fibrosis and cardiovascular disease. Cystic fibrosis occurs as a result of mutations in a gene that encodes a chloride ion channel called cystic fibrosis transmembrane conductance regulator (CFTR) in pulmonary

epithelial cells. A mutation A508F in the protein alters the ability of the first nucleotide-binding domain of CFTR to fold properly and is thus degraded. This prevents the trafficking of this protein to the apical membrane in affected epithelial cells (113).

Accumulation of pre-amyloid oligomers in cardiomyocytes have been observed in human heart failure samples. To test whether protein aggregation in these cells is the cause for heart failure, transgenic mice were created expressing long and short polyQ repeats. A 83 CAG stretch caused intracellular accumulation of oligomers and these aggregates lead to cardiomyocyte death and heart failure in a murine model, confirming that heart failure can be related to protein aggregation (103). Diseases caused by protein aggregation in cells highlight the importance of understanding the PN and the functional roles of its components during protein aggregation (92).

Roles of chaperones in maintaining proteostasis

The protein folding function of the proteostasis network is accomplished by molecular chaperones that bind to intermediate and transition states of proteins. The regulation of genes encoding molecular chaperones is critical to maintain proteostasis and to restore a balance in the cellular proteome during stress. The involvement of PN in protein conformational diseases is underscored by a decrease in toxicity when individual molecular chaperones are overexpressed in various cell-based and animal models. Chaperones contain HSEs in their promoter sequences and hence are principally regulated by Hsf1. Cellular stress increases the demand for the folding machinery and the activation of Hsf1 induces the expression of genes encoding multiple chaperones. Based on their apparent molecular weights, chaperones can be classified into five protein families: the small Hsps (sHsps), which lack ATPase activity, and the ATPases Hsp100, Hsp90, Hsp70 and Hsp60.

The sHsps represent a diverse family of proteins with limited chaperone activity. They are present either transiently or stably in high molecular weight complexes, where they interact with unfolded substrates at a 1:1 monomer-to-substrate ratio (161). Instead of preventing aggregation of misfolded proteins, sHsps appear to co-aggregate with their substrates forming oligomeric complexes within the cell. Refolding of sHsp-associated substrates requires the action of ATP-dependent chaperones. Two well studied sHsps in yeast, Hsp26 and Hsp42 are both required to promote protein solubility during cellular stress and to maintain proteostasis during heat shock (20).

The representative member of the Hsp100 class in yeast is Hsp104, which forms hexameric rings with a large (~15 angstrom) central channel. Hsp104 is unique among the other chaperones as it is capable of extracting misfolded proteins from large aggregates. Hsp104 cannot refold proteins alone and requires the function of Hsp70 to return proteins to their native conformation. Cells lacking *HSP104* are highly sensitive to heat shock suggesting that this chaperone is absolutely required for maintaining proteostasis during heat stress (119). Interestingly, human cells lack a Hsp104 homolog but when yeast Hsp104 is expressed in human cells, it confers thermoprotection (21). This suggests that higher eukaryotes have evolved another strategy to remove large protein aggregates in the cell or utilize a combination of different chaperones to achieve this.

The Hsp90 chaperone family binds a selective group of client proteins, unlike Hsp70 that can associate with nearly any partially unfolded protein it encounters. These clients require Hsp90 for the final stages of native folding after initial interactions with Hsp70, thus linking these two chaperone families. Client proteins include those involved in signal transduction pathways such as kinases (yeast Ste11 analogous to mammalian Raf), steroid

receptors (glucocorticoid receptor) and also transcription factors (Hsf1) (104, 167). In yeast, Hsp90 is encoded by two genes *HSC82* and *HSP82*, which are constitutively and inducibly expressed, respectively, upon heat shock (14).

The Hsp70 chaperone family interacts with proteins at all stages in their lifetimes starting from their biogenesis at the ribosome to their final native state (40). Hsp70 and its cofactors, functions and locations in the cell will be discussed in more detail later in this chapter.

The Hsp60 chaperone family, also called chaperonins, form double-ring complexes and fold proteins within a central cavity in a nucleotide-dependent manner. There are two main groups of chaperonins, group I includes *E. coli* GroEL consisting of a seven-member ring and group II present in eukaryotes called TriC having eight or nine member rings (35, 41). Chaperonins encapsulate unfolded proteins, one molecule at a time and alleviates macromolecular crowding of certain proteins, thus preventing their aggregation during their folding process. The major substrates of TriC include the cytoskeletal proteins, actin and tubulin.

Chaperones thus play diverse roles in the PN by regulating protein folding, assisting the assembly and disassembly of macromolecular complexes and to regulate translocation with cellular organelles. The yeast genome contains chaperones of these families: 7 sHsps, 14 belonging to the chaperonin complex, 2 Hsp90s, 14 Hsp70s, 1 Hsp60 and 3 Hsp104s (48). Thus, it is the function of the cellular PN to regulate the plethora of chaperones during normal and especially stress conditions.

Roles of chaperones in human diseases

A number of studies show molecular chaperones associate with misfolded disease proteins and prevent their aggregation. For example, in a *Drosophila* model, overexpression of Hsp70 and its co-chaperone Hsp40 strongly protected neurons that expressed the mutant form of the Htt protein (157). Similarly, in a *C. elegans* model, overproduction of Hsp104 reduced toxic cellular effects caused by mutant Htt (120). In a PD cell model, overexpression of Hsp70 or its co-chaperone Hdj1 decreased the number of cells that contain Lewy bodies (abnormal protein aggregates that develop inside nerve cells) by more than 50% (80). Hsp70 chaperones have also been found to associate with Lewy bodies in affected brain tissues of patients with PD (82). Hsp27 preferentially interacts with the hyperphosphorylated tau mutant in human brain samples, and cell culture experiments show that increasing the production of this chaperone can decrease hyperphosphorylated tau levels, which in turn suppresses tau-mediated cell death (133). In addition, *in vitro* evidence has established a functional interaction between tau, Hsp70 and Hsp90 (30). Two parallel lines of investigation that decreased the amount of Hsp70/Hsp90 by RNA-mediated interference or induced the amounts of Hsp70/Hsp90 had opposite effects on tau. The former increased the aggregated state of tau while the latter decreased the incidence of aggregation, confirming the role of these two chaperones in maintaining the native fold and function of tau (30).

The evidence that chaperones associate with aggregating proteins involved in the progression of certain diseases suggests that the cellular proteostasis machinery is activated to help prevent aggregation of misfolded proteins. Consistent with this, the accumulation of cellular aggregates is known to trigger the HSR, which in turn induces the expression of chaperones. This was shown by treating cells under normal conditions with puromycin,

which leads to premature nascent chain termination or AZC, an amino acid analog of proline, which prevents normal folding. HSR was induced as a result of unfolded proteins in the cell (47). In the case of a polyQ-containing disease protein, Hsp70 and Hsp40 expression was shown to divert the protein away from its aggregation-prone pathway resulting in the formation of a less stable aggregate form that is more amenable to folding (88, 122).

Alternatively, mutations that cause alterations in genes encoding chaperones may also cause some human diseases and are likely the result of a loss-of-function of chaperone-dependent substrate proteins. For example, a missense mutation in the mitochondrial chaperonin Hsp60 that causes a loss of chaperone function, results in spastic paraplegia SPG13 (37). This disease is characterized by progressive weakness of the lower limbs but it is unclear why a dysfunction in Hsp60 affects only motor neurons of the lower limbs. It is possible that folding of a specific Hsp60-dependent substrate is affected in these cells. Studies involving α-crystallin, a member of the sHsp family showed that missense substitutions in a conserved arginine residue in the core domain of each of its subunits lead to disease progression. Cataracts occur when the mutation is in the A subunit of α-crystallin and desmin-related myopathy when the substitution is in the B subunit (153).

Since structural defects in a variety of proteins can lead to a disease state, the proper functioning of molecular chaperones in the PN is needed to maintain structural integrity of cellular proteins.

Ribosome-associated chaperones

Protein synthesis on the ribosome is the first stage of the proteostasis network where multiple factors directly bind to ribosomes and interact with nascent polypeptides. These include chaperones, processing enzymes that modify the N-termini of nascent polypeptides

and targeting factors such as the signal recognition particle (SRP) that initiate the delivery of secretory proteins to the ER membrane for translocation (69). During polypeptide elongation on the ribosome, approximately four and 20 amino acids are added per second in eukaryotes and bacteria, respectively. The challenge facing the PN is that sequence information of a nascent polypeptide is incomplete and continuously changing depending on the translation rate and therefore polypeptides are exposed in partially folded, aggregation-prone states for relatively long periods of time until the entire protein has been synthesized. Thus, cells utilize chaperones to protect nascent polypeptides during translation. Chaperones involved in *de novo* folding of cytosolic proteins can be classified into two groups. The first group includes chaperones that directly interact with the ribosome and emerging polypeptide to facilitate early peptide folding, and the second group consists of chaperones of the Hsp70 and Hsp60 families that bind polypeptides downstream of their ribosome-associated counterparts. The coordinated function of both groups forms a robust network that safeguards newly synthesized proteins from aggregation.

E. coli Trigger factor (TF) is the best-understood ribosome associated chaperone and its role in cotranslational protein folding is well characterized. TF is present only in bacteria and chloroplasts and contains multiple binding sites that provide several hydrophobic contact points for an unfolded polypeptide chain. In addition, the N-terminal domain of TF contains a linker domain motif that mediates binding to large subunit ribosomal protein Rpl23 situated near the ribosome exit tunnel, which ideally positions TF to associate with emerging polypeptide chains (70). Recent data from ribosome profiling experiments showed that TF is recruited only after a nascent peptide reaches a length of ~100 amino acids (97). This finding suggests that factors such as processing enzymes that remove the formyl moiety and the

initiator methionine from the N-termini of nascent chains have access to nascent peptides before the chaperone is recruited to the ribosome.

In eukaryotes, a TF homolog has not been identified but there are two separate protein complexes that bind to the ribosome and nascent polypeptides: (i) nascent chain associated complex (NAC) and (ii) ribosome associated complex (RAC).

(i) NAC in yeast and higher eukaryotes forms a α-β heterodimer that associates with ribosomes using a ribosome-binding motif (in the β subunit) consisting of a short stretch of positively charged amino acids. Crosslinking experiments localized the NAC binding site on the ribosome to large subunit ribosomal protein Rpl25, the yeast homolog of bacterial Rpl23, suggesting a conserved binding site on the ribosome for these ribosome-associated factors (105, 158). Importantly, ribosome association is a prerequisite for NAC interaction with nascent chains. In contrast to higher eukaryotes, yeast has three NAC subunits: two β-NAC (Egd1 and Btt1) and one α-NAC (Egd2), which result in Egd1-Egd2 and Btt1-Egd2 heterodimers. Btt1 containing heterodimers bind ribosomes that translate mitochondrial or ribosomal proteins while the Egd1-Egd2 heterodimer bind ribosomes that translate metabolic enzymes and secretory and membrane proteins (26).

(ii) In yeast and mammals, RAC forms a heterodimer between an Hsp40, Zuo1 (MPP11 in mammals) and an Hsp70, Ssz1 (Hsp70L1 in mammals). In addition, fungal species contain another ribosome-associated Hsp70, Ssb, which functions together with RAC. Higher eukaryotes lack a ribosome associated Hsp70 and hence utilize cytosolic Hsp70 together with mammalian RAC to facilitate folding of nascent polypeptides. Zuo1 requires stable association with Ssz1 to act as a co-chaperone of Ssb and contains a ribosome binding region that allows RAC to bind near ribosome protein Rpl31, situated at the ribosome exit tunnel

(106). Although direct association of RAC with nascent chains has not been shown, RAC is required for stimulating the binding of Ssb to nascent chains.

Experimental evidence shows that NAC and Ssb associate with aggregated, insoluble amyloid-like fibers and insoluble polyQ repeat proteins artificially expressed in mammalian and yeast cells respectively (98, 156). Although the physiological significance of these findings is not known, the ability of these proteins to play a role in protein biogenesis at the ribosome and associate with cellular aggregates suggests that ribosome-associated chaperones are potent modulators of protein synthesis and folding and represent key elements in the proteostasis network.

The Hsp70 family of chaperones

The 70-kDa family of heat shock proteins (Hsp70s) is evolutionarily conserved and assists in a wide range of cellular functions including protection of nascent polypeptides as they emerge from the ribosome, targeting and translocation of proteins, and either refolding damaged proteins or assisting in their degradation. Hsp70s function by binding to solvent exposed hydrophobic residues that are normally buried in a properly folded protein and ensure that nascent or misfolded proteins do not aggregate as a result of improper folding (Figure 1-2).

Hsp70s are functionally divided into two domains: a ~44 kDa N-terminal nucleotide-binding domain (NBD) joined by a conserved linker to a ~25 kDa C-terminal substrate-binding domain (SBD), which is further subdivided into the (15 kDa) β-sandwich subdomain and the C-terminal α-helical subdomain. The NBD is divided into four subdomains, IA, IB, IIA and IIB (Figure 3-1, green). The region between subdomains IIA and IIB is flexible, which allows subdomain IIB to rotate at this hinge region relative to the other subdomains

(38). The substrate binding characteristics of the SBD are governed allosterically by the nucleotide status of the NBD (154). The NBD has two lobes with an opening between them where the nucleotide binds. The β-sandwich subdomain of the SBD forms a base with a hydrophobic groove for polypeptide binding and the α-helical subdomain forms a lid over the polypeptide binding site. The SBD can bind a short hydrophobic section (~ seven residues) of a polypeptide chain in an extended conformation (116, 168). In the ATP-bound state, Hsp70 has a low affinity for the substrate as a result of increased flexibility between the base and lid of the SBD and effectively opens the peptide-binding site. Hydrolysis of ATP to ADP results in a change in the SBD, which conforms it to a more closed state and hence increases substrate affinity. Ultimately, the release of ADP and replacement with ATP confers the release of the folded or partially folded substrate, allowing the cycle to repeat (Figure 1-3). Two major classes of Hsp70 co-chaperones interact with the NBD of Hsp70 to regulate its protein folding function. The Hsp40/DnaJ family of proteins share a common ~70 amino acid J-domain that mediates binding to Hsp70 and activation of Hsp70's weak ATPase activity. Nucleotide exchange factors (NEFs) catalyze ADP-ATP exchange, which is a critical step in the cycle that releases the substrate and recycles Hsp70 back to its ATP-binding conformation. (Figure 1-3) The role of the NEFs will be discussed below.

As shown in Table1-1, Hsp70 family members are present in the cytoplasm, ER and mitochondria. In the mitochondria, there exists a "specialized" Hsp70 that operates with a "general" Hsp70. The general Hsp70 in the yeast mitochondrial matrix, Ssc1, is involved in refolding of protein substrates after import into the mitochondria, while the specialized Hsp70, Ssq1 is required specifically for maturation of iron-sulfur cluster-containing proteins. In humans, there exists one mtHsp70 (mitochondrial Hsp70), which is 65% homologous to

the yeast Ssc1 (11). Kar2 present in the yeast ER performs general Hsp70 functions in this compartment. BiP, the human homolog of Kar2 performs the same functions of facilitating substrate translocation into the ER lumen and their subsequent folding (53, 91). The cytosol of yeast contains several Hsp70s and will be discussed below.

The cytosolic Hsp70s in yeast

In *S. cerevisiae*, seven cytosolic Hsp70s are classified into two major groups: a) the canonical Ssa1, Ssa2, Ssa3 and Ssa4 proteins and b) the ribosome-associated Ssb1, Ssb2 and Ssz1 proteins. The Ssa and Ssb families share 60% amino acid identity between families but have distinct, non-overlapping functions *in vivo* (13). Constitutive expression of *SSA* and *SSB* genes do not complement each other's deletion phenotypes, indicating that these two classes of Hsp70s have evolved distinct functions (62, 107). The Ssa proteins are highly homologous and differ in their expression patterns with Ssa1/2 being constitutively expressed during normal vegetative growth and Ssa3/4 being induced only upon stress (160). Deletion of all four Ssa proteins is lethal to the cell but the constitutive expression of any one of them can complement lethality, suggestive of redundant functions for these chaperones (160). Cells lacking both Ssa1 and Ssa2 are slow growing and thermosensitive at 37 °C (160). At this temperature, Ssa3 and Ssa4 are induced but do not alleviate the slow growth of the *ssa1Δssa2Δ* strain suggesting that Ssa3/4 cannot fully complement the loss of Ssa1/2 despite the high degree of similarity among them. The protein folding capacity of Ssa proteins is a well-known function, and cells lacking Ssa proteins are defective in their abilities to fold the model protein firefly luciferase (151). Also, it was previously believed that Ssa proteins interacted with their substrate posttranslationally. However, deletion of ribosome-associated Ssb increased the co-translational interaction of nascent polypeptides with Ssa1,

FIGURE 1-2. Model of chaperone action in protein folding. Hsp70 family of chaperone proteins represented by blue circles bind to unfolded polypeptides preventing misfolding/aggregation, while promoting active folding to the native conformation.

FIGURE 1-2. Model of chaperone action in protein folding

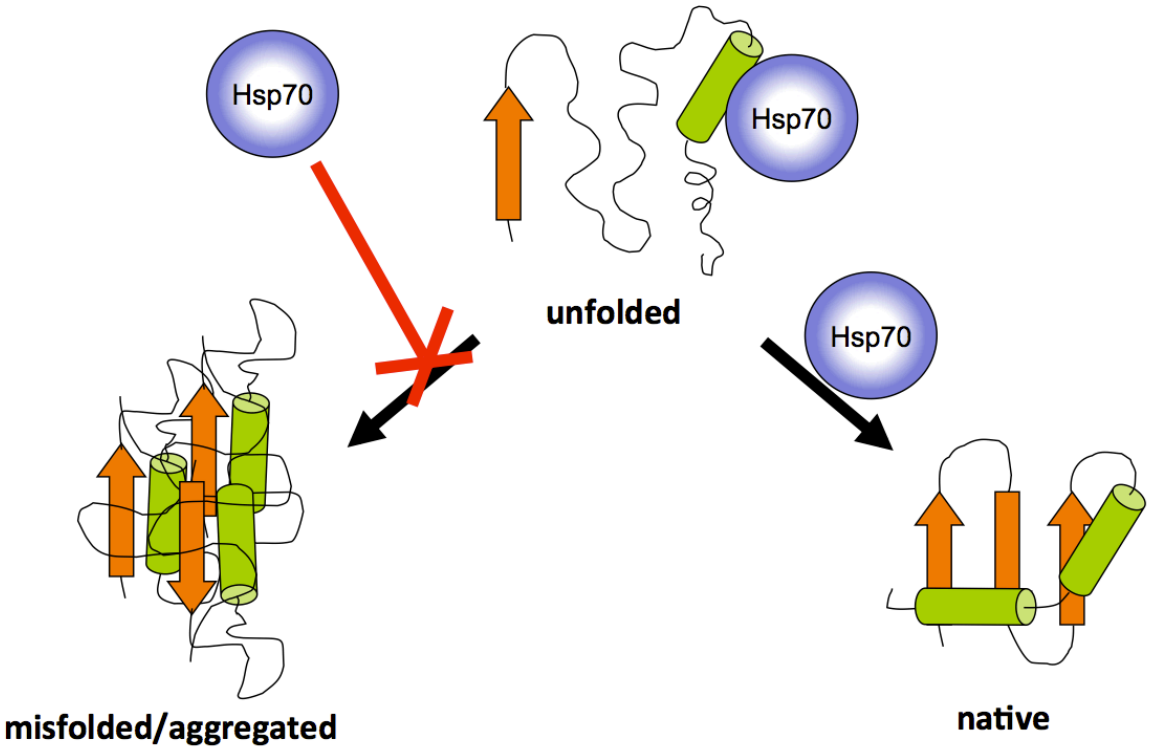

FIGURE 1-3. Hsp70 folding cycle. ATPase-dependent cycle of Hsp70 chaperone illustrating its dependence on ATPase activity and nucleotide exchange activity.

FIGURE 1-3. Hsp70 folding cycle

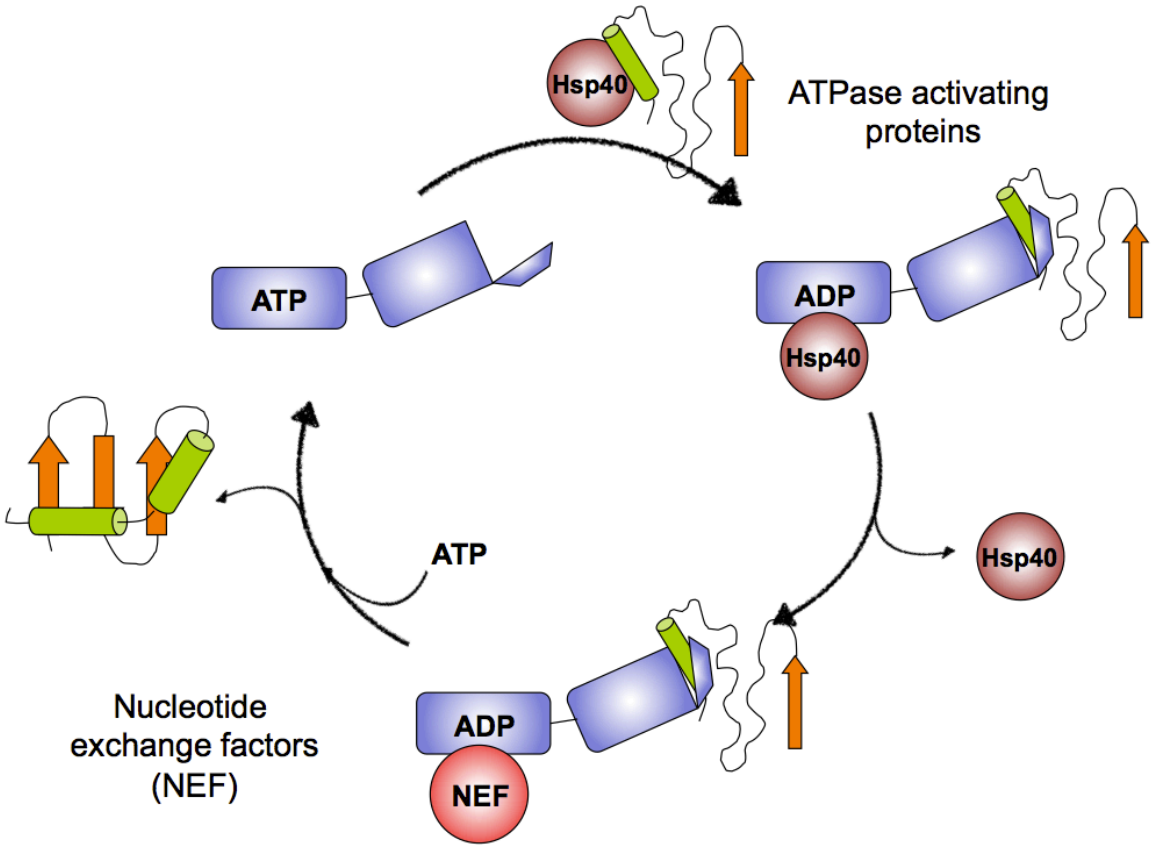

suggesting that Ssa chaperones can interact with nascent chains emerging from the ribosome (163). This corroborates with data showing Ssa interacting with two ribosome-associated factors, Sis1, an Hsp40 and poly(A)-binding protein Pab1, providing a direct link between Ssa and translating ribosomes (56). The Ssa family is also involved in protein translocation across cellular membranes, including the vacuole, the nucleus, mitochondria and the ER (28, 79, 121, 135). Cells lacking Ssa function are defective in translocation of the yeast pheromone, alpha-factor and the β-subunit of the mitochondrial F1-ATP-ase. Another role of Ssa in protein degradation is exemplified using a model substrate for proteasomal degradation, a mutated cytosolic form of the vacuolar protease carboxypeptidase Y (CPY). In the absence of functioning Ssa in the cell (using a temperature sensitive *ssa1-45* strain), CPY aggregated and displayed reduced degradation kinetics at the non-permissive temperature (101). Thus, these diverse functions of Ssa reflect its ability to interact with a variety of different substrates.

The non-essential Ssb family is composed of two proteins, Ssb1 and Ssb2 that share 99% identity and is fungal-specific. The expression of *SSB1/2* is regulated similarly to ribosomal protein genes, supporting their role in cotranslational protein folding (74). The Ssb proteins are associated primarily with translating ribosomes and this interaction is not dependent on but is stabilized by the presence of a nascent polypeptide chain. As mentioned earlier, the Ssb proteins are associated with the ribosome through their interaction with the ribosome-associated complex (RAC) proteins (43). Although the binding site of Ssb on the ribosome has not been identified, it is predicted to be near the exit tunnel in close proximity to the nascent chain and RAC (108). Deletion of *SSB1/2*, *ZUO1* or *SSZ1* causes identical phenotypes including slow growth, cold sensitivity and hypersensitivity to translation-

TABLE 1-1. Hsp70 family of chaperones in *S. cerevisiae*

Protein	Function
Cytosol	
Ssa1, Ssa2	Constitutively expressed, protein folding, translocation
Ssa3, Ssa4	Stress inducible, protein folding, translocation
Ssb1, Ssb2	Ribosome-associated, nascent chain folding
Ssz1	Component of RAC, nascent chain folding through Ssb
ER	
Kar2	Protein folding, translocation, UPR regulation
Mitochondria	
Ssc1	Protein folding, translocation
Ssc3	Protein folding, translocation
Ssq1	Folding of FeS proteins

inhibiting drugs like hygromycin B and paramomycin. These shared phenotypes suggest both their involvement in translation and the formation of a functional triad *in vivo* (43, 60). The ATPase activity of Ssb proteins is stimulated only by Zuo1, which requires stable association with Ssz1 (75, 107). Ssz1 is different from other Hsp70s: it contains an unusually short SBD and lacks the α-helical lid subdomain. ATP binding and hydrolysis by Ssz1 is not required for its function *in vivo*, nor does it seem to interact with nascent polypeptides possibly due to its short SBD.

J domain proteins of Hsp70

J proteins (also referred to as Hsp40 due to their apparent molecular mass) are homologous to DnaJ from *E. coli* and have the ability to accelerate the ATPase activity of Hsp70 (49). J protein structures contain a four-helix bundle approximately 70 amino acids in length and interact with Hsp70 through an invariable histidine-proline-aspartic acid (HPD) motif between helices II and III (148). Thirteen cytosolic J proteins have been identified in *S. cerevisiae*, of which Ydj1 is the best studied. Cells lacking *YDJ1* are slow growing and stress-sensitive and the expression of other cytosolic J proteins can replace its function, suggesting a level of redundancy and functional overlap between these proteins.

Hsp70 nucleotide exchange factors

Nucleotide exchange factors (NEFs) are a group of structurally unrelated proteins that promote ADP release from the NBD of Hsp70, resetting the folding cycle for another round of ATP binding and hydrolysis (Figure 1-3). Much of the initial work on NEFs was done using *E. coli* NEF, GrpE with the *E.coli* Hsp70 homolog, DnaK. The steady-state (when ATP concentration >>> Hsp70 concentration) ATP turnover rate of unstimulated DnaK is very slow (between 0.02 and 0.2 min-1) to drive its chaperone function (99). For the DnaK

system, co-chaperones DnaJ and GrpE stimulate the ATP turnover rate several hundred-fold at saturating conditions (78). The crystal structure of a GrpE monomer reveals a long α-helix followed by a short α-helix and then a compact β-sheet domain at the C-terminus. The co-crystal of GrpE shows that it binds as a dimer to an NBD of DnaK and provides the β-sheet domain at the cleft between the two lobes of the NBD, which causes domain IIB to move outward by 14°, resulting in nucleotide dissociation.

Mge1, an essential mitochondrial matrix protein in *S. cerevisiae* shares 34% identity with *E. coli* GrpE and associates with mitochondrial matrix Hsp70s, Ssc1 and Ssq1 (72). The relative stoichiometry of the three proteins as determined by immunoprecipitation experiments, as the ratio of Ssc1 to Mge1 to Ssq1 is 250:50:1 (123). A conserved loop structure on the surface of the NBD of Ssc1 mediates its interaction with Mge1 and for Mge1-induced nucleotide exchange (84). Mge1 was shown to release both ADP and ATP from Ssc1, suggesting that the Mge1-binding interface of Ssc1 is similar in both the ATP- and ADP-bound forms, thus functioning as a nucleotide release factor for Ssc1. This NEF functions to modulate nucleotide-dependent stability of the Ssc1-Tim44 complex that is required for import of precursor proteins into the matrix. In addition, reduced rates of maturation of Yfh1, the yeast frataxin homolog required for iron homeostasis was seen in an *mge1-100* temperature sensitive strain and in a strain lacking *SSQ1*, which suggests that Mge1 plays a role in posttranslocational folding with regard to Ssq1 function. Interestingly, the inactivation of Ssc1 in *ssc1-3* mitochondria dramatically enhanced the interaction between Ssq1 and Mge1, suggesting a competitive interaction between the two Hsp70s for Mge1 association (123). The mitochondrial matrix thus provides a unique situation where the activity of two Hsp70 chaperones is governed by interactions with a single NEF.

In the early 2000s, three distinct families of NEFs were identified in the cytosol with both yeast and human/mammalian counterparts: the Hsp110s (Sse1/2), HspBP1 (Fes1) and BAG domain-containing proteins (Snl1).

Hsp110 homologs in yeast, Sse1 and Sse2 are 76% identical to each other and are 70% similar to Ssa1 with regard to amino acid sequence. Both Sse1 and Sse2 are expressed under normal conditions but Sse2 is 10 times less abundant than Sse1 (45). Deletion of *SSE1* results in a slow growth phenotype exacerbated by temperature stress, while loss of *SSE2* is not associated with any phenotypic effects (89). Deletion of both genes is lethal, suggesting that both proteins comprise an essential gene product pair. The domain architecture of Sse1/2 is similar to that of all Hsp70s with the exception of two extended spacer regions in the SBD but a number of unusual features of Sse proteins suggested that they might function differently than Hsp70s. Sse1 was found to bind but not hydrolyze ATP and Sse1 holds substrate proteins rather than fold them (130). Our lab and others showed that Sse proteins act as potent NEFs for Ssa and Ssb and that ATP binding by Sse1, but not the Hsp70 partner appears to be a requirement for their association (31, 115, 129). The crystal structure of Sse1 revealed a domain architecture similar to Hsp70 but the α-helical lid subdomain of the SBD of Sse1 exists in an extended conformation that wraps around the distal face of Hsp70 to make additional contacts with lobe II of the Hsp70 NBD (125). The location of the Sse1 SBD in close proximity to the Hsp70 SBD suggests that both proteins may simultaneously bind certain substrates or Sse1 may recruit substrates followed by a "handoff" of the substrate to Hsp70.

The Fes1 cochaperone was initially identified as the cytosolic homolog of the ER NEF Sil1 that interacts with the ER Hsp70 Kar2. Fes1 is also highly homologous to the

mammalian NEF HspBP1 (63, 65). Fes1 was shown to activate nucleotide exchange for Ssa and Ssb and will be discussed further in Chapter 5.

The Bag-1 (Bcl-2-associated athanogene) protein was first identified as a binding partner of apoptosis inhibitor protein, Bcl-2 (144). It was later shown that a conserved domain comprising of about 100 amino acids at the carboxyl end of Bag-1 (BAG domain) directly interacts with the NBD of Hsc70 and stimulates its ATPase rate only in the presence of a J-protein, suggesting its role as an NEF. The crystal structure of the ~13 kDa BAG domain of Bag-1 in complex with the ATPase domain of Hsc70 shows a monomeric three helix bundle architecture with helices two and three making contacts with residues Met 61, Arg 261 and Glu 283 in subdomains IB and IIB of the ATPase domain (140). A structure-based sequence alignment of the BAG domain of different species identified Snl1 as the sole BAG domain-containing protein in *S. cerevisiae*. *In vitro* studies show that Snl1 interacts with yeast Ssa and Ssb and mammalian Hsp70 and regulates the ATPase activity of Hsp70. In addition, two residues (E112, R141) that make contacts with the Hsp70 ATPase domain are absolutely conserved in BAG domain-containing proteins, and their disruption in Snl1 affects its binding to Hsp70, confirming Snl1 as a bonafide BAG domain protein (139). Snl1, was shown to interact with Ssa and Ssb *in vitro* and its nucleotide exchange activity on Hsp70 was comparable with mammalian Bag-1 (139).

Unlike mitochondria, which contain only one NEF, the ER of yeast and higher eukaryotes contains two NEFs, Sil1 and Lhs1 (Grp170 in mammals). Sil1 is a nonessential protein present in the ER lumen and interacts specifically with the NBD of Kar2/BiP, the ER-resident Hsp70 (64, 149). *SIL1* in yeast is synthetically lethal when disrupted in combination with mutant alleles of *KAR2* and *SEC63*, suggesting that Sil1 plays a role in the translocation

of substrates into the ER. Sil1 stimulates Kar2 ATPase activity and preferentially binds to the ADP-bound conformation of Kar2 (64). Human Sil1 shares 20% sequence identity with yeast Sil1 and is suggested to represent a paralog of HspBP1, the Fes1 homolog in mammals (22). Deletion of *SIL1* alone in yeast does not cause any effect but mutations in human Sil1 causes Marinesco-Sjogren syndrome characterized by cerebellar ataxia, cataracts and muscle weakness (127). The crystal structure of Sil1 in complex with NBD of BiP shows Sil1 to contain 16 α-helices (A1-A16) and no β-strands. The central helices A3-A14 form four Armadillo-like repeats (ARM1-ARM4). Each ARM is made of 3 α-helices that pack into a right-handed superhelix to produce a gently curved elongate molecule. Sil1 utilizes its concaved inner surface to embrace lobe IIB of the BiP NBD. Although Sil1 and HspBP1 share limited sequence identity (13%) between them, they share a similar architecture with four central ARM repeats flanked by two amino- and carboxyl- terminal helices, suggesting evolutionary conservation of domain architecture (134, 164). *LHS1* encodes a nonessential glycoprotein that shares 24% amino acid identity with Kar2. It is considered to be an "atypical" Hsp70 family member and is grouped with the Hsp110 family that cannot fold substrates *in vivo*. Lhs1 acts as an NEF for Kar2 and consistent with this evidence, it preferentially binds to the apo- and ADP-bound states of Kar2 (25). Lhs1 and Sse1 share key conserved Hsp70-binding residues and stimulate nucleotide exchange on their Hsp70 partners using similar mechanisms (4). A key difference between Sse1 and Lhs1 is that Kar2 reciprocally stimulates the ATPase activity of Lhs1. Similar to Sse1, Lhs1 and its mammalian homolog Grp170 were shown to also "hold" substrates, suggesting that "holdase" activity is a conserved function of this protein family (159). Since both Sil1 and Lhs1 bind Kar2, it was suggested that they do so in a mutually exclusive manner (143). The

combined deletion of *LHS1* and *SIL1* results in synthetic lethality and suggests a strict requirement of NEF activity for proper Hsp70 function in the ER (149).

Aim of this work

In yeast and human cells, the presence of multiple structurally distinct NEFs that perform the same biochemical function suggests that these NEFs may play distinct and/or overlapping roles as Hsp70 co-chaperones with respect to cellular processes, substrates and location in the cell. An ongoing research focus in the lab is to study the cellular roles of the three families of cytosolic NEFs. In this work, I will focus on two cytosolic NEFs, the unique ER membrane-associated Snl1 and free-floating Fes1. This investigation has provided novel insights into the roles that these proteins play in Hsp70-dependent cellular functions.

Significance of this work

Molecular chaperones are an integral part of the proteostasis network and are vital components needed to maintain homeostasis of the cellular proteome. The proper assembly, processing and transport of cellular proteins requires the function of an ensemble of chaperones under normal and stressed conditions. Improper folding and defects in protein turnover can lead to a variety of diseases, described earlier in this chapter. Hsp70 is, by far, the most evolutionarily conserved protein within this group with many co-chaperones that can bind to it and regulate its substrate-folding cycle. Since the Hsp70 family of chaperones performs different tasks in the cell, regulation of its access to substrates is an important step. This regulatory activity is provided by co-chaperones that connect Hsp70 proteins with their target substrates and also with other chaperones like Hsp90. This occurs through a direct association with both the chaperone and the substrate (73). However, at the molecular level, it is not known how co-chaperones select their Hsp70 partners and substrates. In this study,

using primarily immunoprecipitation techniques, I identified a novel interaction between a cytosolic NEF of Hsp70 tethered to the ER and the ribosome, which might function to recruit Hsp70 to enhance folding at this cellular location. In addition, I discovered a binding specificity between another cytosolic NEF with one class of cytosolic Hsp70 present in yeast cells, suggesting its role in a substrate- or pathway-specific Hsp70 function.

When I first began this study, very little was known about the binding partners of Snl1, an ER-localized cytosolic Hsp70 co-chaperone in yeast cells. A truncated variant of Snl1 that lacked the transmembrane domain was previously described to bind cytosolic Hsp70s, Ssa and Ssb *in vitro* and to facilitate the release of a bound nucleotide from Hsp70. Chapter 3 of the dissertation describes a novel interaction between full length or truncated Snl1 proteins and the ribosomal complex. Several lines of evidence indicate that this interaction is both independent of and concurrent with binding to Hsp70 and is not dependent on membrane localization. I further identify the ribosome-binding site on Snl1 and show that this interaction is conserved in the pathogenic fungus *Candida albicans*. To determine the intricacies of Snl1-Hsp70 interaction, in Chapter 4, I describe a preliminary analysis to find the minimal domains of Snl1 and CaSnl1 (*C.albicans* homolog) that bind Hsp70, and successfully developed a pilot purification strategy that will be used to allow structure determination by X-ray crystallography. This is part of an active collaboration and will be the first structures to be determined for Bag domain-containing proteins in fungi.

In Chapter 5, I describe a preliminary follow-up of my original discovery of Fes1 to exhibit selectivity in binding cytosolic Hsp70s in yeast, as seen in Chapter 3. Previous *in vitro* data showed that Fes1 can bind both Ssa and Ssb but I found that Fes1 interacts specifically with Ssa. I showed that lack of Fes1 binding to Ssb is not due to its stoichiometric levels in the

cell. In addition, two proteins that associate with Ssb at the ribosome do not prevent Fes1 from interacting with Ssb. This is the first evidence of an *in vivo* bias in binding of a cytosolic NEF with Hsp70. While Ssb is present on the ribosome and is involved in co-translational protein folding, Ssa acts downstream to fold polypeptides post-translationally. This suggests that Fes1 functions at a later step in polypeptide folding and is recruited specifically for Ssa-dependent cellular functions. This observation demonstrates that although the three cytosolic NEFs have the same biochemical function, they may be utilized for distinct and/or overlapping cellular processes based on their abilities to bind cytosolic Hsp70s. Thus, targeting Hsp70 co-chaperone proteins to enhance or diminish the ability of the Hsp70 system to modulate substrate recognition, binding and release is an important area of research, especially with regard to protein aggregation diseases.

Taken together, the results presented in this dissertation establish novel binding partners for two distinct Hsp70 co-chaperones in yeast cells. These findings provide a basic framework for future studies into the importance of subcellular localization and binding specificities of Hsp70 co-chaperones in diverse cellular processes.

Chapter 2: Materials and Methods

Strains and plasmids

S. cerevisiae strains used in this study are listed in Table 2-1. The strains were grown in rich medium containing 1% yeast extract, 2% peptone and 2% dextrose (YPD). Synthetic complete (SC) medium lacking the appropriate nutrient for plasmid selection was purchased from Sunrise Science Products (San Diego,CA). Standard yeast propagation and transformation procedures were followed (66). Plasmids used in this work are listed in Table 2-2. All plasmids were built using standard PCR and restriction enzyme cloning techniques.

Polymerase chain reaction mutagenesis and recombination cloning

Site directed mutagenesis was performed via a PCR-based mutagenesis strategy and homologous recombination of PCR products. Plasmids were built by ordering complementary oligonucleotides containing identical changes in the region of interest. Overlap between PCR fragments and the vector backbone was no less than 40 base pairs. Correct plasmids were confirmed by restriction endonuclease analysis and by sequencing the inserts.

pSnl1ΔN-FLAG(E112A,R141A) was constructed in two steps using PCR-based recombination cloning. In brief, p413TEF was digested with Spe I and Xho I and used for gap repair via homologous recombination with pooled PCR products with the incorporated E112A substitution amplified from the template p413TEF-SNL1ΔN-FLAG, with homology to the gapped plasmid ends (*TEF2* promoter and *CYC1* terminator). The second recombination round was performed with pooled PCR products with the incorporated R141A change amplified from the template p413TEF-SNL1ΔN(E112A)-FLAG, with homology to the similar gapped plasmid ends.

Snl1 (5KA)-FLAG was constructed using recombination cloning. In brief, p413TEF was digested with Spe I and Xho I and used for gap repair via homologous recombination with pooled PCR products with the incorporated five lysine-to-alanine changes amplified from the template p413TEF-SNL1-FLAG, with homology to the gapped plasmid ends (*TEF2* promoter and *CYC1* terminator). The construct p413TEF-SNL1-(5KA)-FLAG was used as the template to amplify SNL1ΔN(5KA)-FLAG flanked by 5' Spe I and 3' Xho I sites for subsequent cloning into p413TEF.

SNL1 and SNL1ΔN (Δ40) were amplified from BY4741 genomic DNA by use of standard PCR protocols and cloned into the vector p413TEF by use of 5' Spe I and 3' Xho I sites engineered into the amplifying oligonucleotide primers by use of standard DNA digestion and ligation protocols (90). In each case, a carboxyl-terminal FLAG (DYKDDDDK) epitope tag was also incorporated into the 3'-end primer sequence to facilitate immunoprecipitation of these proteins in the cell. The truncated alleles of *SNL1* (Δ50, Δ60, Δ70, and Δ80) were amplified from p413TEF-SNL1ΔNFLAG flanked by 5' Spe I and 3' Xho I sites for subsequent cloning into p413TEF.

The hypothetical BAG domain-containing protein (ca19.997) from *Candida albicans* was amplified from SC5314 genomic DNA (kindly provided by the Lorenz Lab, Dept. of Microbiology and Molecular Genetics). A C-terminal FLAG tag and 5' Spe I and 3' Xho I sites were incorporated into the amplifying primer sequences for subsequent cloning into p413TEF. *ca19.997* was C-terminally green fluorescent protein (GFP) tagged by using a method described previously (44). Briefly, PCR was performed by using the pGFPHIS1 plasmid template with primers F1 and R2, and this product was transformed by electroporation into *C. albicans* strain SC5314. Transformants were selected by plating the

transformation mix onto histidine plates and verified by PCR.

Plasmid pCDNA3/HA-Bag1 (141)(a gift from R. Morimoto, Northwestern University) was used as a template to amplify *Mus musculus* Bag-1 with a C-terminal FLAG tag and 5' Spe I and 3' Xho I sites that were incorporated into the amplifying primer sequences for subsequent cloning into plasmid p423GPD.

Δ60*SNL1* was amplified from BY4741 genomic DNA by use of standard PCR protocols and cloned into pPRoEX-HtB (Invitrogen, kindly provided by A.Bracher, Max Planck Institute for Biochemistry, Munich, Germany), by use of 5' Spe I and 3' Xho I sites engineered into the amplifying oligonucleotide primers by use of standard DNA digestion and ligation protocols. Δ103*CaSNL1* was amplified from genomic DNA isolated from the *C. albicans* strain SC5314 by use of standard PCR protocols and cloned into pPRoEX-HtB (Invitrogen), by use of 5' Spe I and 3' Xho I sites engineered into the amplifying oligonucleotide primers by use of standard DNA digestion and ligation protocols.

Yeast growth assays

Plate growth assays were carried out by serial dilution using 1/10 dilution steps with a starting culture optical density at 600 nm of 1.0 and the resulting culture was transferred with a multipronged replicating tool from a 96-well plate.

SDS-PAGE and Western blot analysis

Proteins were separated by sodium dodecyl sulfate-polyacrylamide gel electrophoresis (SDS-PAGE) and transferred onto a polyvinylidene difluoride (PVDF) membrane (Millipore) for immunodetection. All antibodies were added in 5% solution of non-fat dry milk resuspended in TBST (0.684 M NaCl, 0.1 M Tris base [pH 7.6], 0.2% Tween-20).

Antibodies used in the study

Antibody	Source	Dilution
Rabbit polyclonal Ssa1/2	Dr. M.Ptashne (Sloan-Kettering Institute)	1:40,000
Rabbit polyclonal Ssb1/2	Dr. E. Craig (University of Wisconsin)	1:5,000
Rabbit polyclonal Rpl8	A. Johnson (University of Texas, Austin)	1:2,000
Mouse polyclonal Rpl3	J. Warner (Albert Einstein College of Medicine)	1:1,000
Mouse monoclonal M2 (FLAG)	Sigma Aldrich, St. Louis, MO	1:1,000
Mouse monoclonal HA (12CA5)	Roche Diagnostics, Indianapolis, IN	1:2,000

Soluble protein extraction from yeast

Cells expressing tagged proteins were harvested and resuspended in TEGN200 buffer (20mM Tris [pH7.9], 0.5 mM EDTA, 10% glycerol, 200 mM NaCl) containing protease inhibitors (2 µg/ml aprotinin, 2µg/ml pepstatin, 1µg/ml leupeptin, 1mM phenylmethylsulfonyl fluoride and 2µg/ml chymostatin [Sigma]), which we refer to as TEGN200+PI. Samples were lysed using acid-washed glass beads in a microtube mixer for five rounds of 1 min of lysis in each round followed by 1 min on ice. The lysate was cleared by centrifugation at 3,000 X *g* for 10 min at 4 °C. For KCl treatment, the lysate was split equally into four tubes containing 0,0.1,0.2 and 0.5 M KCl and incubated on ice for 30 min. For EDTA treatment, the Rps6B-3X hemagglutinin (3XHA) strain (10)(a gift from S. Baserga, Yale University) expressing Snl1ΔN-FLAG was harvested and resuspended in TADM buffer (50 mM Tris [pH 7.5], 50 mM ammonium acetate, 1 mM dithiothreitol [DTT], 5 mM magnesium chloride) with PI (TADM+PI) and lysed as described above. Snl1ΔN was immunoprecipitated from the cell lysate, and the resin was washed two times with TADM+PI. The FLAG resin was split equally, 40 mM EDTA was added to one tube, and samples were incubated on ice for 30 min. The FLAG resin was washed two times, and the

proteins were eluted as mentioned below.

***In vivo* FLAG immunoprecipitation**

Soluble protein extracts were prepared from 25-100 ml of log-phase (A_{600}=0.8) cultures of the appropriate strains. For immunoprecipitations (IPs), 30 µl of a 1:1 slurry of M2 resin (Sigma) in TEGN200 was added to the lysate. The volume was adjusted to 700 µl with TEGN200+PI, followed by incubation with mixing at 4°C for 2 h. Resin was then collected by centrifugation and washed seven times with TEGN+PI. For the elution of bound proteins, 35 µl of 200 µg/ml 2X-FLAG peptide (N-DYKDDDDKDYKDDDDK-C)(GenScript) in TEGN200 was added to the resin pellet and incubated at room temperature for 15 min with occasional shaking. After incubation, the resin was pelleted by centrifugation at 3000 X *g* for 1 min at room temperature and the supernatant combined with an equal volume of 2X sample buffer (200 mM Tris-Cl (pH 6.8), 36% glycerol, 10% SDS, 5% β-mercaptoethanol, 0.012% bromophenol blue). The resulting mixture was boiled for three minutes at 95 °C to denature protein complexes. To immunopurify membrane-bound Snl1, lysates were treated with 1% TritonX-100 to solubilize the protein before performing the immunoprecipitation reaction.

Protein identification

Proteins were identified at the Proteomics Core Facility at the University of Texas Health Science Center at Houston. Tandem mass spectrometry (MS/MS) analysis was performed with an Applied Biosystems QStar Elite liquid chromatography-MS/MS (LC/MS/MS) mass spectrometer equipped with an LC Packings high-performance liquid chromatography (HPLC) instrument for capillary chromatography. The HPLC instrument was coupled to the mass spectrometer by a Nanospray II electrospray ionization (ESI) source

for direct analysis of the eluate. For protein identification, proteins were separated on a 15% SDS-PAGE gel, stained using Coomassie brilliant blue and the gel was sent to the Proteomics Core Facility for band identification.

***In vitro* protein-protein interaction assay**

Snl1ΔN-FLAG was immunoprecipitated from strain BY4741 using anti-FLAG M2 affinity resin. For the competition assay, Snl1ΔN bound to FLAG resin was combined with recombinant His_6-Ssb (1 mg/ml), purified previously by Dr. Lance Shaner, a former member of the lab. The sample was incubated on ice for 30 min. Following incubation, the beads were reisolated and bound proteins were eluted as mentioned above.

Pilot purification of His_6-Δ60SNL1 and His_6-Δ103CaSNL1

Δ60Snl1 and Δ103CaSnl1 were expressed as N-terminally His-tagged fusion proteins using *E. coli* BL21 cells in Luria-Bertani (LB) broth supplemented with 100 µg/ml ampicillin (amp). Cells were sub-cultured into 50 ml LB + ampicillin at a 1:100 dilution and incubated at 37 °C. At two hours (OD600 of 0.6), 1mM IPTG was added to the cultures and grown subsequently for an additional three hours to induce protein expression. Cells were harvested by centrifugation at 8,000 rpm for 20 minutes at 4 °C. The cell mass from a 50 ml culture was resuspended in 5 ml of buffer B (50 mM Tris-HCl (pH 7.6), 5 mM Imidazole, 2 mM MgCl2, 200 mM NaCl) containing protease inhibitors (P.I.)(aprotinin 2 µg/ml; pepstatin A, 2 µg/ml; leupeptin, 1 µg/ml; phenylmethylsulfonyl fluoride, 1 mM; chymostatin, 2 µg/ml; Sigma). Cell lysis via French Press was performed for two rounds of 1000 psi each. After removal of the cell debris by centrifugation at 8,000 rpm for 20 min, the lysate (approx.. 4 ml) was added to a pre-chilled 15 ml centrifuge tube containing 500 µl (1:1slurry) of Ni-NTA (Qiagen), pre-equilibrated using buffer B. The volume was brought to 10 ml to enable

efficient mixing. Samples were incubated for three hours at 4 °C with gentle mixing. Each sample was then loaded onto a Polyprep chromatography column and the flow-through (FT) was collected by gravity flow after the resin was allowed to settle. The resin was washed once with 5 ml buffer B (W1) followed by 5 ml buffer B containing 500 mM NaCl (buffer B500)(W2). The final wash step was done using 5 ml buffer B500 containing 50 mM imidazole (W3). Bound proteins were eluted in two steps; first with 2 ml Buffer B500 containing 200 mM imidazole (E1) and second by 2 mL Buffer B500 supplemented with 500 mM imidazole (E2). The protein content of each fraction was analyzed on a 15% SDS-PAGE gel.

Microscopy

Candida albicans cells were harvested by centrifugation, washed once with water, and resuspended in 70% ethanol for fixation for 1 min. Cells were once again harvested by centrifugation and resuspended in water for visualization. Nuclei of living cells were stained with the vital DNA dye Hoechst 33342 at a concentration of 10 g/ml for 5 min. Cells were observed under a BX60 epifluorescence microscope (Olympus, Tokyo, Japan) equipped with a 100X immersion oil objective and 4',6-diamidino-2-phenylindole or GFP filter cubes. Images were captured with a Photometrics CoolSNAP-fx cooled charge-coupled-device camera driven by QED image-capturing software (Media Cybernetics, Bethesda, MD). All images were processed by using Photoshop CS (Adobe Systems, San Jose, CA).

TABLE 2-1. LIST OF STRAINS USED IN THIS STUDY

Strain Name	Genotype	Source or Reference
BY4741	*MAT*a *his3Δ1/ leu2Δ0/ met15Δ0/ ura3Δ0*	Open Biosystems
snl1Δ	*MAT*a *his3Δ1/ leu2Δ0/ met15Δ0/ ura3Δ0 snl1::KanMX*	Open Biosystems
sse1Δ	*MAT*a *his3Δ1/ leu2Δ0/ met15Δ0/ ura3Δ0 sse1::KanMX*	Open Biosystems
ssz1Δ	*MAT*a *his3Δ1/ leu2Δ0/ met15Δ0/ ura3Δ0 ssz1::KanMX*	Open Biosystems
zuo1Δ	*MAT*a *his3Δ1/ leu2Δ0/ met15Δ0/ ura3Δ0 zuo1::KanMX*	Open Biosystems
egd1Δ	*MAT*a *his3Δ1/ leu2Δ0/ met15Δ0/ ura3Δ0 egd1::KanMX*	Open Biosystems
egd2Δ	*MAT*a *his3Δ1/ leu2Δ0/ met15Δ0/ ura3Δ0 egd2::KanMX*	Open Biosystems
btt1Δ	*MAT*a *his3Δ1/ leu2Δ0/ met15Δ0/ ura3Δ0 btt1::KanMX*	Open Biosystems
sbh1Δ	*MAT*a *his3Δ1/ leu2Δ0/ met15Δ0/ ura3Δ0 sbh1::KanMX*	Open Biosystems
sbh2Δ	*MAT*a *his3Δ1/ leu2Δ0/ met15Δ0/ ura3Δ0 sbh2::KanMX*	Open Biosystems
ssh1Δ	*MAT*a *his3Δ1/ leu2Δ0/ met15Δ0/ ura3Δ0 ssh1::KanMX*	Open Biosystems
sec66Δ	*MAT*a *his3Δ1/ leu2Δ0/ met15Δ0/ ura3Δ0 sec66::KanMX*	Open Biosystems
sec72Δ	*MAT*a *his3Δ1/ leu2Δ0/ met15Δ0/ ura3Δ0 sec72::KanMX*	Open Biosystems
nat4Δ	*MAT*a *his3Δ1/ leu2Δ0/ met15Δ0/ ura3Δ0 nat4::KanMX*	Open Biosystems
nup188Δ	*MAT*a *his3Δ1/ leu2Δ0/ met15Δ0/ ura3Δ0 nup188::KanMX*	Open Biosystems
ubr1Δ	*MAT*a *his3Δ1/ leu2Δ0/ met15Δ0/ ura3Δ0 ubr1::KanMX*	Open Biosystems
ssz1Δsnl1Δ	*MAT*a *his3Δ1/ leu2Δ0/ met15Δ0/ ura3Δ0 ssz1::KanMX snl1::LEU2*	This study
zuo1Δsnl1Δ	*MAT*a *his3Δ1/ leu2Δ0/ met15Δ0/ ura3Δ0 zuo1::KanMX snl1::LEU2*	This study
egd1Δsnl1Δ	*MAT*a *his3Δ1/ leu2Δ0/ met15Δ0/ ura3Δ0 egd1::KanMX snl1::LEU2*	This study
egd2Δsnl1Δ	*MAT*a *his3Δ1/ leu2Δ0/ met15Δ0/ ura3Δ0 egd2::KanMX snl1::LEU2*	This study

btt1Δsnl1Δ	*MAT*a *his3Δ1/ leu2Δ0/ met15Δ0/ ura3Δ0 btt1::KanMX snl1::LEU2*	This study
sbh1Δsnl1Δ	*MAT*a *his3Δ1/ leu2Δ0/ met15Δ0/ ura3Δ0 sbh1::KanMX snl1::LEU2*	This study
sbh2Δsnl1Δ	*MAT*a *his3Δ1/ leu2Δ0/ met15Δ0/ ura3Δ0 sbh2::KanMX snl1::LEU2*	This study
ssh1Δsnl1Δ	*MAT*a *his3Δ1/ leu2Δ0/ met15Δ0/ ura3Δ0 ssh1::KanMX snl1::LEU2*	This study
sec66Δsnl1Δ	*MAT*a *his3Δ1/ leu2Δ0/ met15Δ0/ ura3Δ0 sec66::KanMX snl1::LEU2*	This study
sec72Δsnl1Δ	*MAT*a *his3Δ1/ leu2Δ0/ met15Δ0/ ura3Δ0 sec72::KanMX snl1::LEU2*	This study
nat4Δsnl1Δ	*MAT*a *his3Δ1/ leu2Δ0/ met15Δ0/ ura3Δ0 nat4::KanMX snl1::LEU2*	This study
nup188Δsnl1Δ	*MAT*a *his3Δ1/ leu2Δ0/ met15Δ0/ ura3Δ0 nup188::KanMX snl1::LEU2*	This study
ubr1Δsnl1Δ	*MAT*a *his3Δ1/ leu2Δ0/ met15Δ0/ ura3Δ0 ubr1::KanMX snl1::LEU2*	This study
DS10	*MAT*a *leu2-3,112 trp1-1 ura3-52 lys1 lys2 his3-11,15*	(96)
ssb1Δssb2Δ	*MAT*a Δ*ssb1::HIS3* Δ*ssb2::LEU2 leu2-3,112 trp1-1 ura3-52 lys1 lys2 his3-11,15*	(94)
rps6b-3xHA	*MAT*a *ura3-52 lys2-80 ade2-101trp1-Δ63 his3-Δ200 leu2-Δ1*	(10)
RSY1293 (*sec61*-wt)	*MATa can 1-100 leu2-3,-112 his3-11,-15 trp1-1 ura3-1 ade2-1 sec61::HIS3* [pDQ1]	(109)
RSY1295 (*sec61*-mut^{ts})	as *RSY1293* except [*psec61-41*]	(109)
SC5314	*C. albicans* prototrophic wild type strain	(39)
SC5314 *SNL1::GFP* (CaSnl1)	orf19.997/*orf19.997-GFP*::*HIS1*	This study

TABLE 2-2. LIST OF PLASMIDS USED IN THIS STUDY

Plasmid	Description
p413*TEF*-FLAG-*SSE1*	
p413*TEF*-FLAG-*SSE2*	
p413*TEF*-FLAG-*FES1*	
p413*TEF-SNL1*-FLAG	
p413*TEF-SNL1ΔN*-FLAG	lacks first 40 residues
p413*TEF-SNL1ΔN***-FLAG	*SNL1* mutant,(E112A,R141A),lacks first 40 residues
p413*TEF-SNL1Δ50*-FLAG	lacks first 50 residues
p413*TEF-SNL1Δ60*-FLAG	lacks first 60 residues
p413*TEF-SNL1Δ70*-FLAG	lacks first 70 residues
p413*TEF-SNL1Δ80*-FLAG	lacks first 80 residues
p413*TEF-SNL1ΔN(5KA)*-FLAG	5-Lys to Ala change between residues 52-58
p413*TEF-CaSNL1Δ91*-FLAG	*Candida albicans SNL1*,lacks first 91 residues
p413*TEF-CaSNL1Δ103*-FLAG	*Candida albicans SNL1*,lacks first 103 residues
pGFPHIS1	contains GFP cassette for PCR-mediated gene tagging in *Candida albicans*
pCDNA3/HA-Bag1	Contains 30 kDa small Bag-1 isoform
pPROEX-HtB-*Δ60SNL1*	N-terminally tagged His6-tagged *SNL1*,lacks first 60 residues
pPROEX-HtB-*Δ103CaSNL1*	N-terminally tagged His6-tagged *Candida albicans SNL1*,lacks first 103 residues
p423*GPD*-FLAG-*FES1*	high copy vector

Chapter 3: *SNL1* encodes a novel ribosome associated nucleotide exchange factor in fungi

NOTE: This chapter is derived from work that has been published in 2012: "A lysine-rich region within fungal BAG domain-containing proteins mediates a novel association with ribosomes." "Copyright © American Society for Microbiology, *Eukaryotic Cell* 2012, 11(8):1003. DOI: 10.1128/EC.00146-12. I am the primary author on this paper and was responsible for preparing the original manuscript. I performed all experiments described in this chapter. As an author, I have been granted permission by the publisher of Eukaryotic Cell, the American Society for Microbiology, to reproduce any/all of my manuscript in print or electronically for the purpose of my dissertation.

3A. INTRODUCTION

SNL1 was initially identified in a genetic multicopy suppressor screen for lethality caused by the expression of a truncated mutant allele of the nuclear pore protein Nup116 linking the function of Snl1 to nuclear pore assembly and function (54). Although a direct role for Snl1 in nuclear transport is unclear, the different phenotypes seen here suggest that Snl1 might provide a localized stimulation of Hsp70 in folding certain partially misfolded proteins associated with the nuclear pore complex. However, little else is known about the cellular roles of Snl1. Snl1 is unique among all known Hsp70 NEFs in containing an amino-terminal transmembrane region that tethers it to the ER membrane, with the BAG domain/Hsp70-binding domain facing the cytosol (139). Unlike the phenotypes seen with the loss of *SSE1* or *FES1* in yeast cells, *snl1Δ* cells show no observable phenotype.

The goal of this project was to identify cellular binding partners of full length Snl1 and a truncated variant lacking the amino-terminal transmembrane domain and to determine the function of Snl1 as an Hsp70 co-chaperone at the ER membrane. In this study, I report the novel interaction of Snl1 with the ribosome complex, in addition to its association with Hsp70. I have biochemically characterized this ternary complex and show that Snl1 binds predominantly to the 60S subunit, independent of Hsp70 binding and suggest the presence of two separate interaction surfaces on Snl1. I show that this is a conserved interaction in *Candida* BAG domain-containing proteins using the sole Snl1 homolog in the pathogenic fungus, *Candida albicans*. The ribosome binding interface in these proteins contains a lysine-rich region and is situated in the putative helix one region of the BAG domain (152).

3B. RESULTS

Snl1 is associated with intact ribosomes

Previous *in vitro* results had shown that the cytosolic BAG domain homology region of Snl1 interacts with the yeast cytosolic Hsp70s Ssa and Ssb (139). This interaction is consistent with the mammalian BAG domain protein, Bag-1, which interacts directly with the N-terminal NBD of Hsc70 (Figure 3-1) (140). However, whether Snl1 interacts with the cytosolic Hsp70s *in vivo* was unknown. To test this, I constructed expression vectors to produce FLAG-tagged full length Snl1 (FL-Snl1) and a truncated variant of Snl1 (Snl1ΔN) that lacks the N-terminal transmembrane domain but contains the entire cytosolic region starting at residue 40 and includes the conserved BAG domain. I affinity purified both proteins using M2-agarose resin from cell lysates, which were solubilized with 1% TritonX-100 to release membrane-bound Snl1. In addition to these two Snl1 proteins, I independently expressed FLAG-tagged Sse1, Sse2 and Fes1 fusions from the identical promoter to compare Hsp70 purification patterns. In addition to Ssa and Ssb, Snl1 and Snl1ΔN copurified at least 20 additional bands (Figure 3-2). In contrast, these proteins were absent when the three other FLAG-tagged NEFs were isolated, while Ssa and Ssb were identified in all the pulldowns. I noticed that the amount of Ssa that copurified with the two Snl1 proteins was disproportionately reduced relative to the amounts of the other three NEFs. In addition, FLAG-Fes1 appeared to associate specifically with Ssa *in vivo*, with little to no Ssb copurifying with it. This observation will be discussed further in Chapter 5. To identify individual Snl1-copurifying bands, mass spectrometry was used. This analysis assigned all the bands as large (L) and small (S) ribosomal subunit proteins (Figure 3-2) (Table 3-1). To compare this novel interaction and to identify whether substoichiometric amounts of

ribosomes might be copurifying with the other NEFs, I performed a Western blot using Rpl8, a large subunit ribosomal protein. This verified that the interaction with the ribosome was specific to FL-Snl1 and Snl1ΔN and no interaction was detected with the other NEFs. This is the first report of an interaction between a BAG domain-containing protein and the assembled 80S ribosome. These results also indicate that ribosome binding by Snl1 is independent of its attachment to the ER/nuclear membrane.

Differential binding patterns of Snl1

The ribosome-associated Hsp70, Ssb has been shown to continue associating with ribosomes after a high-salt wash procedure (1 M KCl), suggestive of a tight protein-protein interaction. I sought to determine if Snl1ΔN was an integral part of the ribosome complex or a peripheral ribosome-associated protein by subjecting Snl1ΔN-ribosome complexes to various concentrations of KCl before performing the immunoprecipitation using M2 resin. I observed an association of Snl1ΔN with Hsp70 at all KCl concentrations tested (Figure 3-3). In contrast, the interaction of Sn1ΔN with the ribosome was drastically reduced at KCl concentrations above 0.2 M. Ribosome binding was confirmed by an immunoblot for Rpl3, another large-subunit ribosomal protein. These results show that Snl1ΔN is peripherally associated with ribosomes and suggest that the Snl1ΔN-ribosome interaction is independent of the previously described Snl1ΔN-Hsp70 binding.

FIGURE 3-1. Structure of the BAG domain of Bag-1 with Hsc70 NBD. Co-crystal structure of the BAG domain of human Bag-1 with bovine Hsc70 ATPase domain (NBD) reveals a three-helix bundle where helices 2 and 3 contact Hsc70. The two lobes of the NBD are sub-divided into IA/IB and IIA/IIB. PDB ID:1HX1. (140)

FIGURE 3-1. Structure of the BAG domain of Bag-1 with Hsc70 NBD

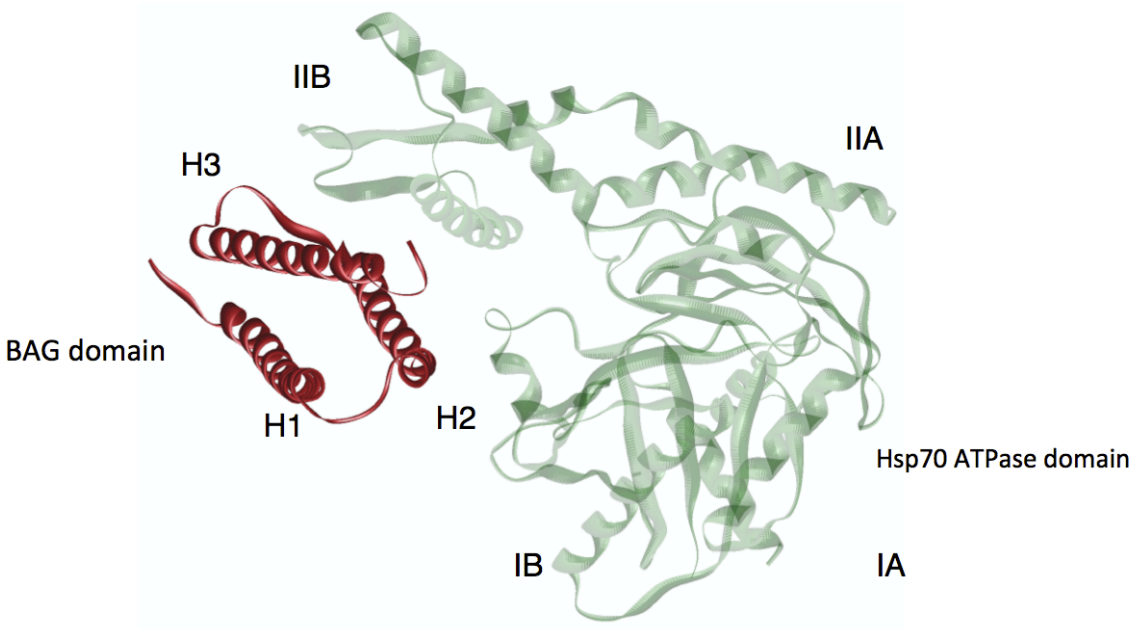

FIGURE 3-2. Snl1 interacts with ribosomal proteins. Amino- or carboxyl-terminally FLAG (F)-tagged NEFs were immunoprecipitated from wild type (BY4741) whole-cell lysates. Immunoblot analysis was used to detect interacting proteins using anti-Ssa, anti-Ssb and anti-Rpl8 antisera. Red letters represent ribosomal proteins of the large (L) and small (S) subunit that were identified by using mass spectrometry. EV, empty vector; CBB, Coomassie brilliant blue; IP, FLAG immunoprecipitation; IB, immunoblot of the whole-cell lysate.

FIGURE 3-2. Snl1 interacts with ribosomal proteins

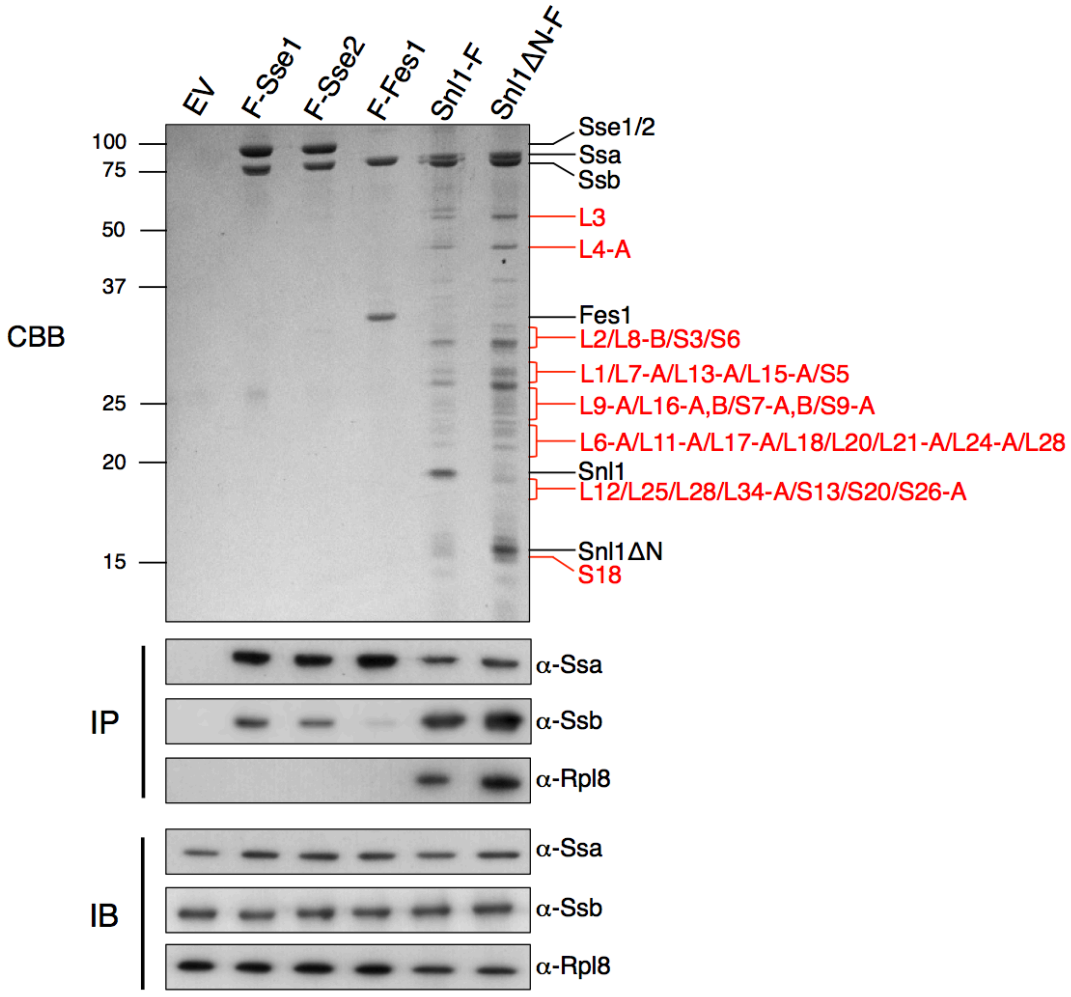

TABLE 3-1. List of Snl1-binding proteins

Protein Score	S. cerevisiae Accession #	Protein mass	Protein description
149	RL3_YEAST	43730	60S ribosomal protein L3
163	RL4A_YEAST	39068	60S ribosomal protein L4-A
183	RL8B_YEAST	28151	60S ribosomal protein L8-B
329	RL7A_YEAST	27621	60S ribosomal protein L7-A
159	RPL2_YEAST	27392	60S ribosomal protein L2
181	RS6_YEAST	27037	40S ribosomal protein S6
94	RS3_YEAST	26543	40S ribosomal protein S3
270	RS5_YEAST	25080	40S ribosomal protein S5
149	RL1_YEAST	24698	60S ribosomal protein L1
44	RL15A_YEAST	24464	60S ribosomal protein L15-A
57	RL13A_YEAST	22540	60S ribosomal protein L13-A
169	RS9A_YEAST	22429	40S ribosomal protein S9-A
205	RL16B_YEAST	22235	60S ribosomal protein L16-B
197	RL16A_YEAST	22187	60S ribosomal protein L16-A
60	RS7B_YEAST	21621	40S ribosomal protein S7-B
398	RL9A_YEAST	21613	60S ribosomal protein L9-A
176	RS7A_YEAST	21609	40S ribosomal protein S7-A
180	RL18_YEAST	20608	60S ribosomal protein L18
36	RL17A_YEAST	20537	60S ribosomal protein L17-A
120	RL20_YEAST	20424	60S ribosomal protein L20
192	RL6A_YEAST	19949	60S ribosomal protein L6-A
172	RL11A_YEAST	19764	60S ribosomal protein L11-A
159	RL21A_YEAST	18288	60S ribosomal protein L21-A
202	RL12_YEAST	17869	60S ribosomal protein L12
96	RL24A_YEAST	17603	60S ribosomal protein L24-A
70	RS18_YEAST	17084	60S ribosomal protein S18
271	RS13_YEAST	17018	40S ribosomal protein S13
25	RL28_YEAST	16712	60S ribosomal protein L28
25	RL28_YEAST	16712	60S ribosomal protein L28
223	RL28_YEAST	16712	60S ribosomal protein L28
124	RL25_YEAST	15748	60S ribosomal protein L25
102	RS20_YEAST	13899	40S ribosomal protein S20
48	RL34A_YEAST	13859	60S ribosomal protein L34-A
70	RS26A_YEAST	13724	40S ribosomal protein S26-A

Proteins reported at <0.05 significance

FIGURE 3-3. Snl1ΔN interaction with ribosomal proteins is salt sensitive. Whole-cell lysate from wild-type BY4741 expressing Snl1ΔN-FLAG was split equally and incubated on ice for 15 min with the indicated concentrations of KCl. Snl1ΔN was immunoprecipitated, and interacting proteins were separated on a 15% SDS-PAGE gel. Rpl3 and Snl1ΔN (anti-FLAG antibody) were detected by immunoblot analysis. Distinct large subunit ribosomal proteins are indicated. CBB, Coomassie brilliant blue; IP, FLAG immunoprecipitation; IB, immunoblot of the whole-cell lysate.

FIGURE 3-3. Snl1ΔN interaction with ribosomal proteins is salt sensitive

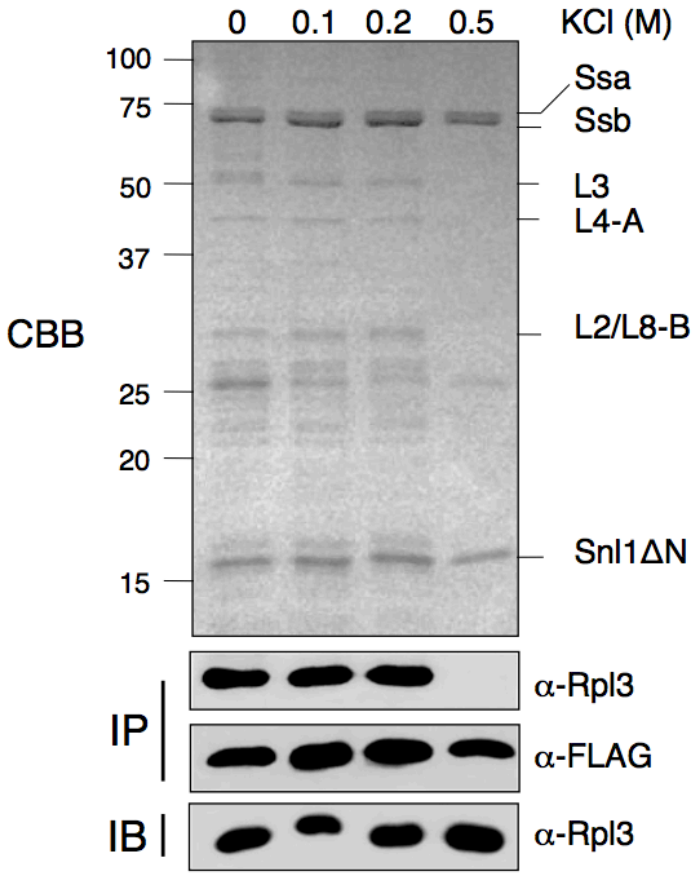

Interaction of Snl1 with the ribosome is Hsp70 independent

It has been previously shown that the cytosolic Hsp70, Ssb is associated with ribosomes (108). Because my results show Snl1 to also associate with Ssb, I sought to determine whether ribosome copurification with Snl1 was dependent on Ssb. Since Ssb1 and Ssb2 are not essential, I first determined whether the Snl1ΔN-ribosome interactions occurred in a strain that lacks these two Hsp70 genes. Snl1ΔN-FLAG was expressed and isolated from a wild type and *ssb1*Δ*ssb2*Δ strain. As shown in (Figure 3-4,A), I found that Snl1 remained associated with the ribosome complex in the *ssb1*Δ*ssb2*Δ strain and the interaction was verified by immunoblotting for Rpl3.

To confirm this result, I took a parallel approach and took advantage of mutation shown previously to drastically reduce binding to Ssa and Ssb by constructing a FLAG-tagged allele of *SNL1* containing alanine substitutions at two residues critical for Hsp70 interaction (Snl1ΔN-FE112A, R141A) (139). To determine if Snl1ΔN interacted with the ribosome in the absence of Hsp70 binding, I immunoprecipitated the mutant variant and the isogenic wild type as a control. In line with previous findings, this mutant exhibited considerably reduced binding to both Ssa and Ssb *in vivo*, as shown by the respective immunoblots (Figure 3-4,B). In contrast, binding to ribosomes, as assessed by an anti-Rpl3 immunoblot was unaffected. Taken together, these two independent approaches show that Hsp70 does not mediate the association of Snl1ΔN with the ribosome.

The ribosome and Hsp70 exhibit non-competitive binding to Snl1

The data presented above shows that Snl1 is associated with ribosomes and this association does not require Hsp70. However, this does not establish whether this binding occurs in a novel or shared binding interface on Snl1. To investigate this question, I

FIGURE 3-4. Snl1ΔN interacts with the ribosome independently of Hsp70. (A) Whole-cell lysates from a *ssb1Δssb2Δ* strain (Δ) or its isogenic wild-type (WT) (DS10) strain expressing either the empty vector (EV) or Snl1ΔN were subjected to FLAG immunoprecipitation (IP). Stably produced proteins were detected with anti-Ssb, anti-Rpl3 and anti-FLAG antisera. (B) FLAG-tagged Snl1ΔN, either wild-type or E112A,R141A mutant, was immunoprecipitated from wild-type (BY4741) cells. Immunoblot analysis was used to detect stably produced protein with anti-Ssa, anti-Ssb, anti-Rpl3 and anti-FLAG antisera. IB, immunoblot of the whole-cell lysate.

FIGURE 3-4. Snl1ΔN interacts with the ribosome independently of Hsp70

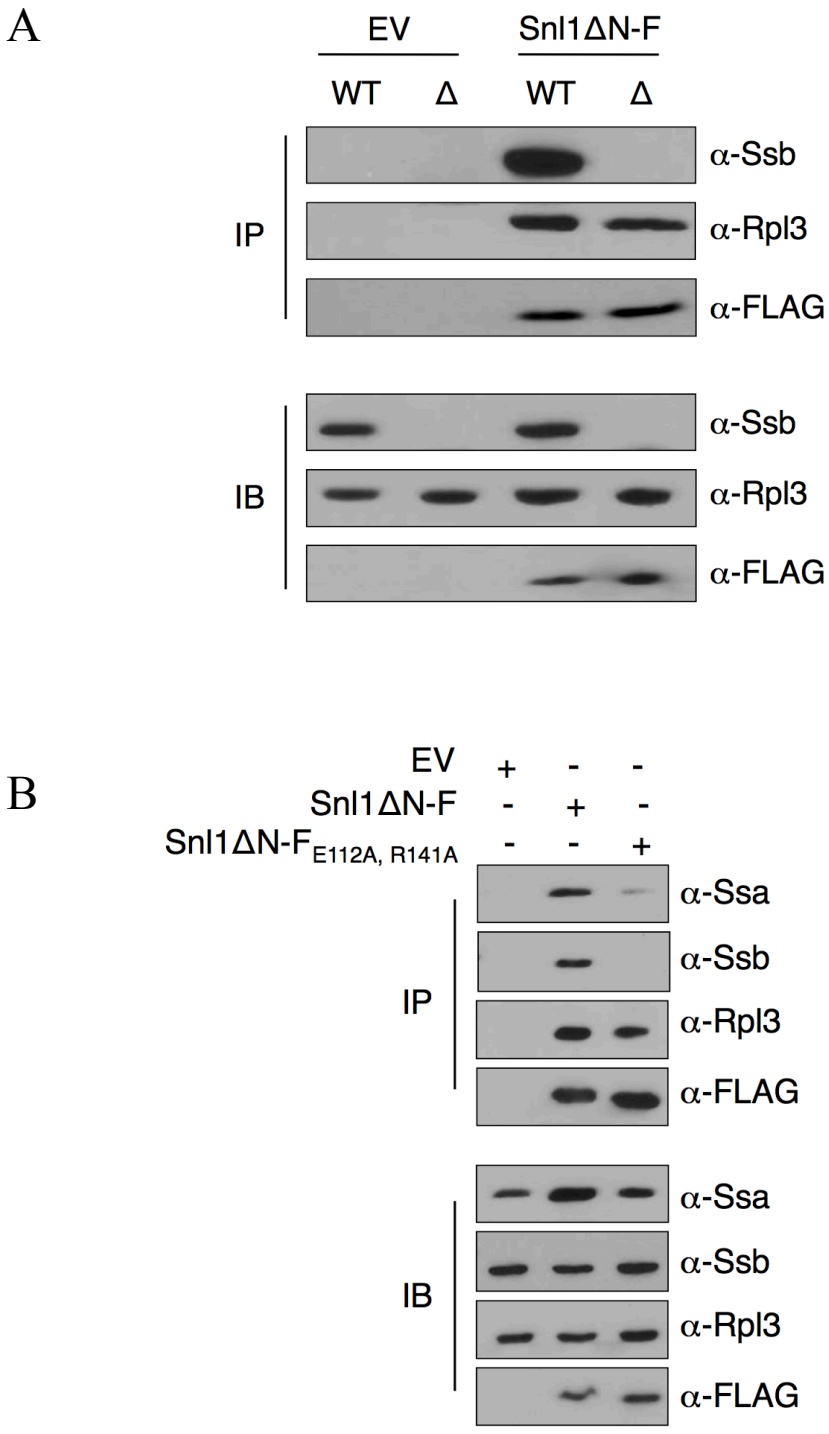

performed a competitive binding experiment using purified Hsp70, Ssb (Figure 3-5,A). Snl1ΔN-ribosome-Hsp70 complexes were first isolated by using M2 resin as described previously. This complex was mixed with 1 mg/ml recombinant His_6-Ssb or buffer alone and then washed and reisolated prior to recovery by elution. (Figure 3-5,B) shows that Snl1ΔN immunoprecipitated from cell extracts copurified with endogenous Ssb and the ribosome. On the addition of exogenous His_6-Ssb, the binding of endogenous Ssb to Snl1ΔN was outcompeted, as expected and seen by the slower migration likely caused by the His_6 tag. Interestingly, the interaction with the ribosome remained intact. This finding suggests that Hsp70 and the ribosome interact with Snl1 in a noncompetitive manner, consistent with the presence of two distinct and independent binding sites on Snl1.

Snl1 binds to the 60S ribosomal subunit

Mass spectrometric analysis of the multiple bands that copurified with Snl1 and Snl1ΔN showed the presence of protein components of both the large and small ribosomal subunits. To determine which subunit might be interacting directly with Snl1, I treated the Snl1ΔN-ribosome-Hsp70 copurified complex with EDTA. EDTA treatment is a well-characterized method used to separate the two subunits of the ribosome by chelating the Mg^{2+} ions required for the 60S-40S subunit assembly. Snl1ΔN-FLAG was expressed in and immunoprecipitated from a yeast strain containing a chromosomally epitope-tagged small subunit of the ribosome (Rps6B-3XHA), which allowed for the detection of the 40S component. Protein complexes were incubated in the absence or presence of 40 mM EDTA and washed to remove unbound proteins. Bound proteins were then eluted. I found a dramatic decrease in the amount of the 40S subunit co-eluting with Snl1ΔN-FLAG, with very little change in the binding capacity of Snl1ΔN with Rpl8 (Figure 3-6). This result can

FIGURE 3-5. The ribosome and Hsp70 exhibit non-competitive binding to Snl1ΔN. (A) Schematic of binding between Snl1 with either the ribosome and/or Hsp70. If the binding of Hsp70 and ribosome with Snl1 is competitive, addition of exogenous Ssb (pink with H6 attached) will titrate Snl1 away from the ribosome. (upper arrow). Non-competitive binding will result in continued binding between Snl1 and the ribosome when exogenous Ssb is added. (lower arrow). (B) Snl1ΔN-FLAG expressed in BY4741 cells was immobilized onto M2 FLAG resin and incubated with His_6-Ssb (1 mg/ml) for 30 min on ice, followed by another round of immunoprecipitation. Bound proteins were eluted as described in Materials and Methods, and immunoblot analysis was performed to detect interacting proteins with anti-Rpl3 and anti-FLAG antisera. The Ssb antibody detected endogenous (bottom band) and recombinant (bottom band) Ssb present in the fractions.

FIGURE 3-5. The ribosome and Hsp70 exhibit non-competitive binding to Snl1ΔN

A

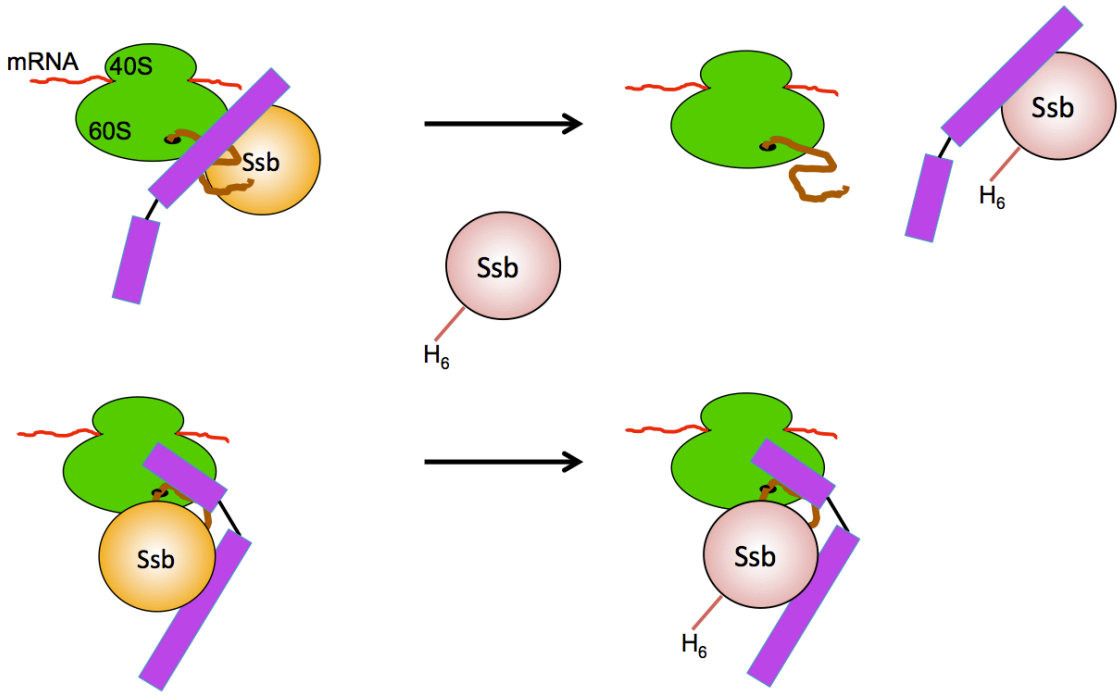

B

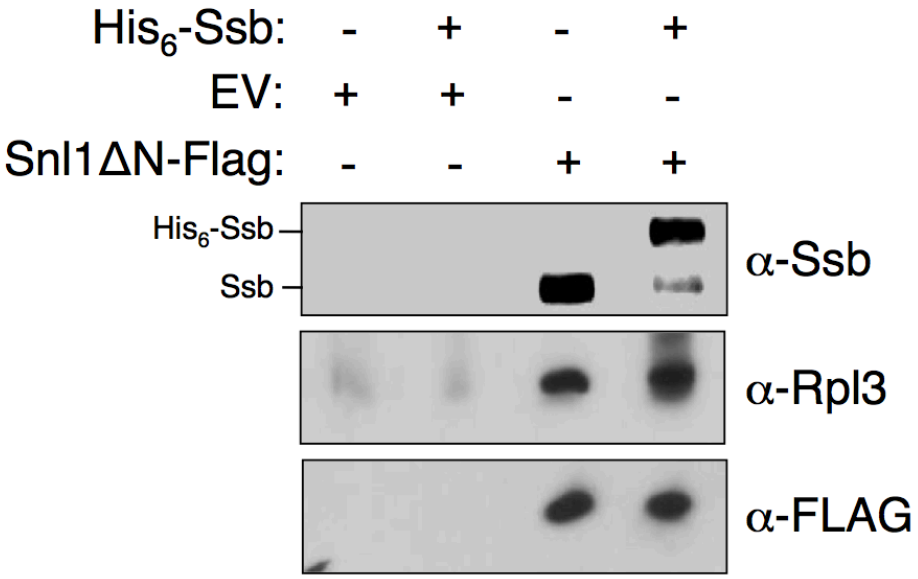

be interpreted to indicate that Snl1 predominantly binds to the large (60S) ribosomal subunit.

Identification of the ribosome binding site in Snl1

Results from the competitive binding experiment demonstrated that the ribosome binding site within Snl1 was distinct from its Hsp70 binding site. Based on the known BAG domain structure of protein Bag-1, the majority of Hsp70 contacts are localized to helices 2 and 3. Because my data suggest that Snl1 can concomitantly bind both Hsp70 and the ribosome, steric hindrance would likely prevent both binding sites being located within these two helices. To identify the ribosome binding site in Snl1, I constructed a series of amino-terminal truncation mutants by sequentially deleting 10 residues starting at the beginning of putative helix 1 of Snl1 (Figure 3-7,A). All constructs were individually expressed in yeast cells and FLAG immunoprecipitated as described in Materials and Methods. With the exception of the Δ80 mutant, all the truncation mutant proteins were stably expressed. In addition, all these proteins except Δ80 mutant retained binding to Ssa and Ssb, as determined by Coomassie-dye staining, suggesting that they were all properly folded (Figure 3-7,B). Strikingly, I noticed that the ribosome interaction was lost in the Δ60 and Δ70 truncation mutants, as indicated by Coomassie-dye staining and the immunoblot for Rpl3. These results suggested that residues required for ribosome binding were found between residues 50 and 60. An evaluation of the amino acids in this region revealed a concentration of five lysine residues (residues 52 to 58), which would be expected to provide a positively charged binding interface, not uncommon in ribosome binding proteins (Figure 3-7,A). To directly determine if this region was indeed responsible for ribosome binding, I constructed a mutant of Snl1ΔN in which the five lysine residues were replaced with an uncharged residue, alanine, which I have named Snl1ΔN (5KA). I separately immunoprecipitated this mutant

FIGURE 3-6. Snl1ΔN binds to the 60S ribosomal subunit. Snl1ΔN-FLAG expressed in an Rps6B-3XHA strain was immobilized on M2 FLAG resin. The resin was equally split and treated with and without 40 mM EDTA for 30 min on ice to dissociate intact ribosomes. Bound proteins were eluted as described in Materials and Methods, and immunoblot analysis was performed to detect proteins with anti-HA, anti-Rpl8, and anti-FLAG antisera.

FIGURE 3-6. Snl1ΔN binds to the 60S ribosomal subunit

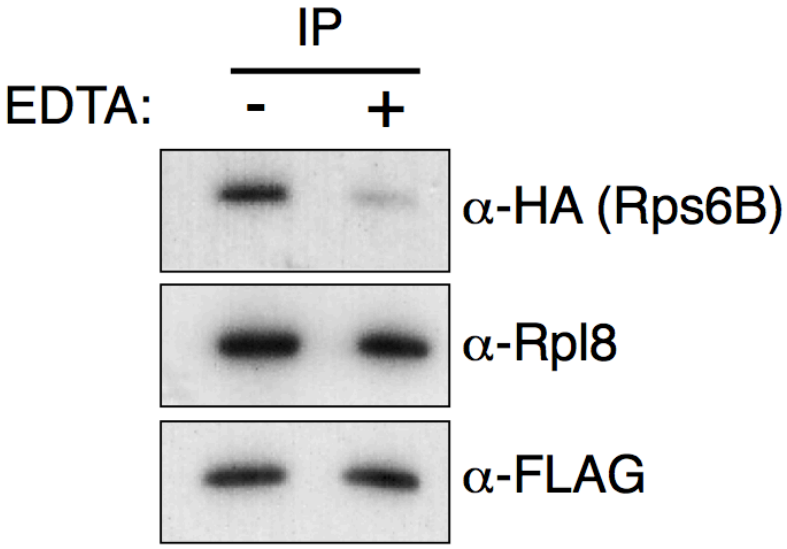

FIGURE 3-7. Identification of the ribosome-binding site in Snl1. (A) N-terminal truncations within putative helix 1 of the Snl1 BAG domain are depicted. The lysine-rich region between resides 50 and 60 in Snl1 are highlighted, and the residue changes are indicated. TM, putative transmembrane domain. (B) FLAG (F)-tagged Snl1ΔN truncations were immunoprecipitated from the wild-type (BY4741) whole-cell lysate. Immunoblot analysis was used to detect ribosomal proteins with anti-Rpl3 antisera. CBB, Coomassie brilliant blue; IP, FLAG immunoprecipitation; IB, immunoblot of the whole-cell lysate.

FIGURE 3-7. Identification of the ribosome-binding site in Snl1

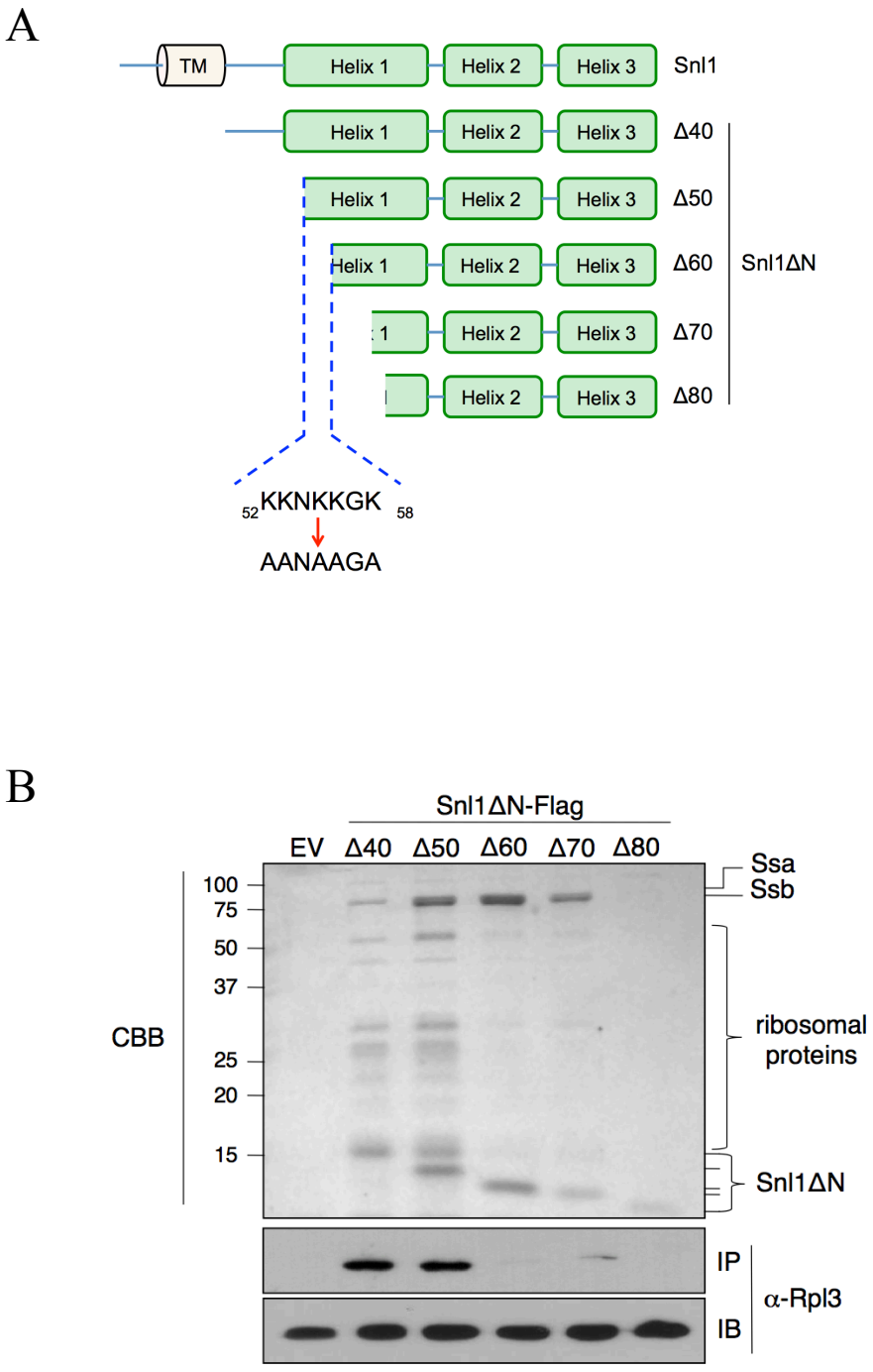

and Snl1ΔN from yeast cell extracts to assess ribosome association. As seen by Coomassie-dye staining and by immunoblotting, the 5KA mutant exhibited a drastic reduction in ribosome binding (Figure 3-8). In contrast, the interactions with Ssa and Ssb remained unchanged. These results demonstrate that this positively charged region within Snl1 is specifically required for ribosome association but not Hsp70 binding.

Conservation of ribosome association in a fungal Bag-1 homolog

The identification of a specific sequence within Snl1 required for ribosome binding prompted me to ask whether this was a conserved or unique feature of Bag-1 homologs. As shown in (Figure 3-9), putative Bag-1 homologs could be identified in a range of eukaryotic organisms, many of which possess positively charged regions in the amino terminus of the predicted BAG domain. Interestingly, the genome of the human pathogenic fungus *Candida albicans* encodes a single predicted protein (orf19.997) that bears a high level of sequence conservation (32% identity and 59% similarity) with Snl1. This predicted protein also contains a putative N-terminal transmembrane region and a domain homologous to the BAG domain with a lysine-rich region in putative helix 1 (Figure 3-10,A). This is in contrast to the small isoform of the mammalian Bag-1 protein (Bag-1S), which, despite significant sequence homology (25% identity), lacks both a transmembrane domain and a lysine-rich region. This led me to speculate that the *C. albicans* Snl1 (CaSnl1) homolog (i) would localize to the ER and (ii) would associate with ribosomes. The next two experiments were performed to test these two predictions.

To test if CaSnl1 associates with ribosomes, I generated two truncated forms of CaSnl1 from *C. albicans* strain SC5314 and expressed them in *S. cerevisiae* cells. CaSnl1Δ91 lacks the first 90 amino acids of the proteins including the predicted transmembrane domain but

FIGURE 3-8. Snl1ΔN interacts with the ribosome via a lysine-rich region. FLAG-tagged Snl1ΔN, either the wild type (WT) or the 5KA mutant, where five lysine residues between residues 50 and 60 were changed to alanine, was immunoprecipitated from wild-type BY4741 cells, and immunoblot analysis was used to detect stably produced proteins with anti-Rpl3 antisera. IP, FLAG immunoprecipitation; IB, immunoblot of the whole-cell lysate.

FIGURE 3-8. Snl1ΔN interacts with the ribosome via a lysine-rich region

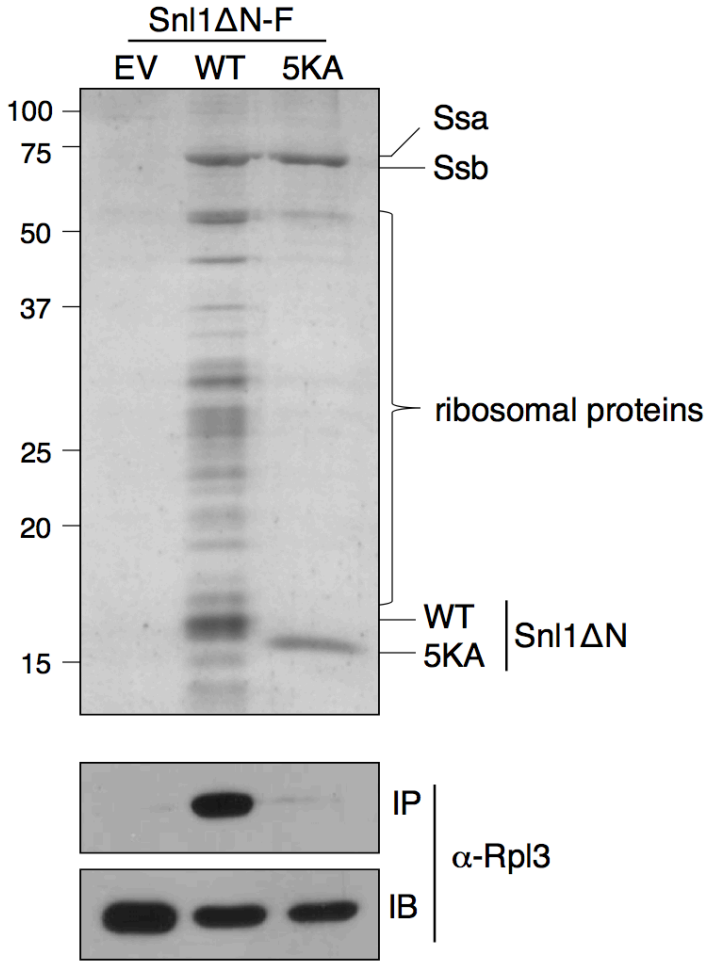

contains the lysine-rich region. CaSnl1Δ103 lacks both regions (Figure 3-10,A). A murine Bag-1 cDNA was also expressed in yeast to determine whether the absence of the lysine-rich region in a distinct Bag-1 homolog would preclude ribosome interactions. I observed that CaSnl1 exhibited the same characteristics for ribosome binding as Snl1, with both variants binding Hsp70 but only the Δ91 construct binding ribosomes (Figure 3-10,C). In addition, murine Bag-1 associated with Hsp70 demonstrating the high level of conservation within the Hsp70 binding domain, but failed to interact with yeast ribosomes. These experiments demonstrate that a lysine-rich region within putative helix 1 of the BAG domain mediates interactions with the assembled ribosomes in two closely related fungi, whereas this interaction is not conserved in Bag-1S in mammalian cells.

To test the prediction that CaSnl1 would localize to the ER, I carboxy-terminally tagged one copy of the gene in *C. albicans* with GFP using a previously described method (44). Due to the limited availability of fluorescent organellar localization markers in this organism, I stained live cell nuclei with the DNA-intercalating Hoechst dye to identify the nucleus. Untagged control cell exhibited discrete nuclear staining, with no background signal in the green channel. In contrast, CaSnl1-GFP was clearly seen to localize around the nucleus and at the cell periphery, consistent with known perinuclear and cortical ER localization patterns and with previous reports of the localization of Snl1 in *S. cerevisiae* (Figure 3-10,B).

Synergistic growth assay between *snl1*Δ and strains lacking ribosome-associated chaperones

Because no detectable phenotype has been assigned to *snl1*Δ cells, I sought to determine if the loss of *SNL1* would have a synthetic growth defect in strains that lacked

FIGURE 3-9. Cartoon sequence alignment of BAG domain-containing proteins in select organisms. Mm; *Mus musculus*, Sp; *Schizosaccharomyces pombe*, Ca; *Candida albicans*, Sc; *Saccharomyces cerevisiae*. Putative transmembrane regions (TM) are shown. Putative positively charged-rich ribosome binding residues are shown in the boxes. Numbers represent the amino acid length of each protein.

FIGURE 3-9. Cartoon sequence alignment of BAG domain-containing proteins in select organisms.

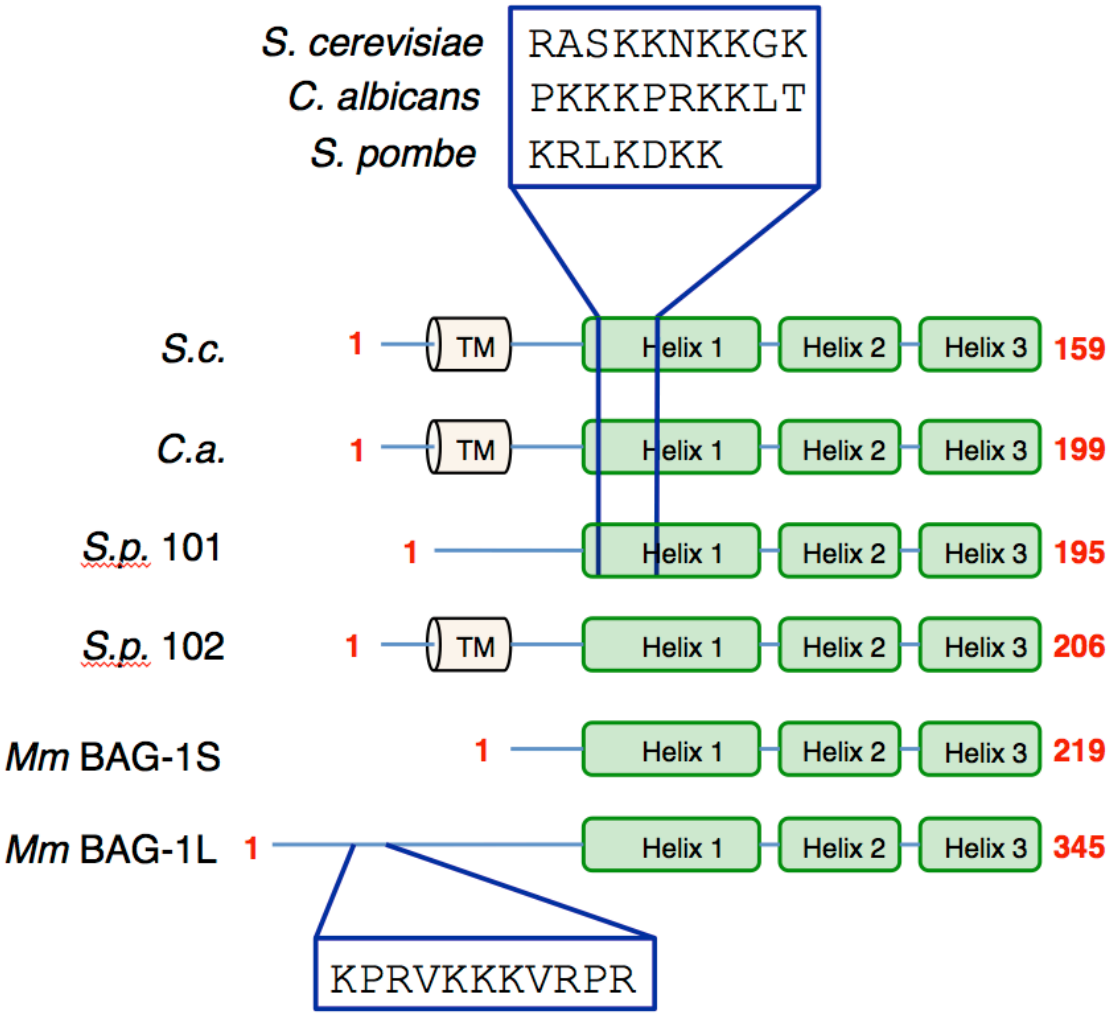

FIGURE 3-10. Ribosome association is conserved in the only BAG domain-containing protein of *Candida albicans*. (A) Illustration of the sequence alignment of BAG domain-containing proteins of *Saccharomyces cerevisiae* (*Sc* Snl1) and *Candida albicans* (*Ca* Snl1) showing the lysine-rich region at the amino terminus of putative helix 1 and the predicted transmembrane (TM) domains. Murine Bag-1 (*Mm* BAG-1) lacks both a TM domain and a lysine-rich region. *Mm*, *Mus musculus*. (B) Localization of the chromosomally tagged *C. albicans* Snl1 homolog (CaSnl1-GFP) in wild-type *C. albicans* strain SC5314 was determined by fluorescence microscopy. Cells were stained with Hoechst 33342 dye to facilitate the assessment of perinuclear ER localization. (C) Snl1ΔN-FLAG from *S. cerevisiae* and the corresponding truncations in the *C. albicans* Snl1 homolog and the mammalian Bag-1 protein were expressed and immunoprecipitated from the wild-type (BY4741) yeast whole-cell lysate. Proteins were separated on a 15% SDS-PAGE gel, and immunoblot analysis was used to detect ribosomal proteins with anti-Rpl8 antisera. CBB, Coomassie brilliant blue; IP, FLAG immunoprecipitation; IB, immunoblot of the whole-cell lysate.

FIGURE 3-10. Ribosome association is conserved in the only BAG domain-containing protein of *Candida albicans*.

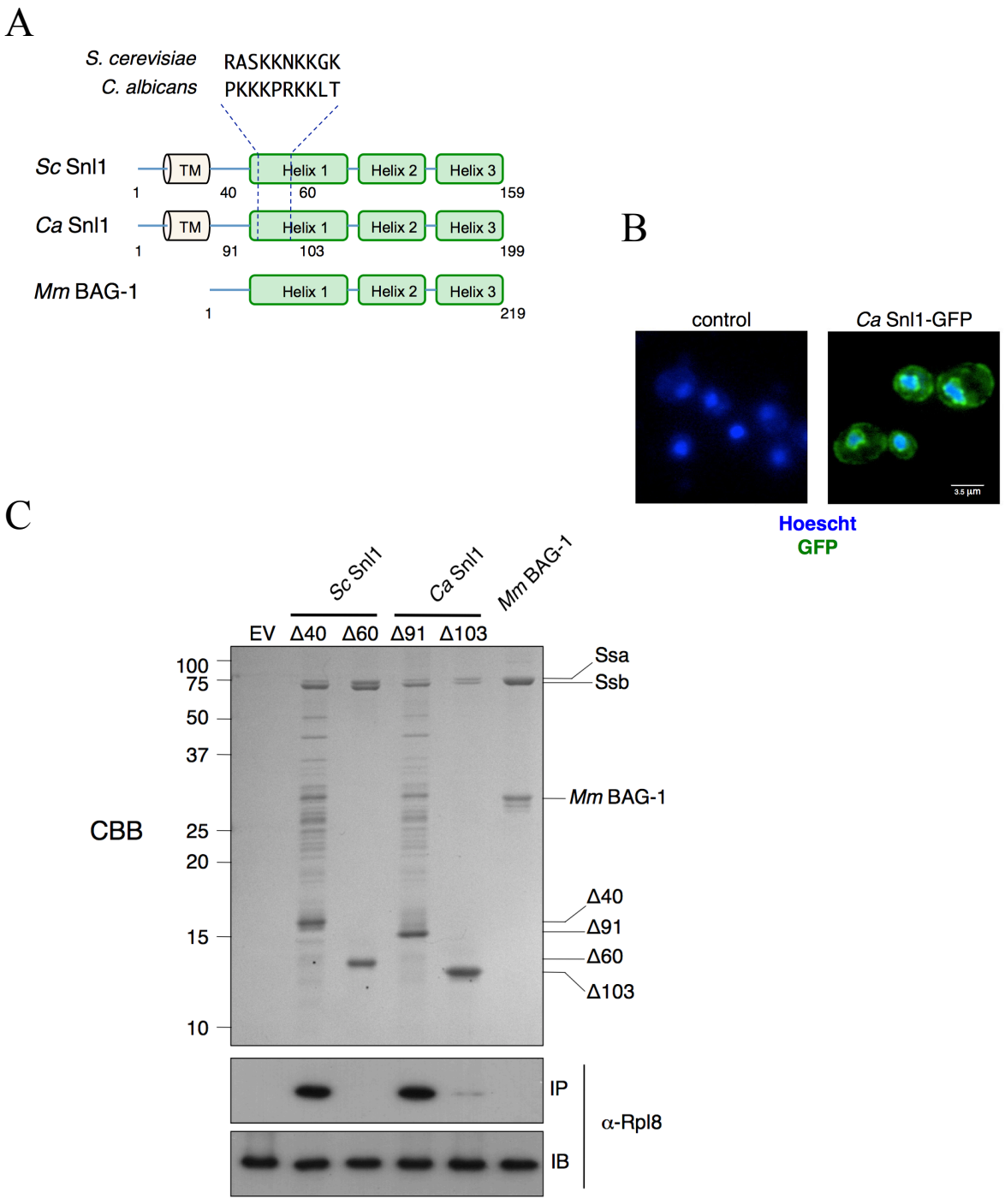

known ribosome associated chaperones. Deletion of *SNL1* in combination with the two proteins that comprise the ribosome associated complex (RAC), *SSZ1* and *ZUO1* caused no detectable growth impairment at normal temperature and heat stress of 39 °C (Figure 3-11,A).

Deletion of *SNL1* from strains lacking individual genes of the nascent chain associated complex (NAC), *EGD1*, *BTT1* and *EGD2* also caused no detectable phenotypes at both temperatures tested (Figure 3-11,B).

I next tested the combined loss of *SNL1* in the strain lacking both ribosome associated Hsp70 chaperones, Ssb1 and Ssb2 (*ssb1*Δ*ssb2*Δ). I was able to corroborate previous reports that cells lacking both *SSB* genes showed slower growth below 30 °C compared to the wild type cells as seen by the smaller colony size and growth defects of the double mutant, whereas cells lacking *SNL1* showed no growth defect. Growth was not further impaired in the *snl1*Δ*ssb1*Δ*ssb2*Δ at these temperatures (Figure 3-11,C). At temperature stress conditions, a slight synthetic growth defect is seen in the triple mutant at 37 °C and 39 °C. These results suggest that there is no genetic interaction between genes encoding *SNL1* and the above mentioned ribosome associated chaperone genes and indicates that they may not be working in parallel or in partly overlapping pathways at the conditions tested. However, it is possible that during temperature stress, Snl1 and the ribosome associated Ssb may be involved together in *de novo* protein folding.

Synergistic growth assay between *snl1*Δ and genes involved in translocation across the ER membrane

Full length Snl1 is attached to the ER membrane and as a result could be involved with protein translocation across the ER. To investigate this, I combined knockout mutations

FIGURE 3-11. s*nl1*Δ cells show no detectable synthetic growth phenotypes with RACΔ, NACΔ and SSBΔ strains. (A, B) Wild-type (WT, BY4741) and indicated single and double-deletion cells were serially diluted and spotted onto plates containing YPD medium and incubated at the indicated temperatures for 2 days. (C) Wild-type (WT, DS10) and indicated mutants in the same genetic background were serially diluted and spotted onto plates as described above.

FIGURE 3-11. s*nl1*Δ cells show no detectable synthetic growth phenotypes with RACΔ, NACΔ and SSBΔ strains.

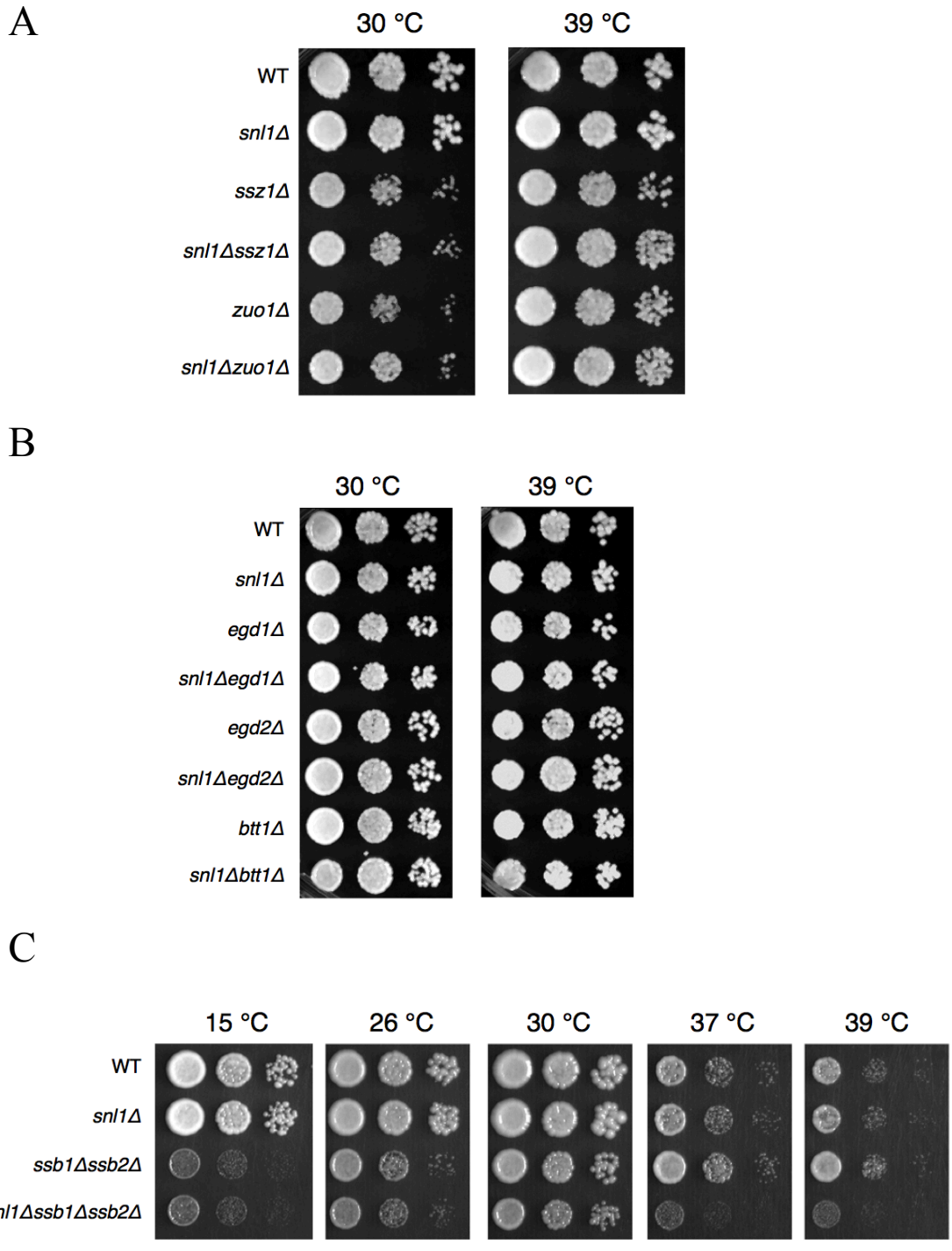

of *SNL1* with deletions of non-essential subunits of the ER translocation pore, *SBH1*, *SBH2*, *SSH1*, *SEC66* and *SEC72*. No detectable growth phenotypes were seen at both temperatures tested (Figure 3-12,A). The combined deletion of *SNL1* from a *sec61*Δ strain complemented with a vector containing a wild type copy of *SEC61* or a *SEC61* temperature sensitive allele showed no discernable growth impairment suggesting that Snl1 may not be working in parallel with these genes at the conditions tested (Figure 3-12,B).

Synergistic growth assay between *snl1*Δ and genes previously identified as synthetic in a genomic screen

As seen in (Figure 3-13), I was unable to recapitulate the synthetic phenotypes reported for *SNL1* by a recently published high-throughput whole-genome screen (24). It is possible that this may be the result of false positives that may have arisen in the screen and will require further testing using conditions other than temperature.

FIGURE 3-12. s*nl1*Δ cells show no detectable synthetic growth phenotypes with genes involved in translocation across the ER membrane. (A) Wild-type (WT, BY4741) and indicated single and double-deletion cells were serially diluted and spotted onto plates containing YPD medium and incubated at the indicated temperatures for 2 days. (B) *SNL1* was deleted from a strain lacking *SEC61* and complemented with a vector containing either a wild-type copy of *SEC61* (p*sec61-WT*) or a *SEC61* temperature sensitive allele (p*sec61-mutTS*). Cells were serially diluted and spotted onto plates containing YPD medium and incubated at the indicated temperatures for 2 days.

FIGURE 3-12. s*nl1*Δ cells show no detectable synthetic growth phenotypes with genes involved in translocation across the ER membrane

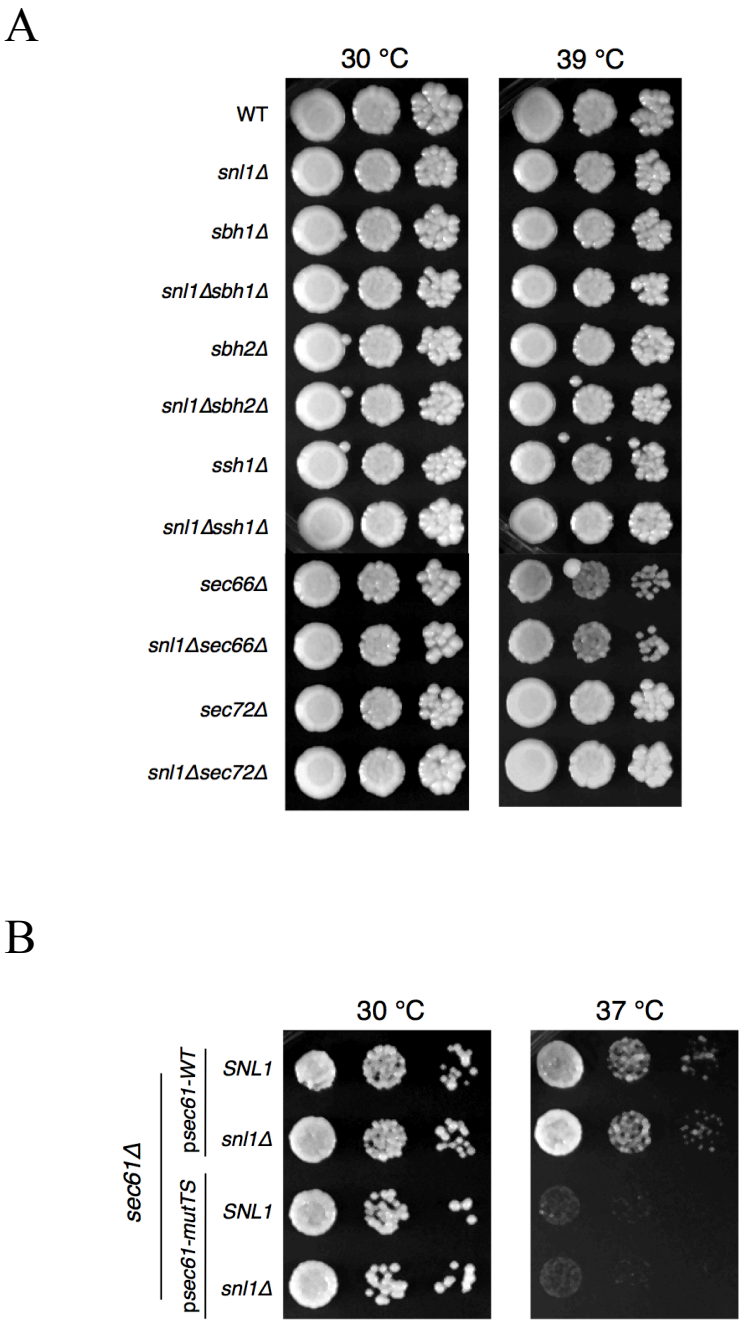

FIGURE 3-13. s*nl1*Δ cells show no detectable synthetic growth phenotypes with genes previously identified as synthetic in a genomic screen. Wild-type (WT, BY4741) and indicated single and double-deletion cells were serially diluted and spotted onto plates containing YPD medium and incubated at the indicated temperatures for 2 days.

FIGURE 3-13. s*nl1*Δ cells show no detectable synthetic growth phenotypes with genes previously identified as synthetic in a genomic screen

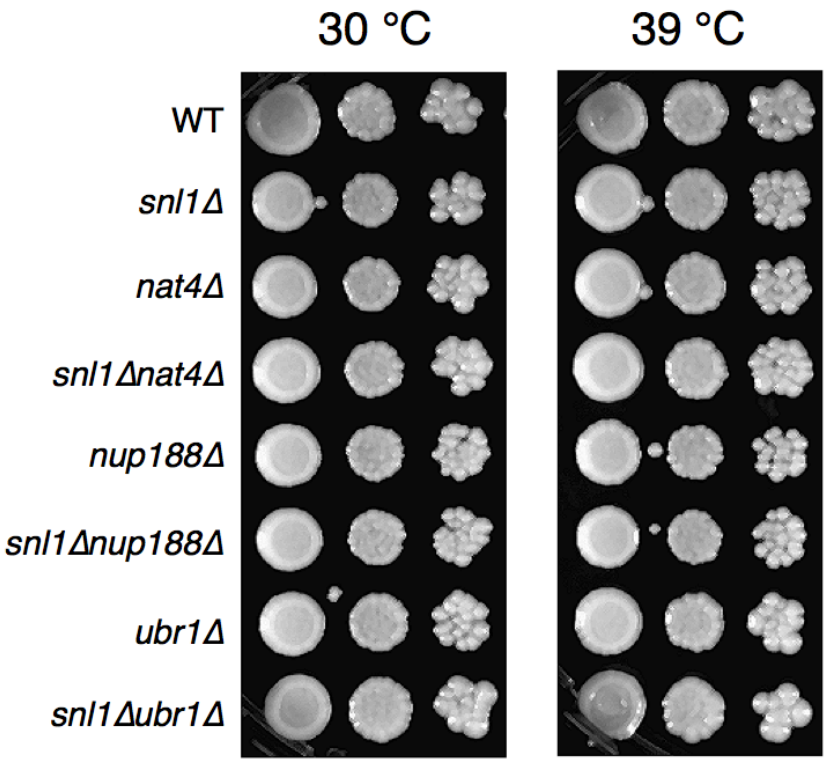

TABLE 3-2 Genes exhibiting correlation with *SNL1* expression identified via SPELL

Rank	Gene	Common name	Score
1	YMR260C	TIF11	2.4
2	YIL008W	URM1	2.4
3	YHR013C	ARD1	2.4
4	YFR001W	LOC1	2.4
5	YPR187W	RPO26	2.3
6	YIL052C	RPL34B	2.3
7	YBR154C	RPB5	2.3
8	YER131W	RPS26B	2.3
9	YIL020C	HIS6	2.3
10	YMR194W	RPL36A	2.2
11	YBR252W	DUT1	2.2
12	YNL162W	RPL42A	2.2
13	YDL191W	RPL35A	2.2
14	YHR010W	RPL27A	2.2
15	YOR210W	RPB10	2.2
16	YGL031C	RPL24A	2.2
17	YOR276W	CAF20	2.2
18	YIL027C	KRE27	2.2
19	YJL124C	LSM1	2.2
20	YLR388W	RPS29A	2.2
21	YDR086C	SSS1	2.2
22	YOL139C	CDC33	2.2
23	YKR094C	RPL40B	2.2
24	YDL166C	FAP7	2.2
25	YGL232W	TAN1	2.1
26	YGR148C	RPL24B	2.1
27	YJL179W	PFD1	2.1
28	YGR195W	SKI6	2.1
29	YML094W	GIM5	2.1
30	YOL077C	BRX1	2.1
31	YGL070C	RPB9	2.1
32	YDR429C	TIF35	2.1
33	YIL021W	RPB3	2.1
34	YGR118W	RPS23A	2.1
35	YGR105W	VMA21	2.1
36	YDR045C	RPC11	2.1
37	YLR333C	RPS25B	2.1
38	YDR471W	RPL27B	2.1
39	YDR339C	FCF1	2.1
40	YDL075W	RPL31A	2.1

41	YHR143W-A	RPC10	2.1
42	YDL092W	SRP14	2.1
43	YDR454C	GUK1	2.1
44	YGR085C	RPL11B	2.1
45	YMR242C	RPL20A	2.1
46	YOR293W	RPS10A	2.1
47	YER074W	RPS24A	2.1
48	YLR344W	RPL26A	2.1
49	YGR081C	SLX9	2.1
50	YLR325C	RPL38	2.1

*Correlation score is calculated for each gene in the genome based on correlation with the query gene *SNL1* using the default settings of the SPELL server. (http://spell.yeastgenome.org/) Only the top 50 hits are shown.

3C. DISCUSSION

In this chapter, I report for the first time a novel interaction between the *S. cerevisiae* BAG domain-containing protein Snl1 and the ribosome and show that this interaction is conserved in the pathogenic fungus *Candida albicans* Snl1/Bag-1 homolog implying a conservation of function. Unlike the other cytosolic NEFs in yeast, Snl1 is unique in being the only known membrane-anchored Hsp70 NEF, and I found that ribosomes associate with both the membrane-bound and soluble truncated Snl1ΔN isoforms. Thus, ER attachment does not block the ribosome-binding site and as a corollary, the localization of Snl1 at the membrane does not govern ribosome binding. As seen in Figure 3-2, all four NEFs readily associated with Hsp70 but Snl1 was unique amongst them in ribosome association.

The ribosome associated Hsp70, Ssb is unique to fungi, compared to other cell types and functions to fold nascent chains as they emerge from the ribosome exit tunnel. The ability of Snl1 to interact with both Ssb and the ribosome suggested that this ternary complex was Ssb-dependent. However, four separate results show that the interaction of Snl1 with the ribosome is independent of its association with Hsp70 and its function as an NEF. First, the strain lacking *SSB1* and *SSB2* had no effect on Snl1-ribosome interaction. Second, a previously characterized mutant of *SNL1* having amino acid changes that abolish Hsp70 interaction still retained ribosome binding. Third, the salt sensitivities of Snl1 with Hsp70 (salt resistant) and Snl1 with ribosomes (salt sensitive) were different. Fourth, the ribosome-binding surface in Snl1 within the predicted helix 1 (based on homology to mammalian Bag-1 BAG domain) is distinct from the Hsp70-interacting residues localized in the predicted helices 2 and 3. From these data, ribosome-associated Snl1 would be predicted to serve two roles: (i) tether an Hsp70 chaperone to the ribosome and (ii) function as an NEF during

Hsp70-dependent protein folding. Genes encoding ribosomal proteins and their binding partners such as Ssb are frequently co-regulated at the transcriptional level. Using the Serial Pattern of Expression Levels Locator (SPELL) database, I found that *SNL1* transcript levels were also co-regulated with ribosomal protein genes and support the idea that Snl1 is a bonafide ribosome binding protein and suggest that cells may regulate levels of Snl1 to correlate with the protein biosynthetic needs of the cell (Table 3-2).

Results from the mass spectrometry analysis and EDTA treatment of the Snl1-ribosome complexes identified two important aspects of Snl1 binding to the ribosome. One, Snl1 interacts with assembled ribosomes since both large (60S) and small (40S) subunit proteins of the ribosome co-purified with Snl1. Two, Snl1 preferentially binds to the large ribosomal subunit via the lysine-rich region that I identified to be in the predicted helix 1 domain and favor the model that it may bind in close proximity to Ssb, which is predicted to be present near the ribosome exit tunnel. Binding to ribosome by means of a positively charged stretch of amino acids seems to be a common binding strategy for ribosome-associated proteins. The identification of a lysine-rich region in Snl1 is consistent with the arginine-lysine-rich region in the β-domains of the nascent chain associated complex (NAC) in yeast and mammals and the bacterial trigger factor (TF), which utilizes a similar charged interface to interact with ribosomes (70).

In this chapter, I show that ribosome binding by Snl1, the Bag-1 homolog in *S. cerevisiae* is not limited to this fungal species but that the Bag-1 homolog in the pathogenic fungus *C. albicans*, which is separated from *S. cerevisiae* by over 250 million years of separation can also bind ribosomes and is also localized to the ER/nuclear membrane, similar to Snl1. This suggests that Bag-1 homologs in fungi are important enough to be conserved

for this long. Interestingly, investigation of Bag-1 homologs in other species identified two in the genome of the fission yeast *Schizosaccharomyces pombe*, one having a transmembrane domain and one that lacks it but contains a lysine-rich region (Figure 3-9). In addition, the human Bag-1 protein is expressed as different isoforms by alternative translation initiation and analysis of the long isoform Bag-1L revealed a short, positively charged sequence at its N-terminus, which was absent in the small isoform used in my experiment (Figure 3-9). The hypothesis that these proteins can bind the ribosome needs to be tested and is therefore possible that cells may express Bag-1 isoforms with or without the ability to associate with ribosomes.

Given the location of Snl1 at the ER membrane, a role in the transport of proteins from the cytoplasm into the ER membrane or lumen can be envisioned. Because of the utilization of the signal recognition particle (SRP) pathway during co-translational translocation, it seemed unlikely that Snl1 would play a role in this pathway. On the contrary, certain proteins that are released into the cytoplasm and require Ssa1 binding to maintain their translocation-competent state do not require the SRP pathway for translocation across the ER membrane (posttranslational translocation). At least one protein, pre-pro-α-factor (ppαF) utilizes this pathway but preliminary analysis of ppαF processing failed to demonstrate a major defect in *snl1*Δ cells. The testing of a functional role for Snl1 in the cell is confounded by the lack of detectable functional phenotypes in cells lacking *SNL1*. Using genetics to detect synthetic growth phenotypes, I tested the loss of *SNL1* in combination with RAC, NAC, SSB, ER translocation mutants and three genes identified to have synthetic growth defects with *SNL1* as reported in a high-throughput whole-genome screen. In all cases, I was unable to detect any synthetic growth defects. It is likely that Snl1 plays a subtle

or condition-specific role in protein biogenesis. Identification of such a role will require unbiased genome-wide and/or proteome-wide studies and it is clear that significant additional work is required to understand the importance of the Snl1-ribosome association. Nevertheless, my discovery of Snl1 as a possible adaptor linking translating ribosomes and Hsp70 represents an important step in understanding the biology of BAG domain-containing proteins.

Chapter 4: Purification of the BAG domain of Snl1 for structural determination

4A. INTRODUCTION

BAG domain-containing protein homologues are found in a variety of organisms including mice, *Xenopus*, *Drosophila*, *Bombyx mori* (silk worm), *Caenorhabditis elegans*, *S. cerevisiae*, *Schizosaccharomyces pombe* and *Arabidopsis thaliana*. Human members of this family include Bag-1, Bag-2, Bag-3 (CAIR-1/Bis), Bag-4 (SODD), Bag-5 and Bag-6 (BAT3/Scythe). The BAG-1 gene encodes four isoforms with varying protein sizes (Figure 4-1). All these proteins share the signature BAG domain near the carboxy-terminal end, except for Bag5, which contains five such domains. Interestingly, Bag proteins contain different N-terminal domain regions that dictate their specificity to protein partners or complexes in the cell and/or their localization. For example, all four Bag-1 isoforms and Bag-6 have an ubiquitin-like domain (UBL) at their amino-terminus. Although two isoforms, Bag-1 and Bag-1M have been shown to interact with the proteasome, the UBL domain of Bag-6 has not yet been linked to a partner protein or function (27). Bag-3 and Bag-6 contain a proline rich repeat, PXXP, which is a binding domain for proteins containing an Src homology 3 (SH3) motif. Unlike the mammalian Bag proteins that are all free floating in the cytosol, the fungal BAG domain-containing homologs Snl1 and CaSnl1 in *S. cerevisiae* and *C. albicans* respectively, are the only known members of this family to contain an N-terminal transmembrane domain and are localized at the ER membrane with majority of the C-terminal BAG domain situated in the cytosol (Figure 4-1). However, the cellular role for membrane attachment is not known.

Snl1 is the yeast homolog of mammalian Bag-1 and has been classified as a member of the BAG domain-containing family of Hsp70 NEFs by sequence analysis (139). In 2001, the crystal structure of the BAG domain of Bag-1M complexed with the NBD of bovine

Hsc70 was determined (Figure 4-2,A) (140). The structure revealed that the BAG domain formed a three-helix bundle with helices 2 and 3 making contacts with subdomains IB and IIB of the NBD. Binding of the BAG domain to the NBD resulted in a 14° rotation of domain IIB. Further, residues Glu-212 and Arg-237 located in helix 2 and helix 3 respectively of Bag-1 are required for Hsp70 interaction and conserved in BAG domain-containing proteins. The domain architecture of the BAG domain of Bag-4 is similar to Bag-1 and contains a 3-helix bundle, however, in Bag-4, each helix in the bundle is three to four turns shorter than in Bag-1 (16). This reduces the length of the domain by one-third and structural comparison defines two sub populations of mammalian BAG proteins, those that contain a long form of the BAG domain (Bag-1) and those that contain a shorter form (Bag-3, Bag-4, Bag-5). As would be expected because of the shorter length of the helices in Bag-4, the contributions and relative importance of some residues that are involved in Hsp70 binding are different. Bag-5 is unique because it contains five shorter BAG domains in tandem in which the fifth alone binds to the Hsp70 NBD. It is not known yet if the other BAG domains in Bag-5 contain a lysine-rich region, which could dictate ribosome interaction. One structure of Bag-5 with the NBD shows it to bind only subdomain IIB, similar to Bag-1, while another structure shows it to interact with both subdomains IB and IIB suggesting that either or both structures may contribute to Bag-5 binding to Hsp70 and its NEF activity (Figure 4-2,C) (5).

Recently, the structure of Bag-2 was determined by X-ray crystallography (Figure 4-2,B). Contrary to the three helix BAG domain present in Bag-1 and Bag-4, Bag-2 forms a dimeric structure, in which a flanking linker helix and loop mediates binding to Hsc70 to promote nucleotide exchange (Figure 4-2,B). This newly defined NEF domain called the ‘brand new bag’ (BNB) also has low homology to BAG domains of other Bag family

members and the crystal structure revealed that conserved residues in other Bag proteins that contact the Hsp70-NBD are poorly conserved or mispositioned in Bag-2. Bag-2 causes the entire domain II of the NBD to rotate about linkages connecting subdomains IA and IIA (162). In addition, Bag-2 can directly bind to misfolded substrates and suppress their aggregation, unlike its other family members. NMR analysis shows that the substrate- and Hsc70-binding sites overlap and that Hsc70 can displace substrates from Bag-2-BNB indicating a distinct mechanism for Hsp70 binding and substrate folding by Bag-2. Taken together, the structures of the BAG domain of these proteins indicate that despite their ability to bind Hsp70, they all have slightly different conformations.

My prediction that the ribosome binding site is present in helix 1 of the putative BAG domain of Snl1 was based on the structure of the mammalian BAG domain of Bag-1 (Figure 4-2,A). In this structure, helices 2 and 3 face the NBD of Hsp70 and are unlikely to be able to bind the ribosome due to steric hindrance. It was plausible from this structure that helix 1 on the opposite side of these two helices would be available for binding other proteins. I have since shown that the putative helix1 of Snl1 binds the ribosome and that this binding is independent of its interaction with cytosolic Hsp70s, Ssa and Ssb. I have also shown that this interaction pattern is present in the closely related pathogenic fungus, *Candida albicans*, suggesting conservation of ribosome association by fungal Bag proteins.

No evidence exists about the structural arrangement of the BAG domain of fungal Bag proteins. This chapter will present the preliminary steps of protein purification and analysis of Hsp70 binding to determine the minimal region of the Snl1 and CaSnl1 BAG domains that are required for Hsp70 interaction. The work presented here is the basis of an

active collaboration with Dr. Andreas Bracher at the Max Planck Institute for Biochemistry in Munich, Germany to determine the structure of the BAG domain in fungal Bag proteins.

FIGURE 4-1. Domain architecture of human and fungal BAG family proteins. The location of the BAG domain (blue) and other domains present in human and fungal BAG family members are indicated. Four isoforms of the Bag-1 protein are depicted on the top. Numbers beside the linear peptide sequence illustration indicate the length of each Bag protein.

FIGURE 4-1. Domain architecture of human and fungal BAG family proteins

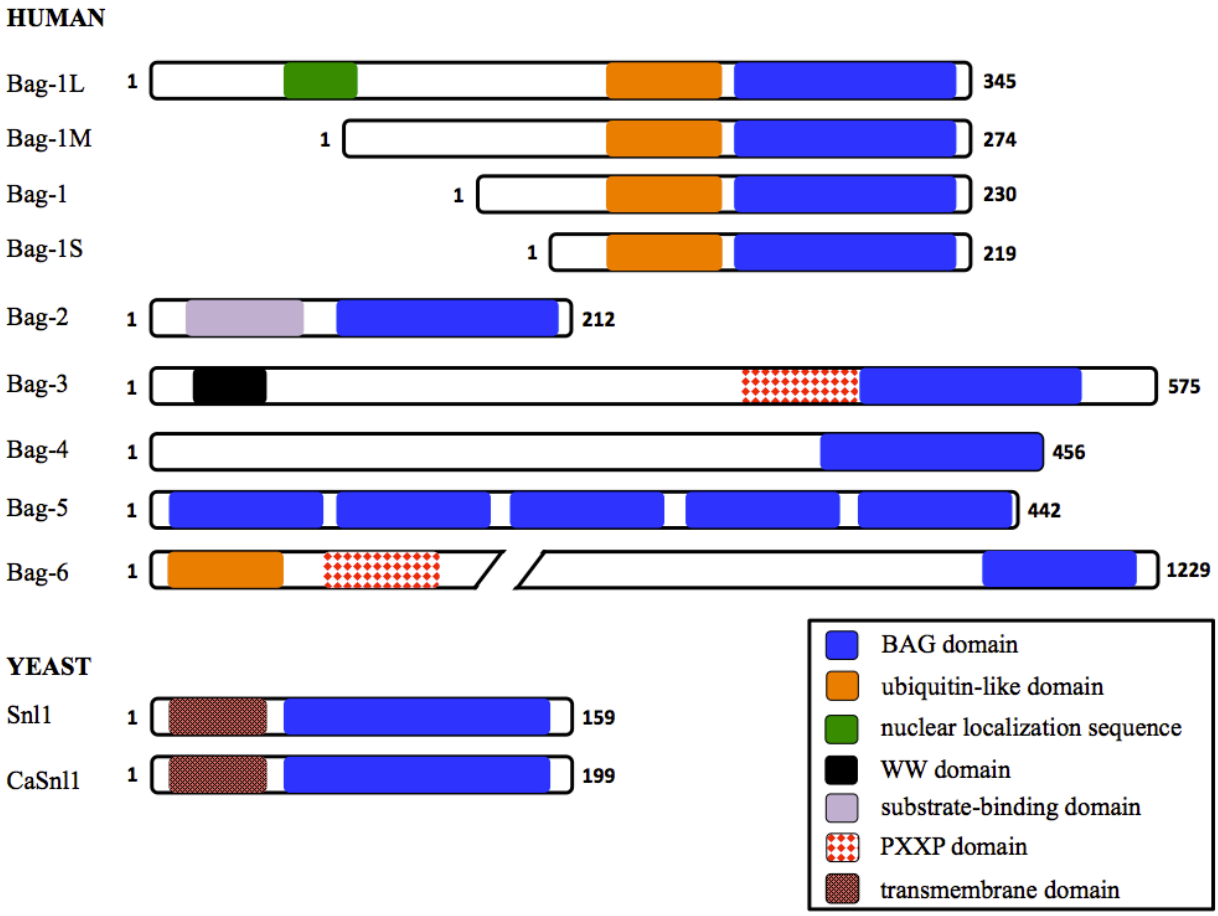

FIGURE 4-2. Structural comparison of known BAG domains. Co-crystal structures of the BAG domain (red) of Bag-1 (A), Bag-2 (B) and the fifth BAG domain of Bag-5 (C) are shown with the ATPase domain of Hsp70 (green). Bag-1 and Bag-5 share a similar three-helix bundle fold while Bag-2 contains a new fold termed “brand new bag.” PDB IDs: 1HX1 (Bag-1), 3CQX (Bag-2) and 3A8Y (Bag-5). (5, 140, 162)

FIGURE 4-2. Structural comparison of known BAG domains

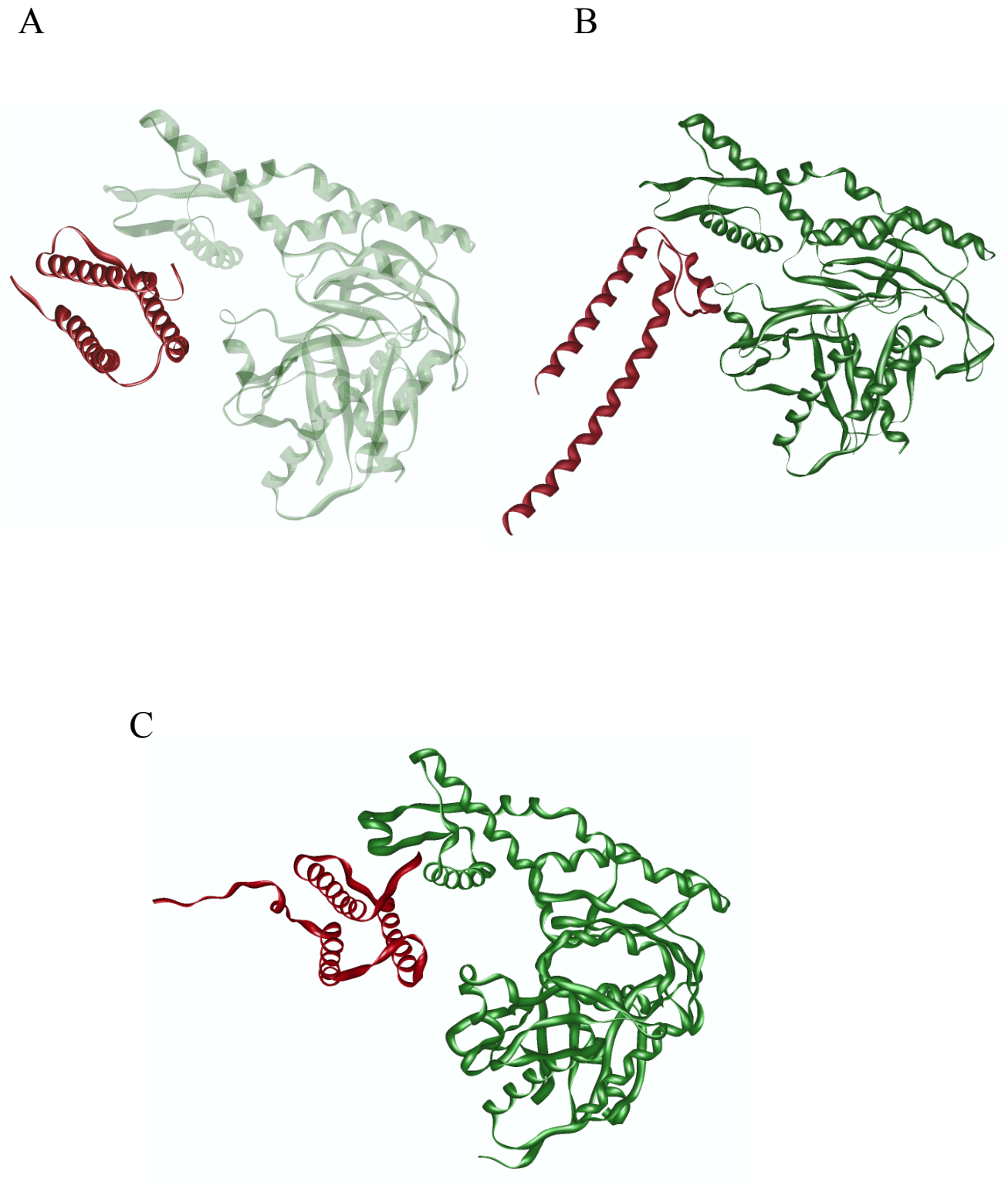

4B. RESULTS

Suppression of *sse1Δ* slow growth phenotype by Snl1 and CaSnl1 truncations

An *sse1Δ* strain was shown previously to exhibit a slow growth phenotype at 30°C and 37°C (89). This growth anomaly is linked to its ability to act as an NEF for the cytosolic Hsp70s, Ssa and Ssb. Our lab has observed that the slow growth of an *sse1Δ* strain can be suppressed when cells moderately overexpress (greater than chromosomal expression) either of the other cytosolic NEFs, Sse2, Fes1 and Snl1ΔN, suggesting that they can replace Sse1 as a NEF for Hsp70-dependent functions in the cell. I utilized this growth assay to determine the minimal region of the BAG domain of *S. cerevisiae* (Snl1) and *C. albicans* (CaSnl1) that can suppress the slow growth phenotype observed in an *sse1Δ* strain. Each truncation of Snl1 and CaSnl1 was FLAG-epitope tagged and individually expressed in the *sse1Δ* strain. If a truncated protein were capable of performing NEF function, it would suppress the slow growth associated with the loss of Sse1. I checked suppression by these constructs at physiological (30°C) and heat-stressed (37°C) conditions (Figure 4-3). With the exception of the Δ80Snl1 mutant, the other truncations of Snl1 and CaSnl1 were able to suppress *sse1Δ* slow growth phenotype at 30°C. However, at 37°C only Δ60Snl1 and to a lesser extent Δ91CaSnl1 and Δ103CaSnl1 were able to suppress slow growth of *sse1Δ* cells. The inability of Δ70Snl1 to suppress the slow growth of *sse1Δ* cells at 37°C suggests that this protein is unable to bind Hsp70 and function as an NEF at high temperature, consistent with a defect in chaperone function. Residues between 60 and 70 may serve to stabilize the Hsp70-binding region of the BAG domain and loss of these ten residues destabilizes this domain at high temperatures.

FIGURE 4-3. *sse1Δ* growth suppression assay. An *sse1Δ* strain expressing FLAG-tagged Sse1 and individual truncated mutants of Snl1 was serially diluted and spotted onto plates containing SC-HIS medium and incubated at the indicated temperatures for 40 hours.

FIGURE 4-3. *sse1Δ* growth suppression assay

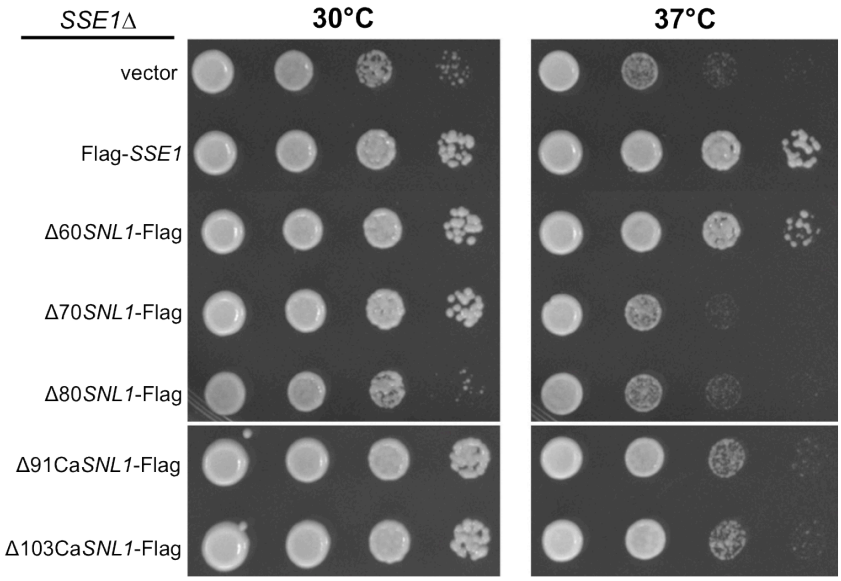

Identification of the minimal region of Snl1 and CaSnl1 that can interact with Ssa and Ssb

To test whether the truncated proteins that were expressed in the previous growth suppression assay were stably produced, I constructed expression vectors to produce FLAG-tagged truncated variants of the proteins. I then affinity purified each protein using M2-agarose resin from whole cell extracts of *S. cerevisiae* cells lacking *SSE1*. As a positive control, I used the previously described Flag-Sse1 protein that binds both Ssa and Ssb (131). This experiment was also performed to identify the minimal BAG domains of Snl1 and CaSnl1 that bind to Ssa and Ssb. With the exception of the Δ80Snl1 mutant, all the truncated proteins appear to be stably expressed (Figure 4-4). In addition, all but the Δ80Snl1 mutant retained binding to Ssa and Ssb as observed by Coomassie- dye staining suggesting that these truncations were properly folded. I noticed that the Snl1 proteins from both *S. cerevisiae* and *C. albicans* interacted with ribosome-associated chaperone Ssb stronger than Sse1 (Figure 4-4). This may suggest that BAG domain-containing proteins have a preference for Ssb. This could be due to the small protein size of fungal Bag proteins compared to Sse1.

Pilot purification of His_6-Δ60Snl1 and His_6-Δ103CaSnl1

How do fungal BAG domain-containing proteins bind Hsp70? Recent evidence of a different BAG domain structure of Bag-2 made us wonder if fungal BAG domains were structurally related to previously known BAG domains or were in a class of their own. From the previous data, it is evident that the stably expressed truncated mutants of Snl1 and CaSnl1 that can bind both Ssa and Ssb in addition to suppressing the slow growth of *sse1Δ* cells at both temperatures tested are Δ60Snl1 and Δ103CaSnl1. As described in the Methods section, Δ60Snl1 and Δ103CaSnl1 were partially purified as N-terminally His_6-tagged fusion proteins

from *E. coli* BL21 cells. Cell extracts expressing His_6-Δ60Snl1 and His_6-Δ103CaSnl1 were isolated using French Press (1200 psi) and incubated with Ni-NTA resin for two hours to facilitate binding. Proteins were purified using a gravity flow column. Most of the proteins present in the cell extract that did not bind the resin were collected in the flow-through (FT) fraction. The resin was washed once with low-ionic-strength buffer containing 5 mM imidazole, which removed almost all non-specifically bound proteins (W1). Both Δ60Snl1 and Δ103CaSnl1 proteins were initially released from the Ni-NTA column using 50 mM imidazole (W3) and all bound proteins were released with 200 mM imidazole (E1) to near purity (Figure 4-5).

FIGURE 4-4. Stably expressed mutants of Snl1 and CaSnl1 bind to Ssa and Ssb. Whole-cell extract from an *sse1Δ* strain expressing individual FLAG-tagged alleles of Snl1 (Δ60-Δ80) and CaSnl1 (Δ91,Δ103) were subjected to FLAG immunoprecipitation and run on a 10% SDS-PAGE gel (top panel) and 15% SDS-PAGE gel (middle panel). The bottom panel represents the load control. An empty vector (EV) and Flag-Sse1 were used as negative and positive controls respectively. CBB, Coomassie brilliant blue.

FIGURE 4-4. Stably expressed mutants of Snl1 and CaSnl1 bind to Ssa and Ssb

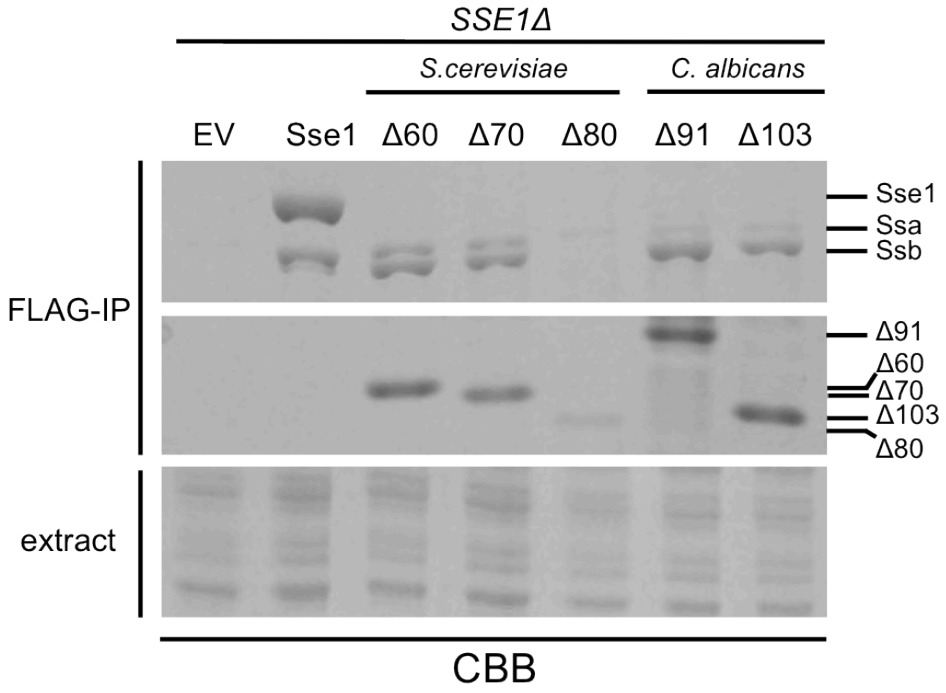

FIGURE 4-5. Pilot purification of His_6-Δ60Snl1 and His_6-Δ103CaSnl1. His_6-tagged Δ60Snl1 and Δ103*Ca*Snl1 were expressed in BL21 cells and affinity purified using Ni-NTA resin from cell lysates. Bound proteins were loaded onto a polyprep chromatography column. The flow through (FT) was initially collected followed by sequential wash steps (W1, W2, W3). Elution of bound protein was done in two steps (E1, E2). All fractions were run on a 15% SDS-PAGE gel. CBB, Coomassie brilliant blue; TP, total extract.

FIGURE 4-5. Pilot purification of His_6-Δ60Snl1 and His_6-Δ103CaSnl1

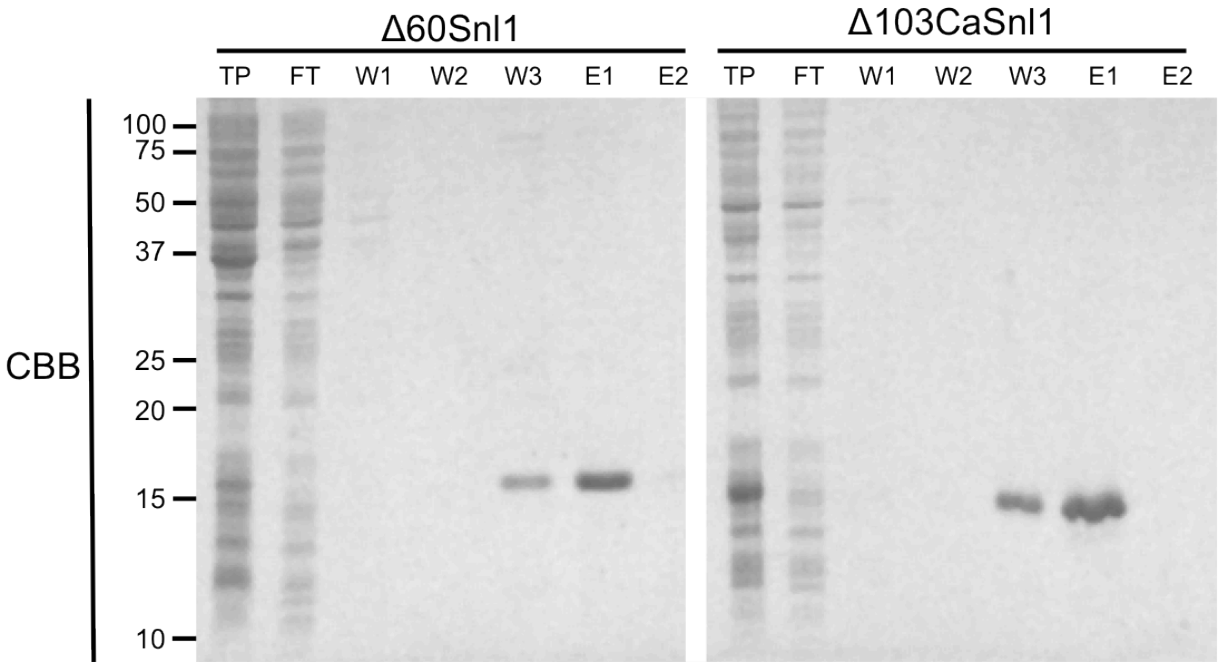

4C. DISCUSSION

The primary goal of the work described in this chapter was to initiate a collaborative project to determine the structure of the fungal BAG domains from *Saccharomyces cerevisiae* and *Candida albicans*. Over the last few years, a number of BAG domain structures from different Bag proteins have been determined. Interestingly, all these structures show nuance differences in their binding surfaces with the NBD of Hsp70. The architecture of fungal BAG domain-containing proteins remains poorly defined and understanding how they interact with Hsp70 may provide clues to better understand their mechanisms and intracellular functions. In addition, my discovery of the ability of fungal BAG domains to also interact with the ribosome adds an additional impetus to determine how they assume their conformation with respect to Hsp70 and the ribosome.

It was previously shown that an *sse1*Δ strain is slow growing at the physiological temperature (30°C) and the growth defect is exacerbated during heat stress (37°C) (89). However, mild overexpression of the other NEFs present in the yeast cytosol can suppress this slow growth phenotype. The ability of these NEFs to overcome the growth defects associated with loss of *SSE1* is due to functional redundancy and their ability to perform the same function as Sse1, namely nucleotide exchange. I used this assay to determine whether truncations of Snl1 and CaSnl1 proteins were able to suppress the growth defect of the *sse1*Δ strain. As seen in Figure 4-3, Δ60Snl1 and a lesser extent Δ91CaSnl1 and Δ103CaSnl1 suppressed the slow growth of cells suggesting that at higher temperatures, Snl1 could efficiently perform its nucleotide exchange function while the CaSnl1 homologs were less efficient. This observation with CaSnl1 homologs could be a result of these proteins being expressed in *S. cerevisiae*. The inability of Δ70Snl1 to suppress the slow growth of *sse1Δ*

cells at 37°C suggests that this truncated protein is unable to perform nucleotide exchange at an elevated temperature. I also determined that suppression of slow growth of *sse1Δ* cells by these proteins was a result of their stable expression. With the exception of the Δ80Snl1 mutant, all the truncated proteins appear to be stably expressed (Figure 4-4). In addition, all but the Δ80Snl1 mutant retained binding to Ssa and Ssb as observed by the Coomassie-stained gel suggesting that these truncations were properly folded. Interestingly, the data show that Snl1 proteins from both *S. cerevisiae* and *C. albicans* interact with ribosome associated chaperone Ssb stronger than Sse1 and suggests a preference for this Hsp70 in the cytosol. Could this be related to the domain architecture of BAG domain-containing proteins since these proteins and Sse1 have different Hsp70 binding domains? One possibility is that the small size of the BAG domain (~13 kDa) compared to Sse1 (~100 kDa) could give Snl1 proteins better access to Ssb present on the ribosome. Association of Sse1 with the ribosome has not been found, although Sse1 can associate with Ssb. It is possible that Sse1 may bind the small population of Ssb (30%) that is not associated with the ribosome. Since Ssb cannot replace most functions of Ssa, binding preferences of Snl1 and Sse1for the two classes of Hsp70 in the cytosol may result in their roles in specific Hsp70-dependent functions.

The structure of fungal Bag proteins is unknown and to initiate the process of determining their crystal structure, I designed and implemented a pilot purification strategy that would efficiently purify the minimal region of the BAG domain of Snl1 and CaSnl1 that could bind Ssa and Ssb (Figure 4-5). The constructs I made were sent to our collaborator for further large-scale purification and crystal structure determination. I predict that the Hsp70 binding domain of these proteins will be consistent with the known BAG domain structure of Bag-1 and contain a three-helix bundle, as residues within this region were also conserved in

the human Bag-1 protein. However, the ribosome-binding site within these proteins might resemble a short helical or loop region that is not part of the rigid structure of the BAG domain and thus makes it more facile for ribosome interaction. Since Snl1 is a small membrane-bound protein, binding to the large ribosomal complex and Hsp70 may be difficult due to steric hindrance effects. A more flexible loop region may subvert these steric effects. In addition to providing a structural explanation for the ability of Snl1 to bind the ribosome and Hsp70, mutagenic confirmation of predicted structural details can be performed.

Chapter 5: Specificity of Fes1 binding to Hsp70

5A. INTRODUCTION

Fes1 was first identified in a yeast genome-wide screen looking for homologs of Sil1, an NEF of Kar2, the resident Hsp70 of the endoplasmic reticulum (ER). Fes1 is related to the mammalian NEF HspBP1 (38% similarity and 25% identity) and binds to and performs nucleotide exchange for Ssa *in vivo* and for both Ssa and Ssb *in vitro* (32). Additionally, the *FES1* gene is required for growth at high temperatures suggesting its important role as an Hsp70 co-chaperone during cellular stress due to elevated temperatures. Structural determination of the conserved core domain of human HspBP1 (BP1c) that binds Hsp70 and shares a similar domain with Fes1, revealed a unique architecture amongst NEFs. The domain is composed of four Armadillo-like repeats that is strikingly different from the three-helix bundle of the BAG domain (Figure 5-1). Compared to the BAG domain, which binds to the central cleft between domains I and II, BP1c associates with lobe II from the side and wraps around subdomain IIB of the NBD and is suggested to displace lobe I due to steric hindrance (134).

In vitro experiments showed that Fes1 binds more efficiently to the ADP-bound state of Ssa1 and rapidly decreased (within 1 min) the amount of bound nucleotide on Hsp70. This classifies Fes1 in the same group of NEFs like Sil1 that preferentially binds to the ADP-bound state of Hsp70. A double mutation in Fes1 (A79R/R195A) abolished its interaction with Ssa1 and was unable to complement the deletion of *FES1* at high temperatures, indicating that a direct interaction between these two proteins is required for function (134). Fes1 was shown to inhibit the ATPase activity of Ssa1 in the presence or absence of Ydj1, a Hsp40 of Ssa1 that stimulates Ssa1 ATPase activity. This observed inhibition by Fes1 is expected since the removal of bound nucleotide in Ssa1 will decrease the apparent rate of

ATP hydrolysis. Binding of Fes1 to ribosome-associated Hsp70, Ssb1 was determined using His_6-tagged Fes1 purified from *E. coli* and incubated with *S. cerevisiae* cell lysate. Interacting proteins were isolated by affinity purification of Fes1. The recombinant double mutant of Fes1 that could not interact with Ssa1 also could not associate with Ssb1, suggesting that the interface of Fes1 that binds Ssa1 and Ssb1 is similar. The binding affinity of the complex between Fes1 and Ssa1 or Ssb1 was determined using surface plasmon resonance. Using this method, Fes1 had a slightly higher affinity for Ssb1 (K_d ~87 nM) compared to Ssa1 (K_d ~193 nM). These values are slightly higher than those determined for BP1c and the BAG domain of Bag-1 with the NBD of mammalian Hsp70 (K_d 62 and 41 nM respectively) (134).

A heterodimeric complex called the ribosome associated complex (RAC) consisting of the non-canonical Hsp70, Ssz1 and Hsp40, Zuo1 functionally cooperates with Ssb to stimulate Ssb ATPase activity. An *in vitro* experiment using purified proteins to test whether Fes1 function as an NEF could further stimulate the ATPase of Ssb in the presence of RAC revealed that Fes1 decreased Ssb1 activity even though Fes1-Ssb affinity was unchanged (32). Based on this evidence, it was proposed that RAC might interfere with binding of Fes1 to Ssb but the direct binding of Fes1 to the Ssb-RAC complex was not assessed.

The function of Fes1 in binding to and releasing bound nucleotide from Ssa and Ssb has been primarily based on *in vitro* evidence using purified proteins. Although these experiments confirm a direct interaction between Fes1 with Ssa and Ssb, there is no *in vivo* evidence of Fes1 binding to these Hsp70s. This chapter will present data that shows Fes1 interacts exclusively with Ssa proteins *in vivo* using a functional FLAG-Fes1 construct and provides preliminary data to test how Fes1 is restricted to Ssa chaperones.

FIGURE 5-1. Structural comparison of Hsp70 binding domains of HspBP1 and Bag-1. (A) Co-crystal structure of the conserved core domain of HspBP1 (red) in complex with subdomain IIB of the Hsp70 ATPase domain (green) showing the Armadillo-like repeats. (B) Co-crystal structure of the three-helix bundle BAG domain (red) of Bag-1 with the ATPase domain of Hsp70 (green). Top views are shown for both structures and aligned for superposition of subdomain IIB in the ATPase domain. PDB IDs: 1XQS (HspBP1), 1HX1 (Bag-1). (134, 140)

FIGURE 5-1. Structural comparison of Hsp70 binding domains of HspBP1 and Bag-1

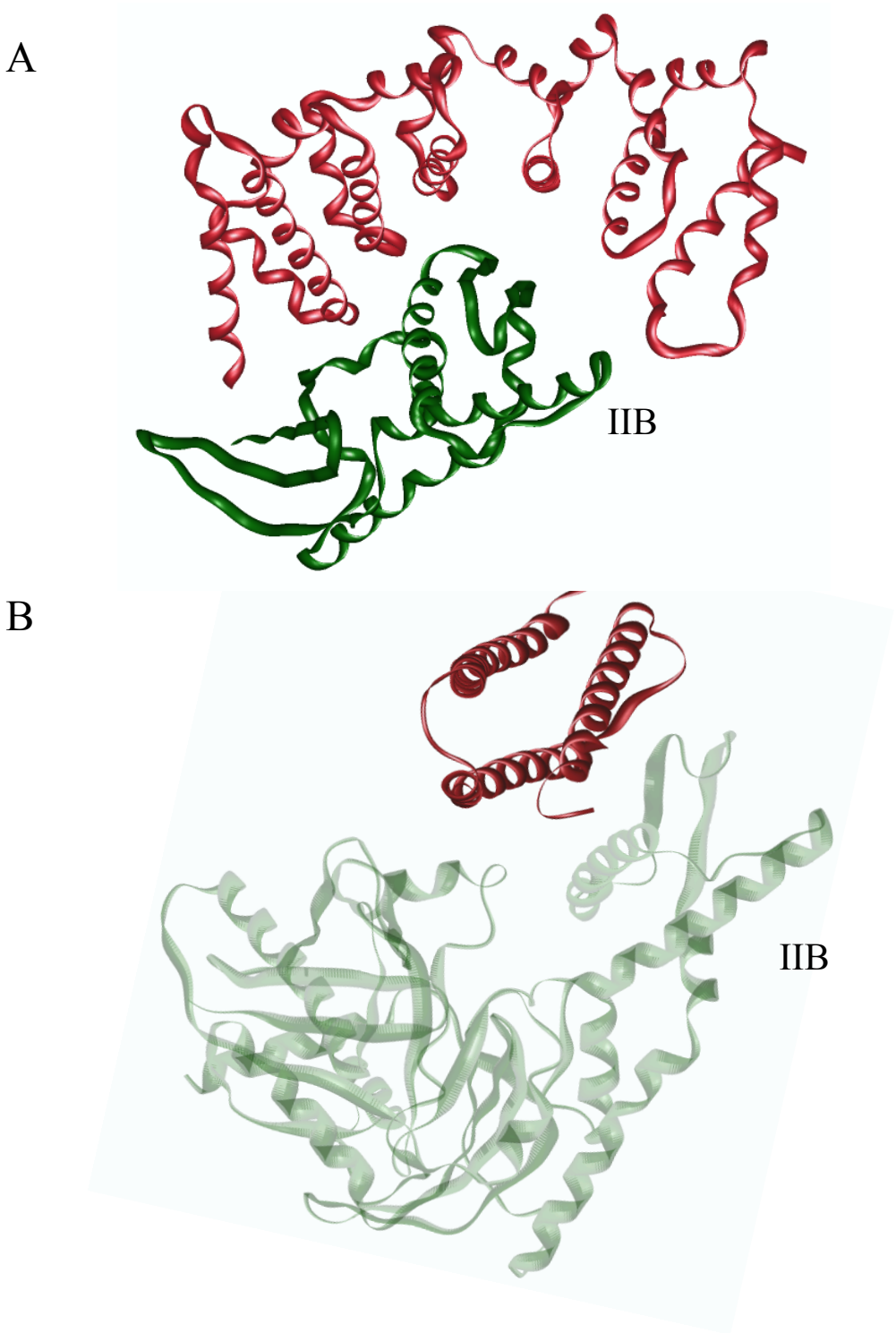

5B. RESULTS

In vivo interactions of Fes1 with Ssa and Ssb

Two separate groups showed that tagged-Fes1 purified from *E. coli* interacted with Ssa and Ssb. The Brodsky group utilized a glutathione-s-transferase (GST) tag on Fes1 to determine direct binding of Fes1 with purified Ssa using a GST pull-down assay (63). The Hartl group utilized a different approach. His_6-Fes1 was incubated with cell lysate isolated from *S. cerevisiae* and binding partners of Fes1 were isolated after co-purification on Ni-agarose resin (32). Using this method, His_6-Fes1 was shown to interact with both Ssa1 and Ssb1. However, in both these cases, Fes1 was not expressed in yeast cells. To determine the co-purifying partners of Fes1 in a yeast cell, I constructed an expression vector to produce low amounts of FLAG-tagged Fes1 (above chromosomal expression levels) in a wild type yeast strain (BY4741). I affinity purified Fes1 using M2–agarose resin from yeast cell extracts as described in Materials and Methods (Chapter 2). Our lab has previously shown that this purification method works efficiently in yeast to determine chaperone interactions in yeast cells. In addition to Fes1, I independently expressed a FLAG-tagged Sse1 fusion using an identical promoter to compare Hsp70 interaction patterns. As shown in (Figure 5-2), Fes1 expressed in a wild-type yeast strain appears to associate specifically with Ssa with little to no Ssb co-purifying with it as determined by Coomassie-dye staining. To confirm this, I performed a Western blot for Ssa and Ssb, which showed that Fes1 interacted exclusively with Ssa1. This result is in contrast to previously described interactions of Fes1 with Ssa and Ssb and suggests that in yeast cells, Fes1 does not associate with Ssb. This is the first reported evidence of a cytosolic NEF to exhibit selectivity in binding cytosolic Hsp70s.

FIGURE 5-2. Fes1 binds predominantly to Ssa *in vivo*. Amino-terminally FLAG (F)-tagged Sse1 and Fes1 were individually expressed and immunoprecipitated from wild type (BY4741) whole-cell lysate. Immunoblot analysis was used to detect interacting proteins using anti-Ssa and anti-Ssb antisera. The positions of Fes1, Sse1, Ssa and Ssb are indicated in the Coomassie brilliant blue (CBB) stained SDS-PAGE gel. IB, immunoblot of the whole-cell lysate.

FIGURE 5-2. Fes1 binds predominantly to Ssa *in vivo*

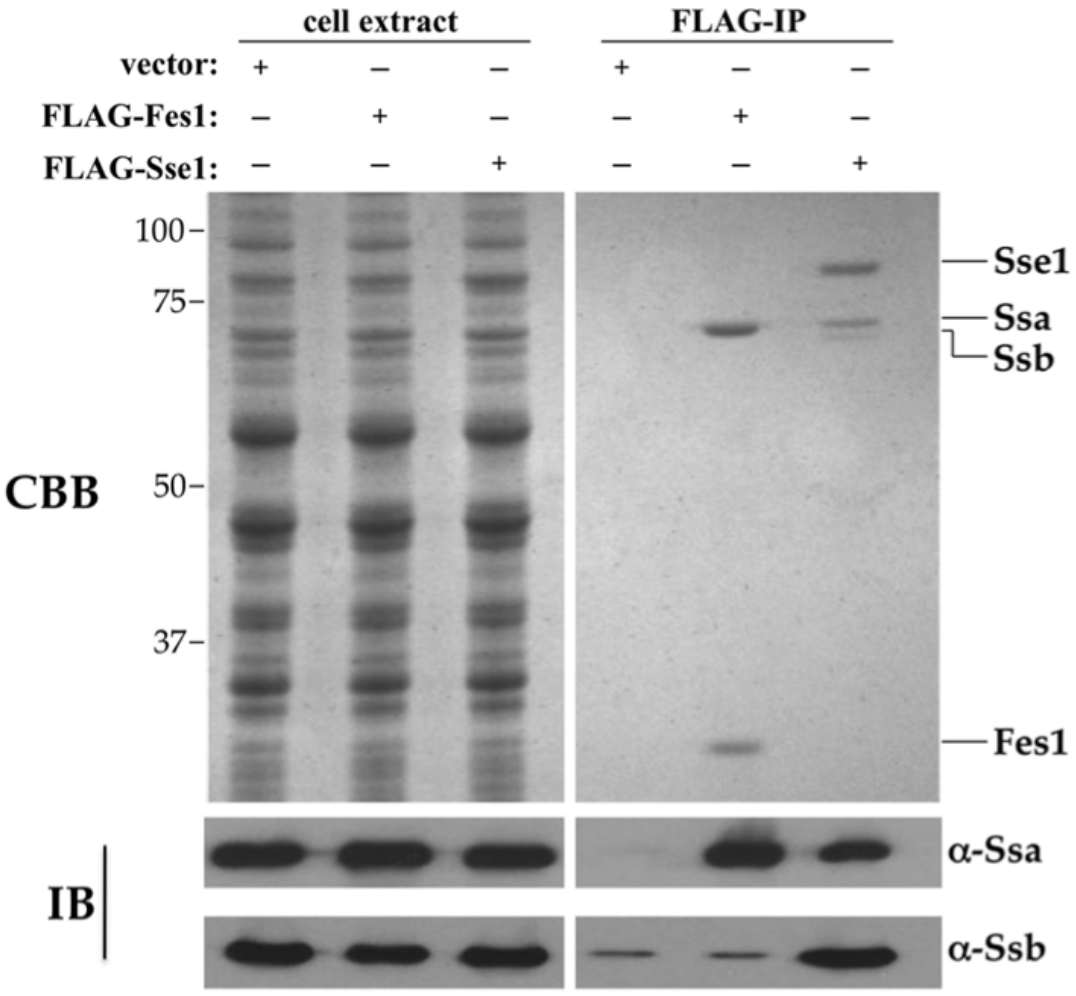

***In vitro* interactions of FLAG-Fes1 with Ssa and Ssb**

In the experiment described above, Fes1 was FLAG-epitope tagged while the Fes1 proteins used previously contained two different epitope tags, GST and His_6. To test the possibility that the selective binding of Fes1 for Ssa was not due to the different tag, I constructed an *E. coli* expression vector to produce FLAG-Fes1 in *E. coli*. I successfully purified FLAG-Fes1 from *E. coli* to apparent homogeneity (1 mg/ml)(data not shown). Keeping the concentration of *E. coli* purified FLAG-Fes1 (3 µg/µl) constant in each sample, a different concentration of cell lysate extracted from *S. cerevisiae* was added to each Fes1 sample and incubated for 2 hours to facilitate complex formation. I affinity purified Fes1 using M2–agarose resin and observed that FLAG-Fes1 bound both Ssa and Ssb (Figure 5-3). This suggests that the tag used in these experiments does not play a role in binding to specific cytosolic Hsp70s. It is possible that Fes1 expressed in yeast may undergo a posttranslational change that is absent when it is produced in *E. coli*. This could alter the Fes1 protein and prevent its interaction with Ssb. Alternatively, factors present in the yeast cytosol may prevent Fes1 binding to Ssb.

Overexpressing Fes1 in the cell still occludes binding to Ssb

Because the above data suggest that Fes1 is precluded from binding Ssb in a yeast cell, I first wanted to determine if the amount of Fes1 present in the cell could be a determining factor. A large-scale analysis of the global protein expression in yeast determined that Fes1 is present at 13,100 molecules/cell compared to Sse1, which is present at 71,700 molecules/cell and binds Ssb (45). To test this hypothesis, I made constructs of FLAG-Fes1 using two vectors that would moderately (~2-fold) and highly (~15-20-fold) overexpress Fes1 in a wild type yeast strain. Fes1 proteins were affinity purified using M2

FIGURE 5-3. Fes1 stably interacts with both Ssa and Ssb *in vitro*. (A) FLAG-Fes1purity. (B) Purified FLAG-Fes1 (3 µg/µl) incubated for two hours with 0, ~4.5 µg/µl and ~7.5 µg/µl of yeast whole-cell lysate was immunoprecipitated using M2 FLAG resin. Bound proteins were eluted as described in Materials and Methods, and immunoblot analysis was performed to detect interacting proteins with anti-Ssa and anti-Ssb antisera. Lysate added to M2 FLAG resin alone served as a control (lane 2). TPE, total extract.

FIGURE 5-3. Fes1 stably interacts with both Ssa and Ssb *in vitro*

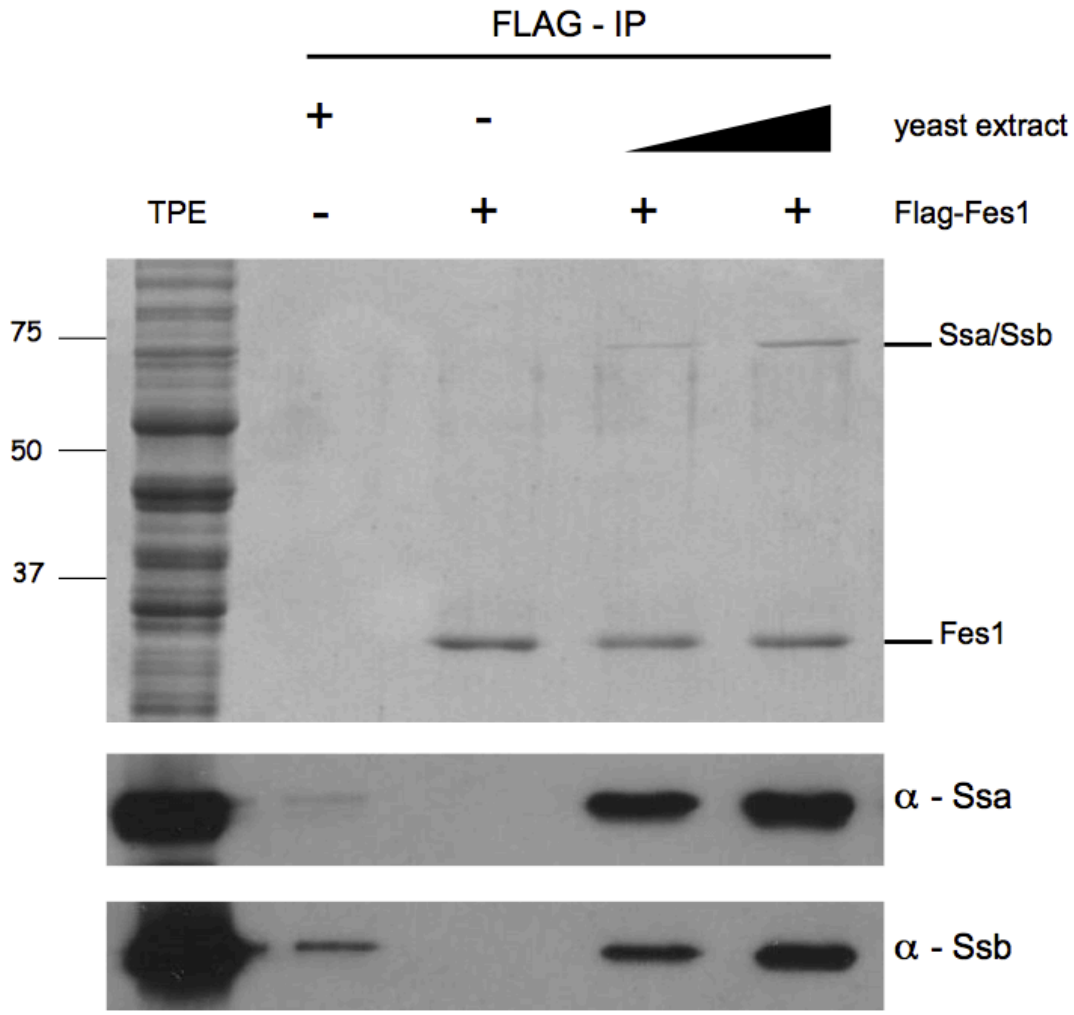

agarose resin and their interactions with Ssa and Ssb was determined by a Western blot using α-Ssa and αSsb. Increasing the level of Fes1 in the cell still did not facilitate Fes1 interaction with Ssb. Interaction of Ssa with Fes1 was concurrent with Fes1 expression levels in the cell (Figure 5-4). This suggests a very distinct bias of Fes1 for cellular Ssa (Figure 5-3).

RAC does not prevent Fes1 binding to Ssb

It was previously proposed that RAC present at the ribosome interferes with the binding of Fes1 to Ssb (32). To determine if the RAC proteins prevented the interaction of Fes1 with Ssb in cells, I expressed FLAG-Fes1 in a strain that lacked either *SSZ1* or *ZUO1*. Fes1 was affinity purified from these two strains using M2 agarose resin and the association of Fes1 with Ssa and Ssb was determined by a Western blot using α-Ssa and α-Ssb (Figure 5-5). The interaction of Fes1 with Ssa was unaffected in the absence of either RAC protein. The amount of Ssb that co-purified with Fes1 in each mutant strain was similar to wild type, but not above background (EV lane). These results indicate that neither RAC protein prevents the association of Fes1 with Ssb and suggests an alternative mechanism that prevents Fes1 binding to Ssb.

FIGURE. 5-4. Overexpressing Fes1 does not facilitate interaction with Ssb. Whole-cell lysate from a wild-type (WT) (BY4741) strain expressing either the empty vector (EV) or FLAG-Fes1 from a low copy (low) or high copy (high) plasmid was subjected to FLAG immunoprecipitation (IP). Interacting proteins were detected with anti-Ssa and anti-Ssb antisera.

FIGURE. 5-4. Overexpressing Fes1 does not facilitate interaction with Ssb

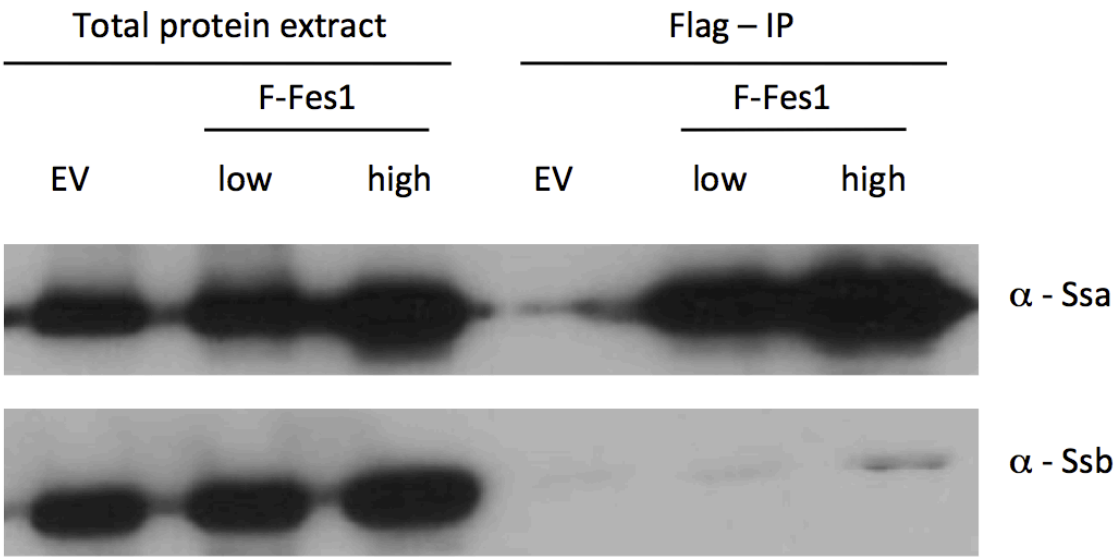

FIGURE 5-5. RAC does not prevent Fes1-Ssb interaction Whole-cell lysate from an *ssz1Δ, zuo1Δ* or wild-type (BY4741) strain expressing FLAG-Fes1 was subjected to FLAG immunoprecipitation (IP). Interacting proteins were detected on a Coomassie-stained gel (above) or by immunoblotting for Ssa and Ssb (below).

FIGURE 5-5. RAC does not prevent Fes1-Ssb interaction

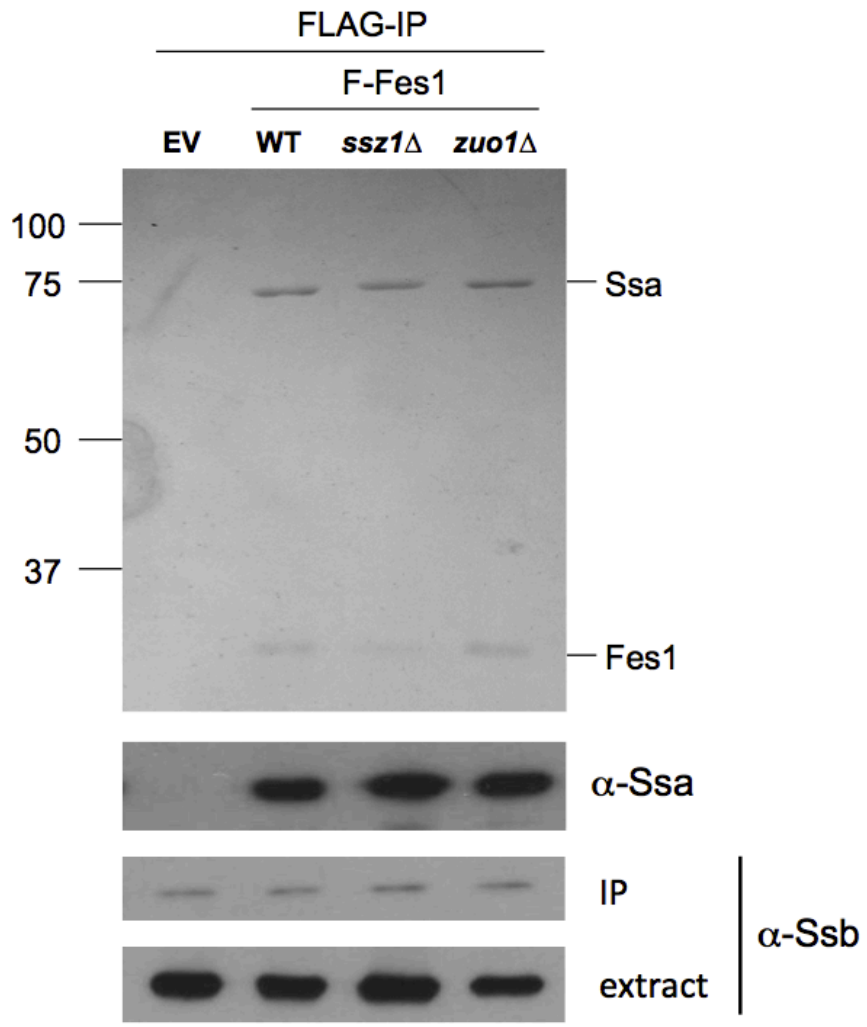

5C. DISCUSSION

In this chapter, I present the first evidence of an *in vivo* bias in binding between a cytosolic NEF and a cytosolic Hsp70. I found that in yeast cells, Fes1 does not bind Ssb. This is in contrast with a previous published report that demonstrated Fes1 binding to Ssb and functioning as an NEF of Ssb *in vitro*. I found that Fes1 purified from *E. coli* and incubated with cell extract isolated from yeast bound both Ssa and Ssb, corroborating previous data. This difference in binding to Ssb whether Fes1 is expressed in *E. coli* versus *S. cerevisiae* is intriguing and in this chapter, I present preliminary data to test how Fes1 is restricted to Ssa chaperones. First, I overexpressed Fes1 in yeast cells to determine if the stoichiometry of the protein relative to Ssb could explain the observation. I found that even when Fes1 was expressed at very high levels, as a measure of the amount of Ssa that interacted with it, Fes1 failed to interact with Ssb, suggesting that this inability to bind Ssb is not due to low affinity coupled with low concentrations. Next, I tested if components of the ribosome associated complex (RAC), Ssz1 and Zuo1 interfered with Fes1 binding to Ssb since both proteins are present with Ssb at the ribosome. In cells lacking *SSZ1* or *ZUO1*, Fes1 was still unable to physically interact with Ssb.

The results presented in this chapter represent a preliminary follow-up of my original discovery of Fes1 binding to only cytosolic Hsp70, Ssa (as shown in Chapter 3). However, there are still many questions that need to be answered for why Fes1 has a bias towards one specific Hsp70. Preliminary data from our laboratory indicate that overexpressing Ssb can increase the amount of Ssb that copurifies with Fes1 (Gibney P, personal communication). This would suggest that during some cellular stress conditions, an increase in *SSB* transcription would then favor Fes1 binding to Ssb. If this were true, under the normal

growth conditions that I was using to test this interaction, Fes1 would not bind Ssb. This possibility is consistent with the observation that cells lacking *FES1* are sensitive to the translation inhibitor cycloheximide and that Fes1 co-migrates with polysomes upon cellular fractionation (63). While this would suggest an Ssb-dependent function, a small population of Ssa exists at the ribosome through its physical association with poly(A)-binding protein, Pab1 and another ribosome-associated Hsp40, Sis1 (56). In addition, a temperature sensitive strain of *SSA* (*ssa1-45*) demonstrates a severe translational defect (8). This evidence along with the discovery that Fes1 specifically binds Ssa suggest that Fes1 migration with polysomes as shown previously may be Ssa-dependent. A comprehensive phenotypic analysis of a *fes1*Δ strain compared to an *ssb1*Δ*ssb2*Δ strain will shed light on which phenotypes are shared between the two proteins, utilizing conditions such as cold and salt sensitivity, and sensitivity to the protein folding inhibitor canavanine. Cells deficient in Ssa chaperones do not share these phenotypes, thus making them a diagnostic for Ssb function alone. In addition, the role of Fes1 with respect to only Ssa-dependent functions such as protein translocation and protein folding need to be assessed. Initial analysis showed that Fes1 is not involved in the translocation of ppαF and in refolding the model substrate, firefly luciferase (Abrams *et al*., unpublished data). However, it is possible that Fes1 might be substrate- and cellular pathway-specific with respect to binding Ssa1 similar to that observed with the plethora of J proteins present in the cell (67). Finally, to test if Fes1 is differentially modified when produced in yeast versus *E. coli*, comparative mass spectrometry on both Fes1 proteins needs to be performed to identify any posttranslational modifications including phosphorylation and acetylation, both of which are well known modifiers of protein behavior

in the cell. This work provides a foundation to further investigate the functional roles of Fes1 in the cell.

Chapter 6: Conclusions and perspectives

Summary and conclusions

Proper folding of cellular proteins is crucial for survival and the assistance of molecular chaperones or 'heat shock proteins' in preventing protein misfolding is vital. In mammalian cells, approximately 180 different chaperones and co-chaperones form a complex folding network that helps maintain the conformational integrity of the cellular proteome (52). The Hsp70 protein family plays an important role in this network. In addition to participating in co- and post-translational folding of newly synthesized proteins, Hsp70s are also involved in protein assembly, refolding of stress-denatured proteins, protein degradation, transport of proteins across cellular membranes such as the ER and mitochondria and in the regulation of protein substrates involved in signal transduction. However, Hsp70s do not perform this plethora of cellular functions by themselves, but depend on the function of J-proteins and NEFs, which regulate their nucleotide-dependent folding cycle and thereby their substrate binding ability.

In the present study, I focused on two classes of NEFs in yeast: Snl1 and Fes1. My experiments with Snl1 lead to the identification of a novel ribosome interaction site in BAG domain-containing proteins in fungi and I found that this interaction was independent of Snl1 binding to cytosolic Hsp70s, Ssa and Ssb. Furthermore, I discovered that Fes1 bound specifically to Ssa with little to no interaction with ribosome-associated Hsp70, Ssb. These two lines of investigation highlight the first evidence of a novel ribosome association among fungal BAG domain-containing proteins and the first distinct binding specificity of an NEF with a cytosolic Hsp70.

Fungal BAG domain containing proteins bind ribosomes

At the outset of these studies, Snl1 in *S. cerevisiae* was identified as a homolog of the human BAG domain-containing protein, Bag-1 (139). Like Bag-1 in human cells, Snl1 interacts with free-floating, cytosolic Hsp70, Ssa. In addition, Snl1 was shown to interact with the fungal-specific, ribosome-associated Hsp70, Ssb (139). However, both these interactions were determined *in vitro* using recombinant Snl1 that lacks its N-terminal transmembrane domain (Snl1ΔN). To characterize the cellular role of Snl1, I first sought to determine its binding partners in the cell. I did this by expressing FLAG-epitope tagged Snl1 in yeast, which allowed me to immunoprecipitate it from cell extracts and identify co-purifying proteins. I found that full length, membrane-associated Snl1 and free-floating Snl1ΔN bound to Ssa and Ssb. In addition, both Snl1 proteins also physically interacted with the assembled ribosome. However, this specific interaction with the ribosome is not seen with Bag proteins in higher eukaryotes. In humans, there are eight BAG domain-containing proteins that can bind different protein partners apart from Hsp70. This is accomplished by different N-terminal motifs located upstream of the Hsp70-binding BAG domain, which serves to target Bag proteins to their substrates (Figure 4-1). For example, the ubiquitin-like (UBL) domain present in Bag-1 and Bag-1M was shown to be responsible for co-immunoprecipitating the Bag proteins with the 20S core and the 19S subunit of the proteasome. This suggests that both Bag proteins perform an adapter-like function linking the protein degradation machinery with Hsp70. Bag-1 is the only known BAG domain-containing protein to also utilize the BAG domain to bind a substrate. Bag-1 interacts with the serine/threonine kinase Raf-1 or Hsc70 in a mutually exclusive manner (141). When Hsp70 levels increase during cellular stress, they compete with Raf-1 for binding to Bag-1,

which leads to lower Raf-1 signaling and subsequent inhibition of DNA synthesis and cell cycle arrest. This suggests that Bag-1 acts like a molecular switch that enables cell proliferation in normal conditions and cell growth inhibition during a stressful environment. These results support the idea that in addition to binding the NBD of Hsp70, BAG domain-containing proteins can also bind other cellular substrates through their N-termini or directly through their BAG domains.

Conservation in fungal BAG domain proteins with ribosome association

How widespread in fungi is this interaction between the *S. cerevisiae* BAG domain-containing protein and the ribosome? To answer this, I examined the sole Snl1 homolog in the pathogenic fungus, *Candida albicans*. *S. cerevisiae* and *C. albicans* are separated by more than 250 million years and it seemed appropriate to test if another fungal BAG domain-containing protein could bind the ribosome. Utilizing a similar copurification method, I found that the *C. albicans* Snl1 homolog (CaSnl1) also associated with the ribosome, suggesting a common evolutionary function for these proteins to bind the ribosomal complex. However, this specific interaction with the ribosome has not yet been identified in Bag proteins in higher eukaryotes. The genome of the fission yeast *Schizosaccharomyces pombe* contains two putative BAG domain-containing proteins; bag102, which contains a putative N-terminal transmembrane domain and bag101 that contains a short positively charged string of residues. This suggests that in *S. pombe*, the transmembrane domain and ribosome binding are not connected and may function in distinct cellular pathways. The human BAG domain family consists of six members; Bag-1 to Bag-6. The Bag-1 gene encodes four isoforms of the Bag-1 protein expressed through alternative translation initiation sites. Bag-1L is located primarily in the nucleus while Bag-1, Bag-1M and Bag-1S

are localized to the cytoplasm. The human Bag-1 isoform that was used in this study (Chapter 3) was the shortest isoform, Bag-1S. Sequence analysis of Bag-1M and Bag-1L reveal a short, positively charged sequence at their N-terminal that is absent in Bag-1S (Figure 3-9). Therefore, it is possible that mammalian cells may express distinct Bag-1 isoforms with or without the capacity to associate with ribosomes.

BAG domain proteins interact with the ribosome through a short lysine-rich region

The results in Chapter 3 show that *S. cerevisiae* and *C. albicans* BAG domain-containing proteins interact with the ribosome through a short sequence of lysine-rich residues. This region was first identified in Snl1 during a sequential N-terminal deletion analysis of the BAG domain to determine the ribosome-binding site. These lysine residues in Snl1 had not been previously assigned a function. Based on homology to mammalian Bag-1, this region of Snl1 lies in putative helix 1 of the anti-parallel BAG domain. Recent data on the heterodimeric nascent chain-associated complex (NAC) showed a short region of positively charged residues located at the amino-terminus of each β-subunit that mediated ribosome association (158). A similar charged interface is utilized by bacterial trigger factor (TF) to bind ribosomes, which enables the protein to bind nascent chains emerging from the ribosome (114). Interestingly, SecA, the motor protein in *E. coli* that assists in posttranslational substrate translocation across the bacterial membrane was shown to associate with ribosomes utilizing two lysine residues (59). These discoveries show that proteins interacting with the ribosome only require a short positively charged region. My discovery of the cytosolic NEF, Snl1 in fungi to associate with the ribosomal complex is the first of its kind for Hsp70 NEFs.

Structural determination of the fungal BAG domain

How does the small size of the BAG domain of Snl1 (~110 amino acids) accommodate binding to Hsp70 and to the large ribosome complex? The ribosome-binding region in the β-subunit of NAC proteins is located in an exposed loop of a predicted helix-loop-helix motif. This strategy to bind ribosomes is similar to trigger factor in bacteria. In both cases, the binding region is localized in a flexible loop region that is flanked by two α-helices. From these two structures, it seems like a trend is emerging for ribosome associated chaperone domains; an exposed loop of positively charged residues inserted between α-helical structures. Whether BAG domain proteins in fungi follow this trend or are in a structural class of their own needs further evaluation and our lab has initiated a collaboration to determine the structure of Snl1ΔN and CaSnl1ΔN. It will be interesting to determine if the Snl1 BAG domain forms a rigid three-helix bundle structure like the human Bag-1 protein. A recent crystal structure of Bag-2 shows a new domain conformation termed "brand new BAG" (BNB), which forms a dimer with each monomer contacting an Hsc70 NBD by binding to subdomains Ib and IIb in an end-on fashion (162). In addition to its NEF function, the BNB domain is able to interact with hydrophobic residues of a short polypeptide sequence derived from the cystic fibrosis transmembrane conductance regulator (CFTR) protein. Since substrate- and Hsc70-binding sites on this domain overlap, Bag-2 might coordinately transfer substrate peptides to the substrate-binding domain (SBD) of Hsc70. Alternatively, Bag-2 might by recruited to Hsp70-client complexes through its ability to bind substrates. Determining the structure of Snl1 and CaSnl1 would shed light on whether BAG domain folds are also conserved in fungi.

Snl1 binds to the large subunit (60S) of the ribosome

Ribosomes are composed of two subunits, each containing RNA and protein. The large subunit (60S) of the eukaryotic ribosome consists of three rRNAs (25S, 5.8S and 5S) and 46 proteins while the small subunit (40S) includes one rRNA (18S) and 33 proteins (68). While the small subunit is responsible for proper codon-anti-codon recognition and mRNA surveillance, the large subunit contains the active site where new peptide bonds are created during protein synthesis and the exit tunnel through which the polypeptide exits. Snl1-ribosome complexes were treated with EDTA to dissociate the 80S-assembled ribosome into its subunits and then determine which ribosomal subunit Snl1 binds. I found that Snl1 predominantly binds to the 60S large ribosomal subunit. Previous data shows that both signal recognition particle (SRP) and NAC bind to the large ribosomal subunit near ribosomal protein L23 and that SRP and NAC can interact directly with each other and compete for nascent polypeptide access (158). This is because protein L23 is situated near the polypeptide exit tunnel of the ribosome. Some secretory polypeptides require NAC to efficiently interact with SRP, whereas others are prevented from interacting with SRP when NAC is present (26). Thus, the observation that different factors compete with each other for binding to L23 and the fact that Snl1 preferentially binds to the large subunit may add another layer of complexity in substrate recognition between proteins that bind near the ribosome exit tunnel. Identification of the exact binding site of Snl1 on the large ribosome subunit by crosslinking experiments could determine if Snl1 adds to the binding dynamics that exists between these non-homologous ribosome binding factors at the exit tunnel. On the contrary, Zuo1, the J domain protein component of the RAC complex that stimulates the ATPase activity of Ssb, was shown to bind the ribosome near the large subunit ribosomal protein L31, also situated at

the ribosome exit tunnel. Interestingly, it was previously suggested that the aminopeptidase from *Mycobacterium tuberculosis* might interact via a tandem proline-rich repeat motif, PXXP, with the Src homology 3 (SH3)-domain of the conserved large subunit ribosomal protein L24, a protein located in the vicinity of the chaperone-docking site L23 (2). The human BAG domain-containing protein, Bag-3 contains several PXXP motifs upstream of the BAG domain and it will be interesting to discern if this protein can bind the ribosome.

I predict that Snl1 will interact at or near the ribosome exit tunnel and as a result may function to recruit cytosolic Hsp70, Ssa to sample nascent polypeptides emerging for the ribosome. The position of Ssb near the ribosome exit tunnel suggests that Snl1 might be utilized as an NEF of Ssb for specific substrates. The hypothesis that Snl1 can directly interact with nascent polypeptides chains also needs to be investigated. Since both large and small subunits of the ribosome co-purify with Snl1, it is possible that Snl1 associates with an intact translating ribosome but further work will have to be done to test this.

Snl1 binds to ribosomes independently of Hsp70

Using three different approaches, I was able to provide evidence that the interaction of Snl1 with the ribosome was independent of its association with Hsp70 and its function as an NEF. However, the functional basis for this separation in binding is unknown. Snl1 might be recruiting Hsp70 to ribosomes, inviting comparisons to the recruitment of Ssb by RAC in fungi and more recently, the recruitment of cytosolic Hsp70 in mammals by the Zuo1 ortholog, Mpp11 (58). In both cases, the ribosome associated proteins served to (i) tether an Hsp70 to the ribosome and (ii) perform its function as a J protein to stimulate the ATPase activity of Hsp70. Snl1 might also fulfill both roles.

Genes encoding ribosomal proteins and other components of the translational machinery display coordinated regulation in response to environmental changes. This allows efficient adjustment of the protein synthetic capability of the cell. For example, upon carbon upshift the mRNA levels for ribosomal proteins increase and upon amino acid starvation, the mRNA levels for these proteins are decreased. It was shown that the mRNA levels of Ssb, the ribosome associated chaperone are co-regulated with ribosomal protein encoding mRNA under three different growth conditions tested (74). Using the Serial Pattern of Expression Levels Locator (SPELL) database, I found that *SNL1* mRNA levels correlated with those of ribosomal protein genes when queried over all available data sets (Table 3-2). This evidence along with the physical association of Snl1 with Ssb and the ribosome supports the contention that Snl1 is a component of the translational apparatus and suggests that cells may regulate the levels of Snl1 to match protein biosynthetic needs.

Functional roles for Snl1 at the ER membrane

What roles might Snl1 play while tethered to the endoplasmic reticulum (ER) membrane and associating with ribosomes? Determining the function of Snl1 in the cell is confounded by the lack of a detectable phenotype associated with cells lacking the protein. However, some speculations can be made on how Snl1 might function to bridge its interactions with Hsp70 and the ribosome. Because of the unique location of this Hsp70 NEF at the ER membrane, a role in protein translocation from the cytosol into the ER membrane or lumen can be envisioned. However, since co-translationally translocated proteins are recruited to the ER membrane in a signal recognition particle (SRP)-dependent manner, it seems unlikely that Snl1 would play a role in this pathway. In contrast, post-translationally translocated proteins must be directed to the ER translocon for import and require Hsp70/Ssa

binding while in the cytosol. Snl1 might serve to recruit an Ssa-substrate complex to the ER membrane through its Hsp70 binding site and in the process help to target non-SRP dependent substrates to the ER membrane. Testing this hypothesis is inhibited by the lack of a detectable phenotype for *snl1*Δ cells. In apparent disagreement with this idea, preliminary analysis of pre-pro-α-factor, a known post-translationally translocated substrate of Ssa1 showed no major defect in translocation in *snl1*Δ cells. However, other posttranslational substrates cannot be ruled out. Another area for investigation would be to test whether Snl1 is required for the translocation of membrane-tethered secretory pathway-dependent proteins that either remain in the ER or are secreted to the outer membrane. In line with this, Snl1 might function as an ER-localized NEF that assists Hsp70 to maintain and properly fold cytosolic domains of integrated ER membrane proteins.

Because Snl1 interacts with several ribosomal proteins, an area for investigation would be to test whether Snl1 plays a role in ribosome biogenesis. It was previously shown that ribosome-associated Hsp40, Jjj1 co-migrates with 60S ribosome subunits when total cellular extract from wild type yeast cells was separated on a sucrose gradient (83). This co-migration was related to ribosome biogenesis where exit and subsequent re-entry of biogenesis factors from the nucleus shuttled pre-60S particles into the cytosol for maturation. Since Snl1 preferentially binds the 60S ribosomal subunit (Chapter 3) and is tethered to the ER/nuclear membrane, a role in ribosome biogenesis is suggested. One way to test this would be to compare the growth of the individual mutants with the combined deletion of *SNL1* and *JJJ1* to assess synthetic growth defects. In cells lacking ribosome-associated components (RAC-Ssb and NAC), a reporter construct with a GFP-tagged ribosomal protein, L25, was visualized in the nucleus, indicating defects in assembly and export of pre-60S subunits into

the cytoplasm. This protein incorporates into the mature ribosome and therefore the fluorescent signal should be seen in the cytosol. Nuclear or cytosolic accumulation of this reporter in *snl1*Δ cells will determine if Snl1 is involved in ribosome biogenesis. In addition, it has been suggested that Ssb cycles between the cytoplasm and the nucleus and Snl1, which is at the ER/nuclear membrane could function as a targeting protein for Ssb at this location to enable Ssb to translocate efficiently through pores. Given the complexity of the ribosome biogenesis process, further efforts are needed to understand the functions of these chaperones in this process.

Although association of Snl1 with the ribosome suggests its involvement in protein biogenesis, a degradation process exists in yeast that requires the function of the cytosolic Hsp70 chaperone, Ssa. Because Snl1 co-purifies Ssa, it is possible that Snl1 may be involved in the ER-associated protein degradation (ERAD) pathway, which is a quality control process that selectively degrades terminally misfolded or unassembled secretory proteins. The ERAD of membrane and soluble proteins requires the 26S proteasome located in the cytosol and hence these proteins must be retrotranslocated from the ER to the cytosol. Ssa1 is required for the ERAD of several membrane proteins but is dispensable for ERAD of lumenal proteins. Snl1 could act as the ER-bound NEF for Ssa1 to maintain the solubility of misfolded cytosolic domains on some integral membrane ERAD substrates. This model for Snl1 function in ERAD requires further testing.

As observed in (Figure 3-2), in addition to the novel association of Snl1 with the ribosome, Fes1 was found to specifically interact with Ssa. The work done in Chapter 5 is a preliminary follow-up of my initial discovery and is discussed below.

Fes1 has a distinct preference to bind Ssa but not Ssb

To determine the binding preference of Fes1 for different types of Hsp70 proteins, I performed a co-immunoprecipitation experiment using FLAG-tagged Fes1. Interestingly, I found that Fes1 exhibited a strong bias for binding Ssa. This is the first reported evidence of an NEF that shows preference for one class of cytosolic Hsp70s in yeast and is in contrast to a previously published report that found His_6-tagged Fes1 to bind Ssb and perform its function of nucleotide exchange *in vitro*. A major difference in the previous report that identified Ssb to bind Fes1 was that recombinant tagged-Fes1 (expressed and purified from *E. coli*) was incubated with cell lysates from yeast and then affinity purified to determine Fes1 interacting partners. In the experimental set-up I used, tagged Fes1 was expressed and purified from *S. cerevisiae* before it was incubated with yeast cell lysates. How could the Fes1 expression system cause such a stark difference in binding to Ssb? To determine if the previous findings were in fact due to whether Fes1 was expressed in *E. coli* versus *S. cerevisiae*, I purified FLAG-Fes1 from *E. coli* to near homogeneity and incubated it with yeast cell lysate to determine Hsp70 binding partners. I found that Fes1 bound both Ssa and Ssb, corroborating previous data and implying that Fes1 produced in *S. cerevisiae* may be post-translationally different than Fes1 made in *E. coli*.

What are the conditions that prevent Fes1 made in yeast to interact with Ssb? One possible explanation for the lack of Fes1 binding to Ssb is its stoichiometric balance with respect to Ssb. Based on the number of protein molecules of Fes1 in the cell (13,100) compared to Sse1 (71,700), it could be argued that the abundance of Sse1 in the cell could preclude Fes1 from associating with Ssb (45). To test this, I moderately (2-fold) or highly (15-20-fold) overproduced Fes1 above chromosomal levels in a wild-type yeast strain to

determine if increased Fes1 expression would allow binding to Ssb. This was not the case as Fes1 expressed at both levels failed to bind Ssb. This suggests that the abundance of Fes1 in the cell is not a determinant for Ssb binding. Another possibility is that Sse1 might prevent Fes1 to associate with Ssb even when Fes1 is expressed at high levels in wild type cells. To test this, increasing expression levels of Fes1 in *sse1Δ* cells will determine if Sse1 precludes Fes1-Ssb interaction.

Another possible explanation why Fes1 does not bind Ssb *in vivo* could be because of the ribosome associated complex (RAC), which is known to associate with Ssb and regulate its ATPase activity at the ribosome. To test whether Zuo1 and Ssz1, the two components of RAC inhibited Fes1-Ssb interaction, I individually expressed and immunopurified tagged-Fes1 in a strain lacking either *ZUO1* or *SSZ1* to check if binding to Ssb was restored. From this experiment, I concluded that RAC components do not inhibit the interaction of Fes1 with Ssb. The other complex situated close to the ribosome exit tunnel and hence in close proximity to Ssb, is NAC. Whether Fes1 binds Ssb in the absence of NAC components is yet to be determined.

A third explanation is that Fes1 in yeast is posttranslationally modified. The activity and localization of proteins inside the cell can be regulated by reversible posttranslational modifications (PTMs) including acetylation, phosphorylation and ubiquitylation, which lead to regulation of protein domain activity or mediation of protein-protein interactions. A recent publication used mass spectrometry to identify PTMs in proteins and compiled a list of nearly 200,000 modification sites across 11 eukaryotic species in order to develop predictors of PTM functional relevance (9). When Fes1 was queried in this database, two residues were identified for PTM, lysine 16 (predicted ubiquitylated site) and threonine 143 (predicted

phosphorylation site). The human homolog HspBP1 was identified to contain one ubiquitylation site on residue 94. Further work is needed to test whether mutating these residues changes the ability of Fes1 to bind to Ssb in yeast cells.

Understanding the role of Hsp70 NEFs in difference cellular processes

Information obtained from the crystal structures of the Hsp70 NEFs and their nucleotide exchange mechanisms suggest that despite their different binding modes, most NEF families, which include their homologs in other organisms, appear to utilize similar nucleotide release mechanisms. The end result is the stabilization of the Hsp70 NBD in an open conformation by slightly tilting subdomain IIb. In addition, Sse1 homologs utilize their SBD, which exists in an extended conformation to wrap around the distal face of Hsp70. Fes1 and its homologs seem to utilize a different mechanism to bind Hsp70 and displace bound ADP. These proteins stabilize the outward rotation of subdomain IIb and induce local unfolding of lobe I of Hsp70. Structurally, the Hsp70-binding domain of Bag-1 and Fes1/HspBP1 are different, the former having a three helix bundle and the latter containing a succession of four Armadillo-like repeats (ARM1-ARM4). Each ARM is made of 3 α-helices that pack into a right-handed superhelix to produce a gently curved elongate molecule (Figure 5-1).

Overexpression of Fes1 or Snl1ΔN can rescue an otherwise synthetic *sse1*Δ*sse2*Δ strain suggesting some degree of functional redundancy among the NEFs. The proteins Swi6 and Swi4 form a heterodimeric transcription factor responsible for cell morphology and is activated by the MAP kinase Slt2. Our lab has shown that Sse1 in partnership with Hsp70 and Hsp90 is required for Slt2 maturation, which in turn is required for signaling through the cell wall integrity pathway (128). Loss of both *SSE1* and *SWI6* causes cells to become

amorphous and elongated and can be suppressed by overexpressing Fes1. This indicates that either NEF can partner with Hsp70 to facilitate cell integrity signaling and morphogenesis.

This redundancy amongst NEFs is not limited to the cytoplasm. Overexpression of the ER HspBP1 homolog Sil1 suppresses growth defects of a *ire1*Δ*lhs1*Δ yeast strain, where Lhs1 is the yeast ER Hsp110 homolog and Ire1 is a transmembrane kinase that is essential for the unfolded protein response pathway. However, recent experiments to determine which NEFs are involved in spindle organization revealed that only Sse1 played a role as an NEF of Ssa1/2 to maintain the proper distribution of the widely conserved kinesin-5 motor, Cin8 within the spindle, which in turn is required for bipolar spindle assembly in S phase. In mice, deletion of the ER Hsp110 homolog, Grp170 is lethal and indicates that the alternative NEF Sil1 also present in the ER cannot replace the function of Grp170. Mutations in *SIL1* disrupt Sil1 function resulting in a rare autosomal recessive neurodegenerative disorder called Marinesco-Sjögren syndrome that is characterized by the abnormal accumulation of ubiquitinated proteins in the ER and nucleus of Purkinje cells of the cerebellum. Grp170 cannot compensate for these mutations in Sil1. This evidence and other unpublished data from our lab suggest that different NEFs can act on Hsp70s with respect to cellular substrates. How Hsp70 surveys the available NEFs to determine a binding partner, who then enables Hsp70 to interact with its substrate, is still an open question. Specialization of NEFs especially BAG domain-containing proteins suggests only partial redundancy among the members of this family. These proteins do not seem to be regulators of protein folding by Hsp70 but appear to help target Hsp70 for specific functions. Apart from the BAG domain, which is a common feature of all Bag proteins, the N-terminal region of these proteins is uniquely different and allows individual Bag proteins to interact with distinct target proteins.

For instance, all four Bag-1 isoforms along with Bag-6 contain a ubiquitin-like domain and a nuclear localization signal, which means that these proteins can enter the nucleus. Bag-3 contains several tandem proline rich repeats, PXXP, which is a canonical binding domain for proteins that contain a Src homology 3 (SH3) motif. These findings indicate that Bag proteins may function as adaptor molecules that can recruit molecular chaperones to cellular targets through their N-terminal domains and motifs and this alter cellular functions including protein degradation, cell proliferation and apoptosis. In line with these findings, I have shown that two fungal BAG domain-containing proteins interact with the ribosome and suggest that this protein may act as a bridge between protein biogenesis and folding at the ER membrane.

Role of yeast in modeling chaperone function

Model organisms have been used frequently to determine the functions of chaperones in preventing the aggregation of relevant disease-causing proteins. The remarkable homology between these organisms has provided many good reasons to use model systems to study cellular processes and find targets that will lead to treatments of human disease. For example, the etiology of Aβ in Alzheimer's disease has been the concerted effort of research done using fruitflies, worms, budding yeast and mice. It is becoming evident that multiple approaches within these model systems will be needed to make significant advances towards developing therapies.

The budding yeast, *S. cerevisiae* is a good model to study human disease because (i) 25% of positionally cloned human disease-causing genes has a close yeast homolog and (ii) yeast is readily amenable to analysis (7). In addition, 60% of yeast genes have human homologs or contain at least one conserved domain with human genes (15, 138). In 1996, the

complete genome of *S. cerevisiae* was sequenced and this lead to the identification of orthologs of human genes. Orthologs are genes in different species that are related by vertical descent from a common ancestor and normally perform the same function. Thus, yeast has been used extensively as a model to dissect the functions of chaperones, which has expanded into manipulating the proteostasis network in the cell in order to prevent protein misfolding and aggregation. As discussed in chapter 1, there are numerous chaperones involved in maintaining protein homeostasis, most of which are evolutionarily conserved from yeast to humans. Thus, the roles of chaperones in preventing protein aggregation in the cell can be analyzed using in a tractable model organism like yeast. For example, the cooperation of different chaperones during polyQ aggregation was tested in a yeast model using sequential immunoprecipitations and mass spectrometry to identify proteins associated with an aggregation-prone Q103 fragment in the early and late stages following induction of its expression (155). Hsp70, Hsp90, Hsp26 and other chaperones interacted with this fragment within two hours, followed by partial release of these chaperones prior to the maturation of the aggregates and before the recruitment of Hsp104. Use of a small chemical molecule 115-7c, which stimulates ATP turnover of Hsp70 by favoring its interaction with co-chaperone Hsp40 and locking it in the substrate-binding state retained Hsp70 and Hsp90 on the Q103 fragment and limited the exchange for Hsp104, resulting in incomplete disaggregation and suggests that partial release of Hsp70 may be an essential step in expanded polyQ processing in yeast.

Yeast is also becoming an attractive tool in drug discovery. Compound screens have led to the successful identification of inhibitors of α-synuclein aggregation and toxicity, which may prove to be effective pharmaceutical therapeutics in the future (50). Similarly,

compound screens in a yeast model can be used to target chaperones, which can either enhance their function and prevent protein aggregation or reduce their function in cases involving premature degradation of cellular proteins. For example, mutation of either Hsp70 or its co-chaperone Ydj1 reduces degradation of CFTR in models of cystic fibrosis (166). Consistent with this, co-chaperones that regulate Hsp70 functions are also thought to be important in disease. For example, the interaction of Hsp70 with Bag-2 is important for the clearance of misfolded tau, involved in Alzheimer's disease (19). However, there is much more work needed to understand chaperone functions, their interacting substrates, how co-chaperones direct a substrate to them and shape its activities and the cooperation of chaperones with the protein degradation machinery to maintain proteostasis. In all these cases, the study of chaperones in yeast is proving to be an efficient and quick way to discern their functions, which can later be applied to mammalian and human systems.

Perspectives

The genome sequence of *S. cerevisiae* was completed in 1996 followed by the first genome-wide "bar-coded" yeast gene knockout (YKO) mutant collection made available in 2002, ushering in the era of yeast genomics and proteomics (46). Our understanding of protein quality control in cells has been made possible from decades of pathway- and gene-specific investigations and we now know most of the players involved in maintaining the integrity of the cellular proteome. The challenge for the future will be to determine how these components interact and how they are organized into functional networks to promote the life of a cell. This knowledge can then be translated to understanding similar questions in human cells, with the key goal to devise methods to modulate the network to further human health.

Identification of a function of Snl1 in yeast cells with relation to its interaction with ribosomes has been hindered due to the lack of a detectable phenotype associated with loss of *SNL1*. Studies involving genetic interactions have been extremely useful to characterize gene function and identifying pathways that the gene product is involved in the cell. Previously, systematic analysis of genome-wide gene-gene synthetic lethality interactions has provided an effective way to study gene functions but have been unsuccessful with identifying a pathway-specific function for *SNL1* (146). A new technique, dSLAM (heterozygous diploid-based synthetic lethality analysis on microarrays) has been developed that combines heterozygous diploid YKO mutants in pooled form and the efficiency of a microarray analysis of abundance of YKOs in the population (100). For each YKO, its relative growth rate as a single and double mutant (in combination with *SNL1*) can be indirectly compared by microarray analysis of the abundance of "bar-codes" in both the haploid single (control) and double (experiment) mutant pools. This technique may deliver a set of putative interactors of *SNL1* to test. Another approach that would enable potential capture of Snl1-dependent substrates during protein translation is ribosome profiling. This approach maps the position of ribosomes on mRNA transcripts by nuclease footprinting. The abundance of various footprint fragments in deep sequencing data will indicate the amount of translation of a gene (61). This technique was used previously to quantitatively monitor translation rates and to identify when the *E. coli* ribosome-associated chaperone trigger factor engages polypeptides (97). Since we have shown that membrane associated Snl1 can efficiently bind ribosomes, selective profiling of ribosomes that are bound to Snl1 and affinity purified from yeast cells may enable the identification of mRNA transcripts being translated by ribosomes bound by Snl1. Thus, these global analyses using genetic and biochemical approaches should help to

discern a functional role for Snl1. Future efforts to determine the coordinated action of various ribosome-associated chaperones, processing enzymes and targeting factors that ensure the efficient biogenesis of cellular proteins is warranted. In line with this, kinetic flux of newly synthesized proteins that transit through the cytosolic Hsp70s, Ssa and Ssb, and their NEFs can be determined using pulse chase analysis. This technique was used previously to show the transient rate of association of Sse1, Ssa and Ssb with newly synthesized polypeptides during *de novo* folding and the effect of the loss of *SSB* on chaperone utilization during translation. (163). A similar approach may provide additional insights into the role of Snl1 in cellular protein biogenesis.

Eukaryotic cells employ a number of complex targeting pathways to efficiently and accurately deliver nascent polypeptides to organelles. Hsp70 and Hsp90 chaperones are utilized for targeting to mitochondria and chloroplasts and receptors capable of recognizing these chaperones have been identified on the surface of both organelles (36, 132). Although the role of these receptors is not fully understood, they may help to increase the efficiency of protein targeting. It is also less clear whether these membrane receptors contribute to targeting specificity. Since Hsp70 is involved in targeting to many cellular organelles, targeting to a cellular localization must be more than a substrate recognition event. For instance, a single chaperone or a combination of chaperones may function in tandem to properly deliver a substrate to its precise location in the cell. If this is true, how is targeting regulated and how do co-chaperones play a role? The localization of Snl1 at the ER membrane and its ability to bind ribosomes and Hsp70 independent of the other suggests that this BAG domain-containing protein may serve as a targeting receptor for Hsp70 in yeast cells. Targeting tail-anchored (TA) membrane proteins to the ER in yeast was shown to

require a highly coordinated sequence of events and involved a conserved set of proteins. This guided entry of TA proteins (GET) pathway was shown to be independent of the well-studied signal recognition particle (SRP) complex-dependent pathway. It is possible that ribosomes translating TA proteins may be associated with Snl1, which then recruits Hsp70 to the ER for substrate folding. Loss of GET complex components leads to mislocalization of a number of TA proteins including Sbh1/2 and Scs2 (126). Proper ER localization of these fluorescent-tagged proteins can be tested in *snl1Δ* cells and can be complemented by the Hsp70- and ribosome- binding mutants of Snl1 to determine whether either binary complex is involved in this pathway. A key step in the GET pathway is formation of a complex between Get3 and the TA protein being translated. Unlike SRP, Get3 does not associate with ribosomes (76) and it remains unclear whether this protein surveys all TA proteins and commits only ER-bound ones or whether TA protein-containing signals are sorted at an earlier step. It is possible that Snl1 present at the ER membrane and associated with translating ribosomes could assist in Get3 detection of its substrates.

One area ripe for further investigation involves identifying the coordinated functions of NEFs and J domain-containing proteins in Hsp70 regulation. In yeast cells, the cytosol contains 11 J proteins and three NEFs. The functional overlap and differences between these co-chaperones for specific substrates is an active area for research. For example, it has been shown that the Hsp70 co-chaperone Ydj1 possesses a C-terminal CAAX sequence, where A is an aliphatic amino acid and X is any residue, and this sequence specifies the addition of a farnesyl modification group to Ydj1, which converts the cytosolic protein to one that can attach to the ER and perinuclear membranes (18). It is tempting to speculate that under certain cellular conditions, farnesylation of Ydj1 may target it to the cytosolic face of the ER

membrane, which along with Snl1 could enhance Hsp70-dependent folding at this specific location. This modification has been shown to have specific roles in protein-protein interactions, particularly those that facilitate protein trafficking and subcellular localization (137). Further, the specific Snl1 binding site on the ribosome and how its interaction is coordinated with several other ribosome-associated factors including SRP, NAC complex and RAC complex remain important questions for future studies.

Fes1 and Ydj1 have been suggested to play antagonistic functions with regard to their respective negative and positive regulation of Ssa1 ATPase activity (63). However, it is not clear whether these two proteins compete for binding to Ssa1 or if substrates regulate the temporal interaction of Ssa1 with its co-chaperones. An *ab initio* construction of the *S. cerevisiae* transcriptome by parallel mRNA sequencing identified a previously uncharacterized intron in the *FES1* gene with full reads through the splice junction and inside the intron, suggesting alternative splicing (165). In the spliced variant, the annotated stop codon is removed and a later stop codon is introduced resulting in a 10 amino acid extension, which was validated by RT-PCR showing bands consistent with both forms. It is therefore possible that under certain conditions, unknown at present, Fes1 is available in an alternate form, which then dictates its Hsp70-binding function. It will be interesting to discern whether spliced Fes1 could play a role in Fes1 interaction with Ssb. HspBP1, the Fes1 homolog in human cells, is the least efficient NEF as measured by ADP dissociation constants in vitro, and is inhibitory of Hsc70 refolding function (150). In addition, HspBP1 was shown to promote degradation of proteins and block anti-apoptotic functions of stress-induced Hsp70. These findings are consistent with HspBP1 acting as an inhibitor of Hsp70, possibly as a function of relative NEF/70 stoichiometry (3, 145). It seems likely that cytosolic NEFs can

accommodate three functions: Fes1 and its homologs inhibit Hsp70 and may be utilized when protein degradation as opposed to protein refolding is a better survival strategy for cells. The Sse family is the strongest activator of Hsp70 ATPase and may be better suited to assist in refolding. The ability of Snl1 and its homologs to associate with other functional domains in proteins suggests a more specialized role for these NEFs in Hsp70 targeting and recruitment.

The Hsp70 chaperone system has been subject to intense evaluation for a number of years with regard to identifying components and pathways that are required to maintain homeostasis of the cellular proteome. The next decade or more will be focused on identifying how these components and pathways are interconnected to promote cellular survival under normal and stress conditions and in designing pharmacological chaperones to modulate these pathways. I anticipate that a combined effort by various groups using different model organisms will help to understand these networks and will be key to elucidating their *in vivo* functional significance.

Bibliography

1. **Abate, C., L. Patel, F. J. R. III, and T. Curran**. 1990. Redox regulation of Fos and Jun DNA-binding activity in vitro. Science **249**:1157-1161.
2. **Addlagatta, A., M. L. Quillin, O. Omotoso, J. O. Liu, and B. W. Matthews**. 2005. Identification of an SH3-binding motif in a new class of methionine aminopeptidases from Mycobacterium tuberculosis suggests a mode of interaction with the ribosome. Biochemistry **44**:7166-7174.
3. **Alberti, S., K. Bohse, V. Arndt, A. Schmitz, and J. Hohfeld**. 2004. The cochaperone HspBP1 inhibits the CHIP ubiquitin ligase and stimulates the maturation of the cystic fibrosis transmembrane conductance regulator. Mol Biol Cell **15**:4003-4010.
4. **Andreasson, C., H. Rampelt, J. Fiaux, S. Druffel-Augustin, and B. Bukau**. 2010. The endoplasmic reticulum Grp170 acts as a nucleotide exchange factor of Hsp70 via a mechanism similar to that of the cytosolic Hsp110. J Biol Chem **285**:12445-12453.
5. **Arakawa, A., N. Handa, N. Ohsawa, M. Shida, T. Kigawa, F. Hayashi, M. Shirouzu, and S. Yokoyama**. 2010. The C-terminal BAG domain of BAG5 induces conformational changes of the Hsp70 nucleotide-binding domain for ADP-ATP exchange. Structure **18**:309-319.
6. **Balch, W. E., R. I. Morimoto, A. Dillin, and J. W. Kelly**. 2008. Adapting proteostasis for disease intervention. Science **319**:916-919.
7. **Bassett, D. E., Jr., M. S. Boguski, and P. Hieter**. 1996. Yeast genes and human disease. Nature **379**:589-590.

8. **Becker, J., W. Walter, W. Yan, and E. A. Craig**. 1996. Functional interaction of cytosolic hsp70 and a DnaJ-related protein, Ydj1p, in protein translocation in vivo. Mol Cell Biol **16**:4378-4386.

9. **Beltrao, P., V. Albanese, L. R. Kenner, D. L. Swaney, A. Burlingame, J. Villen, W. A. Lim, J. S. Fraser, J. Frydman, and N. J. Krogan**. 2012. Systematic functional prioritization of protein posttranslational modifications. Cell **150**:413-425.

10. **Bernstein, K. A., J. E. Gallagher, B. M. Mitchell, S. Granneman, and S. J. Baserga**. 2004. The small-subunit processome is a ribosome assembly intermediate. Eukaryotic cell **3**:1619-1626.

11. **Bhattacharyya, T., A. N. Karnezis, S. P. Murphy, T. Hoang, B. C. Freeman, B. Phillips, and R. I. Morimoto**. 1995. Cloning and subcellular localization of human mitochondrial hsp70. J Biol Chem **270**:1705-1710.

12. **Bienz, M., and H. R. Pelham**. 1986. Heat shock regulatory elements function as an inducible enhancer in the Xenopus hsp70 gene and when linked to a heterologous promoter. Cell **45**:753-760.

13. **Boorstein, W. R., T. Ziegelhoffer, and E. A. Craig**. 1994. Molecular evolution of the HSP70 multigene family. J Mol Evol **38**:1-17.

14. **Borkovich, K. A., F. W. Farrelly, D. B. Finkelstein, J. Taulien, and S. Lindquist**. 1989. hsp82 is an essential protein that is required in higher concentrations for growth of cells at higher temperatures. Mol Cell Biol **9**:3919-3930.

15. **Botstein, D., S. A. Chervitz, and J. M. Cherry**. 1997. Yeast as a model organism [comment]. Science **277**:1259-1260.

16. **Briknarova, K., S. Takayama, S. Homma, K. Baker, E. Cabezas, D. W. Hoyt, Z. Li, A. C. Satterthwait, and K. R. Ely**. 2002. BAG4/SODD protein contains a short BAG domain. J Biol Chem **277**:31172-31178.

17. **Bukau, B., J. Weissman, and A. Horwich**. 2006. Molecular chaperones and protein quality control. Cell **125**:443-451.

18. **Caplan, A. J., J. Tsai, P. J. Casey, and M. G. Douglas**. 1992. Farnesylation of YDJ1p is required for function at elevated growth temperatures in Saccharomyces cerevisiae. J Biol Chem **267**:18890-18895.

19. **Carrettiero, D. C., I. Hernandez, P. Neveu, T. Papagiannakopoulos, and K. S. Kosik**. 2009. The cochaperone BAG2 sweeps paired helical filament- insoluble tau from the microtubule. J Neurosci **29**:2151-2161.

20. **Cashikar, A. G., M. Duennwald, and S. L. Lindquist**. 2005. A chaperone pathway in protein disaggregation. Hsp26 alters the nature of protein aggregates to facilitate reactivation by Hsp104. J Biol Chem **280**:23869-23875.

21. **Chernoff, Y. O., S. L. Lindquist, B. Ono, S. G. Inge-Vechtomov, and S. W. Liebman**. 1995. Role of the chaperone protein Hsp104 in propagation of the yeast prion-like factor [psi+]. Science **268**:880-884.

22. **Chung, K. T., Y. Shen, and L. M. Hendershot**. 2002. BAP, a mammalian BiP-associated protein, is a nucleotide exchange factor that regulates the ATPase activity of BiP. J Biol Chem **277**:47557-47563.

23. **Cohen, E., J. Bieschke, R. M. Perciavalle, J. W. Kelly, and A. Dillin**. 2006. Opposing activities protect against age-onset proteotoxicity. Science **313**:1604-1610.

24. **Costanzo, M., A. Baryshnikova, J. Bellay, Y. Kim, E. D. Spear, C. S. Sevier, H. Ding, J. L. Koh, K. Toufighi, S. Mostafavi, J. Prinz, R. P. St Onge, B. VanderSluis, T. Makhnevych, F. J. Vizeacoumar, S. Alizadeh, S. Bahr, R. L. Brost, Y. Chen, M. Cokol, R. Deshpande, Z. Li, Z. Y. Lin, W. Liang, M. Marback, J. Paw, B. J. San Luis, E. Shuteriqi, A. H. Tong, N. van Dyk, I. M. Wallace, J. A. Whitney, M. T. Weirauch, G. Zhong, H. Zhu, W. A. Houry, M. Brudno, S. Ragibizadeh, B. Papp, C. Pal, F. P. Roth, G. Giaever, C. Nislow, O. G. Troyanskaya, H. Bussey, G. D. Bader, A. C. Gingras, Q. D. Morris, P. M. Kim, C. A. Kaiser, C. L. Myers, B. J. Andrews, and C. Boone**. 2010. The genetic landscape of a cell. Science **327**:425-431.

25. **de Keyzer, J., G. J. Steel, S. J. Hale, D. Humphries, and C. J. Stirling**. 2009. Nucleotide binding by Lhs1p is essential for its nucleotide exchange activity and for function in vivo. J Biol Chem **284**:31564-31571.

26. **del Alamo, M., D. J. Hogan, S. Pechmann, V. Albanese, P. O. Brown, and J. Frydman**. 2011. Defining the specificity of cotranslationally acting chaperones by systematic analysis of mRNAs associated with ribosome-nascent chain complexes. PLoS Biol **9**:e1001100.

27. **Demand, J., S. Alberti, C. Patterson, and J. Hohfeld**. 2001. Cooperation of a ubiquitin domain protein and an E3 ubiquitin ligase during chaperone/proteasome coupling. Curr Biol **11**:1569-1577.

28. **Deshaies, R. J., B. D. Koch, M. Werner-Washburne, E. A. Craig, and R. Schekman**. 1988. A subfamily of stress proteins facilitates translocation of secretory and mitochondrial precursor polypeptides. Nature **332**:800-805.

29. **Diez, S., B. L. Gomez, A. Restrepo, R. J. Hay, and A. J. Hamilton**. 2002. Paracoccidioides brasiliensis 87-kilodalton antigen, a heat shock protein useful in diagnosis: characterization, purification, and detection in biopsy material via immunohistochemistry. J Clin Microbiol **40**:359-365.

30. **Dou, F., W. J. Netzer, K. Tanemura, F. Li, F. U. Hartl, A. Takashima, G. K. Gouras, P. Greengard, and H. Xu**. 2003. Chaperones increase association of tau protein with microtubules. Proc Natl Acad Sci U S A **100**:721-726.

31. **Dragovic, Z., S. A. Broadley, Y. Shomura, A. Bracher, and F. U. Hartl**. 2006. Molecular chaperones of the Hsp110 family act as nucleotide exchange factors of Hsp70s. EMBO J **25**:2519-2528.

32. **Dragovic, Z., Y. Shomura, N. Tzvetkov, F. U. Hartl, and A. Bracher**. 2006. Fes1p acts as a nucleotide exchange factor for the ribosome-associated molecular chaperone Ssb1p. Biol Chem **387**:1593-1600.

33. **Ellis, R. J., and A. P. Minton**. 2003. Cell biology: join the crowd. Nature **425**:27-28.

34. **Ellis, R. J., and A. P. Minton**. 2006. Protein aggregation in crowded environments. Biol Chem **387**:485-497.

35. **Ewalt, K. L., J. P. Hendrick, W. A. Houry, and F. U. Hartl**. 1997. In vivo observation of polypeptide flux through the bacterial chaperonin system. Cell **90**:491-500.

36. **Faou, P., and N. J. Hoogenraad**. 2012. Tom34: a cytosolic cochaperone of the Hsp90/Hsp70 protein complex involved in mitochondrial protein import. Biochim Biophys Acta **1823**:348-357.

37. **Fink, J. K.** 2002. Hereditary spastic paraplegia: the pace quickens. Ann Neurol **51**:669-672.

38. **Flaherty, K. M., C. DeLuca-Flaherty, and D. B. McKay**. 1990. Three-dimensional structure of the ATPase fragment of a 70K heat-shock cognate protein. Nature **346**:623-628.

39. **Fonzi, W. A., and M. Y. Irwin**. 1993. Isogenic strain construction and gene mapping in Candida albicans. Genetics **134**:717-728.

40. **Frydman, J.** 2001. Folding of newly translated proteins in vivo: the role of molecular chaperones. Annu Rev Biochem **70**:603-647.

41. **Frydman, J., E. Nimmesgern, H. Erdjument-Bromage, J. S. Wall, P. Tempst, and F. U. Hartl**. 1992. Function in protein folding of TRiC, a cytosolic ring complex containing TCP-1 and structurally related subunits. EMBO J **11**:4767-4778.

42. **Gasch, A. P., P. T. Spellman, C. M. Kao, O. Carmel-Harel, M. B. Eisen, G. Storz, D. Botstein, and P. O. Brown**. 2000. Genomic expression programs in the response of yeast cells to environmental changes. Mol Biol Cell **11**:4241-4257.

43. **Gautschi, M., H. Lilie, U. Funfschilling, A. Mun, S. Ross, T. Lithgow, P. Rucknagel, and S. Rospert**. 2001. RAC, a stable ribosome-associated complex in yeast formed by the DnaK-DnaJ homologs Ssz1p and zuotin. Proc Natl Acad Sci U S A **98**:3762-3767.

44. **Gerami-Nejad, M., J. Berman, and C. A. Gale**. 2001. Cassettes for PCR-mediated construction of green, yellow, and cyan fluorescent protein fusions in Candida albicans. Yeast **18**:859-864.

45. **Ghaemmaghami, S., W. K. Huh, K. Bower, R. W. Howson, A. Belle, N. Dephoure, E. K. O'Shea, and J. S. Weissman**. 2003. Global analysis of protein expression in yeast. Nature **425**:737-741.

46. **Giaever, G., A. M. Chu, L. Ni, C. Connelly, L. Riles, S. Veronneau, S. Dow, A. Lucau-Danila, K. Anderson, B. Andre, A. P. Arkin, A. Astromoff, M. El-Bakkoury, R. Bangham, R. Benito, S. Brachat, S. Campanaro, M. Curtiss, K. Davis, A. Deutschbauer, K. D. Entian, P. Flaherty, F. Foury, D. J. Garfinkel, M. Gerstein, D. Gotte, U. Guldener, J. H. Hegemann, S. Hempel, Z. Herman, D. F. Jaramillo, D. E. Kelly, S. L. Kelly, P. Kotter, D. LaBonte, D. C. Lamb, N. Lan, H. Liang, H. Liao, L. Liu, C. Luo, M. Lussier, R. Mao, P. Menard, S. L. Ooi, J. L. Revuelta, C. J. Roberts, M. Rose, P. Ross-Macdonald, B. Scherens, G. Schimmack, B. Shafer, D. D. Shoemaker, S. Sookhai-Mahadeo, R. K. Storms, J. N. Strathern, G. Valle, M. Voet, G. Volckaert, C. Y. Wang, T. R. Ward, J. Wilhelmy, E. A. Winzeler, Y. Yang, G. Yen, E. Youngman, K. Yu, H. Bussey, J. D. Boeke, M. Snyder, P. Philippsen, R. W. Davis, and M. Johnston**. 2002. Functional profiling of the Saccharomyces cerevisiae genome. Nature **418**:387-391.

47. **Goff, S. A., and A. L. Goldberg**. 1985. Production of abnormal proteins in E. coli stimulates transcription of lon and other heat shock genes. Cell **41**:587-595.

48. **Gong, Y., Y. Kakihara, N. Krogan, J. Greenblatt, A. Emili, Z. Zhang, and W. A. Houry**. 2009. An atlas of chaperone-protein interactions in Saccharomyces cerevisiae: implications to protein folding pathways in the cell. Mol Syst Biol **5**:275.

49. **Greene, M. K., K. Maskos, and S. J. Landry**. 1998. Role of the J-domain in the cooperation of Hsp40 with Hsp70. Proc Natl Acad Sci U S A **95**:6108-6113.

50. **Griffioen, G., H. Duhamel, N. Van Damme, K. Pellens, P. Zabrocki, C. Pannecouque, F. van Leuven, J. Winderickx, and S. Wera**. 2006. A yeast-based model of alpha-synucleinopathy identifies compounds with therapeutic potential. Biochim Biophys Acta **1762**:312-318.

51. **Hartl, F. U.** 1996. Molecular chaperones in cellular protein folding. Nature **381**:571-579.

52. **Hartl, F. U., A. Bracher, and M. Hayer-Hartl**. 2011. Molecular chaperones in protein folding and proteostasis. Nature **475**:324-332.

53. **Hendershot, L. M., V. A. Valentine, A. S. Lee, S. W. Morris, and D. N. Shapiro**. 1994. Localization of the gene encoding human BiP/GRP78, the endoplasmic reticulum cognate of the HSP70 family, to chromosome 9q34. Genomics **20**:281-284.

54. **Ho, A. K., G. A. Raczniak, E. B. Ives, and S. R. Wente**. 1998. The integral membrane protein snl1p is genetically linked to yeast nuclear pore complex function. Mol Biol Cell **9**:355-373.

55. **Hoffner, G., and P. Djian**. 2002. Protein aggregation in Huntington's disease. Biochimie **84**:273-278.

56. **Horton, L. E., P. James, E. A. Craig, and J. O. Hensold**. 2001. The yeast hsp70 homologue Ssa is required for translation and interacts with Sis1 and Pab1 on translating ribosomes. J Biol Chem **276**:14426-14433.

57. **Hsu, A. L., C. T. Murphy, and C. Kenyon**. 2003. Regulation of aging and age-related disease by DAF-16 and heat-shock factor. Science **300**:1142-1145.

58. **Huang, P., M. Gautschi, W. Walter, S. Rospert, and E. A. Craig**. 2005. The Hsp70 Ssz1 modulates the function of the ribosome-associated J-protein Zuo1. Nat Struct Mol Biol **12**:497-504.

59. **Huber, D., N. Rajagopalan, S. Preissler, M. A. Rocco, F. Merz, G. Kramer, and B. Bukau**. 2011. SecA interacts with ribosomes in order to facilitate posttranslational translocation in bacteria. Mol Cell **41**:343-353.

60. **Hundley, H., H. Eisenman, W. Walter, T. Evans, Y. Hotokezaka, M. Wiedmann, and E. Craig**. 2002. The in vivo function of the ribosome-associated Hsp70, Ssz1, does not require its putative peptide-binding domain. Proc Natl Acad Sci U S A **99**:4203-4208.

61. **Ingolia, N. T., G. A. Brar, S. Rouskin, A. M. McGeachy, and J. S. Weissman**. 2012. The ribosome profiling strategy for monitoring translation in vivo by deep sequencing of ribosome-protected mRNA fragments. Nature protocols **7**:1534-1550.

62. **James, P., C. Pfund, and E. A. Craig**. 1997. Functional specificity among Hsp70 molecular chaperones. Science **275**:387-389.

63. **Kabani, M., J. M. Beckerich, and J. L. Brodsky**. 2002. Nucleotide exchange factor for the yeast Hsp70 molecular chaperone Ssa1p. Mol Cell Biol **22**:4677-4689.

64. **Kabani, M., J. M. Beckerich, and C. Gaillardin**. 2000. Sls1p stimulates Sec63p-mediated activation of Kar2p in a conformation-dependent manner in the yeast endoplasmic reticulum. Mol Cell Biol **20**:6923-6934.

65. **Kabani, M., C. McLellan, D. A. Raynes, V. Guerriero, and J. L. Brodsky**. 2002. HspBP1, a homologue of the yeast Fes1 and Sls1 proteins, is an Hsc70 nucleotide exchange factor. FEBS Lett **531**:339-342.

66. **Kaiser, C., S. Michaelis, and A. Mitchell**. 1994. Methods in Yeast Genetics, p. 234. Cold Spring Harbor Laboratory Press, New York.

67. **Kampinga, H. H., and E. A. Craig**. 2010. The HSP70 chaperone machinery: J proteins as drivers of functional specificity. Nat Rev Mol Cell Biol **11**:579-592.

68. **Klinge, S., F. Voigts-Hoffmann, M. Leibundgut, S. Arpagaus, and N. Ban**. 2011. Crystal structure of the eukaryotic 60S ribosomal subunit in complex with initiation factor 6. Science **334**:941-948.

69. **Kramer, G., D. Boehringer, N. Ban, and B. Bukau**. 2009. The ribosome as a platform for co-translational processing, folding and targeting of newly synthesized proteins. Nat Struct Mol Biol **16**:589-597.

70. **Kramer, G., T. Rauch, W. Rist, S. Vorderwulbecke, H. Patzelt, A. Schulze-Specking, N. Ban, E. Deuerling, and B. Bukau**. 2002. L23 protein functions as a chaperone docking site on the ribosome. Nature **419**:171-174.

71. **Kruger, R., W. Kuhn, T. Muller, D. Woitalla, M. Graeber, S. Kosel, H. Przuntek, J. T. Epplen, L. Schols, and O. Riess**. 1998. Ala30Pro mutation in the gene encoding alpha-synuclein in Parkinson's disease. Nat Genet **18**:106-108.

72. **Laloraya, S., B. D. Gambill, and E. A. Craig**. 1994. A role for a eukaryotic GrpE-related protein, Mge1p, in protein translocation. Proc Natl Acad Sci U S A **91**:6481-6485.

73. **Lindquist, S., and E. A. Craig**. 1988. The heat-shock proteins. Annu Rev Genet **22**:631-677.

74. **Lopez, N., J. Halladay, W. Walter, and E. A. Craig**. 1999. SSB, encoding a ribosome-associated chaperone, is coordinately regulated with ribosomal protein genes. J Bacteriol **181**:3136-3143.

75. **Lopez-Buesa, P., C. Pfund, and E. A. Craig**. 1998. The biochemical properties of the ATPase activity of a 70-kDa heat shock protein (Hsp70) are governed by the C-terminal domains. Proc Natl Acad Sci U S A **95**:15253-15258.

76. **Mariappan, M., X. Li, S. Stefanovic, A. Sharma, A. Mateja, R. J. Keenan, and R. S. Hegde**. 2010. A ribosome-associating factor chaperones tail-anchored membrane proteins. Nature **466**:1120-1124.

77. **Martinez-Pastor, M. T., G. Marchler, C. Schuller, A. Marchler-Bauer, H. Ruis, and F. Estruch**. 1996. The *Saccharomyces cerevisiae* zinc finger proteins Msn2p and Msn4p are required for transcriptional induction through the stress response element (STRE). EMBO J **15**:2227-2235.

78. **McCarty, J. S., A. Buchberger, J. Reinstein, and B. Bukau**. 1995. The role of ATP in the functional cycle of the DnaK chaperone system. J Mol Biol **249**:126-137.

79. **McClellan, A. J., and J. L. Brodsky**. 2000. Mutation of the ATP-binding pocket of SSA1 indicates that a functional interaction between Ssa1p and Ydj1p is required for post-translational translocation into the yeast endoplasmic reticulum. Genetics **156**:501-512.

80. **McLean, P. J., H. Kawamata, S. Shariff, J. Hewett, N. Sharma, K. Ueda, X. O. Breakefield, and B. T. Hyman**. 2002. TorsinA and heat shock proteins act as molecular chaperones: suppression of alpha-synuclein aggregation. J Neurochem **83**:846-854.

81. **McMillan, D. R., X. Xiao, L. Shao, K. Graves, and I. J. Benjamin**. 1998. Targeted disruption of heat shock transcription factor 1 abolishes thermotolerance and protection against heat-inducible apoptosis. J Biol Chem **273**:7523-7528.

82. **McNaught, K. S., P. Shashidharan, D. P. Perl, P. Jenner, and C. W. Olanow**. 2002. Aggresome-related biogenesis of Lewy bodies. Eur J Neurosci **16**:2136-2148.

83. **Meyer, A. E., N. J. Hung, P. Yang, A. W. Johnson, and E. A. Craig**. 2007. The specialized cytosolic J-protein, Jjj1, functions in 60S ribosomal subunit biogenesis. Proc Natl Acad Sci U S A **104**:1558-1563.

84. **Miao, B., J. E. Davis, and E. A. Craig**. 1997. Mge1 functions as a nucleotide release factor for Ssc1, a mitochondrial Hsp70 of Saccharomyces cerevisiae. J Mol Biol **265**:541-552.

85. **Morimoto, R. I., P. E. Kroeger, and J. J. Cotto**. 1996. The transcriptional regulation of heat shock genes: a plethora of heat shock factors and regulatory conditions. EXS **77**:139-163.

86. **Morley, J. F., H. R. Brignull, J. J. Weyers, and R. I. Morimoto**. 2002. The threshold for polyglutamine-expansion protein aggregation and cellular toxicity is dynamic and influenced by aging in Caenorhabditis elegans. Proc Natl Acad Sci U S A **99**:10417-10422.

87. **Morley, J. F., and R. I. Morimoto**. 2004. Regulation of longevity in Caenorhabditis elegans by heat shock factor and molecular chaperones. Mol Biol Cell **15**:657-664.

88. **Muchowski, P. J., G. Schaffar, A. Sittler, E. E. Wanker, M. K. Hayer-Hartl, and F. U. Hartl**. 2000. Hsp70 and hsp40 chaperones can inhibit self-assembly of

polyglutamine proteins into amyloid-like fibrils. Proc Natl Acad Sci U S A **97**:7841-7846.

89. **Mukai, H., T. Kuno, H. Tanaka, D. Hirata, T. Miyakawa, and C. Tanaka**. 1993. Isolation and characterization of SSE1 and SSE2, new members of the yeast HSP70 multigene family. Gene **132**:57-66.

90. **Mumberg, D., R. Muller, and M. Funk**. 1995. Yeast vectors for the controlled expression of heterologous proteins in different genetic backgrounds. Gene **156**:119-122.

91. **Munro, S., and H. R. Pelham**. 1986. An Hsp70-like protein in the ER: identity with the 78 kd glucose-regulated protein and immunoglobulin heavy chain binding protein. Cell **46**:291-300.

92. **Naeem, A., and N. A. Fazili**. 2011. Defective protein folding and aggregation as the basis of neurodegenerative diseases: the darker aspect of proteins. Cell biochemistry and biophysics **61**:237-250.

93. **Nakai, A.** 1999. New aspects in the vertebrate heat shock factor system: Hsf3 and Hsf4. Cell Stress Chaperones **4**:86-93.

94. **Nelson, R. J., T. Ziegelhoffer, C. Nicolet, M. Werner-Washburne, and E. A. Craig**. 1992. The translation machinery and 70 kd heat shock protein cooperate in protein synthesis. Cell **71**:97-105.

95. **Neumann, M., D. M. Sampathu, L. K. Kwong, A. C. Truax, M. C. Micsenyi, T. T. Chou, J. Bruce, T. Schuck, M. Grossman, C. M. Clark, L. F. McCluskey, B. L. Miller, E. Masliah, I. R. Mackenzie, H. Feldman, W. Feiden, H. A. Kretzschmar, J. Q. Trojanowski, and V. M. Lee**. 2006. Ubiquitinated TDP-43 in

frontotemporal lobar degeneration and amyotrophic lateral sclerosis. Science **314**:130-133.

96. **Nicolet, C. M., and E. A. Craig**. 1989. Isolation and characterization of STI1, a stress-inducible gene from Saccharomyces cerevisiae. Mol Cell Biol **9**:3638-3646.

97. **Oh, E., A. H. Becker, A. Sandikci, D. Huber, R. Chaba, F. Gloge, R. J. Nichols, A. Typas, C. A. Gross, G. Kramer, J. S. Weissman, and B. Bukau**. 2011. Selective ribosome profiling reveals the cotranslational chaperone action of trigger factor in vivo. Cell **147**:1295-1308.

98. **Olzscha, H., S. M. Schermann, A. C. Woerner, S. Pinkert, M. H. Hecht, G. G. Tartaglia, M. Vendruscolo, M. Hayer-Hartl, F. U. Hartl, and R. M. Vabulas**. 2011. Amyloid-like aggregates sequester numerous metastable proteins with essential cellular functions. Cell **144**:67-78.

99. **Packschies, L., H. Theyssen, A. Buchberger, B. Bukau, R. S. Goody, and J. Reinstein**. 1997. GrpE accelerates nucleotide exchange of the molecular chaperone DnaK with an associative displacement mechanism. Biochemistry **36**:3417-3422.

100. **Pan, X., D. S. Yuan, S. L. Ooi, X. Wang, S. Sookhai-Mahadeo, P. Meluh, and J. D. Boeke**. 2007. dSLAM analysis of genome-wide genetic interactions in Saccharomyces cerevisiae. Methods **41**:206-221.

101. **Park, S. H., N. Bolender, F. Eisele, Z. Kostova, J. Takeuchi, P. Coffino, and D. H. Wolf**. 2007. The cytoplasmic Hsp70 chaperone machinery subjects misfolded and endoplasmic reticulum import-incompetent proteins to degradation via the ubiquitin-proteasome system. Mol Biol Cell **18**:153-165.

102. **Parsell, D. A., A. S. Kowal, M. A. Singer, and S. Lindquist**. 1994. Protein disaggregation mediated by heat-shock protein Hsp104. Nature **372**:475-478.

103. **Pattison, J. S., A. Sanbe, A. Maloyan, H. Osinska, R. Klevitsky, and J. Robbins**. 2008. Cardiomyocyte expression of a polyglutamine preamyloid oligomer causes heart failure. Circulation **117**:2743-2751.

104. **Pearl, L. H., and C. Prodromou**. 2006. Structure and mechanism of the Hsp90 molecular chaperone machinery. Annu Rev Biochem **75**:271-294.

105. **Pech, M., T. Spreter, R. Beckmann, and B. Beatrix**. 2010. Dual binding mode of the nascent polypeptide-associated complex reveals a novel universal adapter site on the ribosome. J Biol Chem **285**:19679-19687.

106. **Peisker, K., D. Braun, T. Wolfle, J. Hentschel, U. Funfschilling, G. Fischer, A. Sickmann, and S. Rospert**. 2008. Ribosome-associated complex binds to ribosomes in close proximity of Rpl31 at the exit of the polypeptide tunnel in yeast. Mol Biol Cell **19**:5279-5288.

107. **Pfund, C., P. Huang, N. Lopez-Hoyo, and E. A. Craig**. 2001. Divergent functional properties of the ribosome-associated molecular chaperone Ssb compared with other Hsp70s. Mol Biol Cell **12**:3773-3782.

108. **Pfund, C., N. Lopez-Hoyo, T. Ziegelhoffer, B. A. Schilke, P. Lopez-Buesa, W. A. Walter, M. Wiedmann, and E. A. Craig**. 1998. The molecular chaperone Ssb from Saccharomyces cerevisiae is a component of the ribosome-nascent chain complex. EMBO J **17**:3981-3989.

109. **Pilon, M., R. Schekman, and K. Romisch**. 1997. Sec61p mediates export of a misfolded secretory protein from the endoplasmic reticulum to the cytosol for degradation. EMBO J **16**:4540-4548.

110. **Piper, P. W.** 1997. The yeast heat shock response, p. 75-99. *In* S. Hohmann, and W. E. Mager (eds.), Yeast Stress Responses. Chapman and Hall, New York.

111. **Polymeropoulos, M. H., C. Lavedan, E. Leroy, S. E. Ide, A. Dehejia, A. Dutra, B. Pike, H. Root, J. Rubenstein, R. Boyer, E. S. Stenroos, S. Chandrasekharappa, A. Athanassiadou, T. Papapetropoulos, W. G. Johnson, A. M. Lazzarini, R. C. Duvoisin, G. Di Iorio, L. I. Golbe, and R. L. Nussbaum**. 1997. Mutation in the alpha-synuclein gene identified in families with Parkinson's disease. Science **276**:2045-2047.

112. **Qu, B. H., E. H. Strickland, and P. J. Thomas**. 1997. Localization and suppression of a kinetic defect in cystic fibrosis transmembrane conductance regulator folding. J Biol Chem **272**:15739-15744.

113. **Quinton, P. M.** 1990. Cystic fibrosis: a disease in electrolyte transport. FASEB J **4**:2709-2717.

114. **Rauch, T., H. A. Hundley, C. Pfund, R. D. Wegrzyn, W. Walter, G. Kramer, S. Y. Kim, E. A. Craig, and E. Deuerling**. 2005. Dissecting functional similarities of ribosome-associated chaperones from Saccharomyces cerevisiae and Escherichia coli. Mol Microbiol **57**:357-365.

115. **Raviol, H., H. Sadlish, F. Rodriguez, M. P. Mayer, and B. Bukau**. 2006. Chaperone network in the yeast cytosol: Hsp110 is revealed as an Hsp70 nucleotide exchange factor. EMBO J **25**:2510-2518.

116. **Rudiger, S., A. Buchberger, and B. Bukau**. 1997. Interaction of Hsp70 chaperones with substrates. Nat Struct Biol **4**:342-349.

117. **Sanchez, Y., and S. L. Lindquist**. 1990. HSP104 required for induced thermotolerance. Science **248**:1112-1115.

118. **Sanchez, Y., D. A. Parsell, J. Taulien, J. L. Vogel, E. A. Craig, and S. Lindquist**. 1993. Genetic evidence for a functional relationship between Hsp104 and Hsp70. J Bacteriol **175**:6484-6491.

119. **Sanchez, Y., J. Taulien, K. A. Borkovich, and S. Lindquist**. 1992. Hsp104 is required for tolerance to many forms of stress. EMBO J **11**:2357-2364.

120. **Satyal, S. H., E. Schmidt, K. Kitagawa, N. Sondheimer, S. Lindquist, J. M. Kramer, and R. I. Morimoto**. 2000. Polyglutamine aggregates alter protein folding homeostasis in Caenorhabditis elegans. Proc Natl Acad Sci U S A **97**:5750-5755.

121. **Satyanarayana, C., S. Schroder-Kohne, E. A. Craig, P. V. Schu, and M. Horst**. 2000. Cytosolic Hsp70s are involved in the transport of aminopeptidase 1 from the cytoplasm into the vacuole. FEBS Lett **470**:232-238.

122. **Schaffar, G., P. Breuer, R. Boteva, C. Behrends, N. Tzvetkov, N. Strippel, H. Sakahira, K. Siegers, M. Hayer-Hartl, and F. U. Hartl**. 2004. Cellular toxicity of polyglutamine expansion proteins: mechanism of transcription factor deactivation. Mol Cell **15**:95-105.

123. **Schmidt, S., A. Strub, K. Rottgers, N. Zufall, and W. Voos**. 2001. The two mitochondrial heat shock proteins 70, Ssc1 and Ssq1, compete for the cochaperone Mge1. J Mol Biol **313**:13-26.

124. **Schmitt, A. P., and K. McEntee**. 1996. Msn2p, a zinc finger DNA-binding protein, is the transcriptional activator of the multistress response in Saccharomyces cerevisiae. Proc Natl Acad Sci U S A **93**:5777-5782.

125. **Schuermann, J. P., J. Jiang, J. Cuellar, O. Llorca, L. Wang, L. E. Gimenez, S. Jin, A. B. Taylor, B. Demeler, K. A. Morano, P. J. Hart, J. M. Valpuesta, E. M. Lafer, and R. Sousa**. 2008. Structure of the Hsp110:Hsc70 nucleotide exchange machine. Mol Cell **31**:232-243.

126. **Schuldiner, M., J. Metz, V. Schmid, V. Denic, M. Rakwalska, H. D. Schmitt, B. Schwappach, and J. S. Weissman**. 2008. The GET complex mediates insertion of tail-anchored proteins into the ER membrane. Cell **134**:634-645.

127. **Senderek, J., M. Krieger, C. Stendel, C. Bergmann, M. Moser, N. Breitbach-Faller, S. Rudnik-Schoneborn, A. Blaschek, N. I. Wolf, I. Harting, K. North, J. Smith, F. Muntoni, M. Brockington, S. Quijano-Roy, F. Renault, R. Herrmann, L. M. Hendershot, J. M. Schroder, H. Lochmuller, H. Topaloglu, T. Voit, J. Weis, F. Ebinger, and K. Zerres**. 2005. Mutations in SIL1 cause Marinesco-Sjogren syndrome, a cerebellar ataxia with cataract and myopathy. Nat Genet **37**:1312-1314.

128. **Shaner, L., P. A. Gibney, and K. A. Morano**. 2008. The Hsp110 protein chaperone Sse1 is required for yeast cell wall integrity and morphogenesis. Curr Genet **54**:1-11.

129. **Shaner, L., R. Sousa, and K. A. Morano**. 2006. Characterization of Hsp70 binding and nucleotide exchange by the yeast Hsp110 chaperone Sse1. Biochemistry **45**:15075-15084.

130. **Shaner, L., A. Trott, J. L. Goeckeler, J. L. Brodsky, and K. A. Morano**. 2004. The function of the yeast molecular chaperone Sse1 is mechanistically distinct from the closely related hsp70 family. J Biol Chem **279**:21992-22001.

131. **Shaner, L., H. Wegele, J. Buchner, and K. A. Morano**. 2005. The yeast Hsp110 Sse1 functionally interacts with the Hsp70 chaperones Ssa and Ssb. J Biol Chem **280**:41262-41269.

132. **Shi, L. X., and S. M. Theg**. 2010. A stromal heat shock protein 70 system functions in protein import into chloroplasts in the moss Physcomitrella patens. Plant Cell **22**:205-220.

133. **Shimura, H., Y. Miura-Shimura, and K. S. Kosik**. 2004. Binding of tau to heat shock protein 27 leads to decreased concentration of hyperphosphorylated tau and enhanced cell survival. J Biol Chem **279**:17957-17962.

134. **Shomura, Y., Z. Dragovic, H. C. Chang, N. Tzvetkov, J. C. Young, J. L. Brodsky, V. Guerriero, F. U. Hartl, and A. Bracher**. 2005. Regulation of Hsp70 function by HspBP1: structural analysis reveals an alternate mechanism for Hsp70 nucleotide exchange. Mol Cell **17**:367-379.

135. **Shulga, N., P. Roberts, Z. Gu, L. Spitz, M. M. Tabb, M. Nomura, and D. S. Goldfarb**. 1996. In vivo nuclear transport kinetics in Saccharomyces cerevisiae: a role for heat shock protein 70 during targeting and translocation. J Cell Biol **135**:329-339.

136. **Silva, M. C., S. Fox, M. Beam, H. Thakkar, M. D. Amaral, and R. I. Morimoto**. 2011. A genetic screening strategy identifies novel regulators of the proteostasis network. PLoS Genet **7**:e1002438.

137. **Sinensky, M.** 2000. Functional aspects of polyisoprenoid protein substituents: roles in protein-protein interaction and trafficking. Biochim Biophys Acta **1529**:203-209.

138. **Smith, M. G., and M. Snyder**. 2006. Yeast as a model for human disease. Current protocols in human genetics / editorial board, Jonathan L. Haines ... [et al.] **Chapter 15**:Unit 15 16.

139. **Sondermann, H., A. K. Ho, L. L. Listenberger, K. Siegers, I. Moarefi, S. R. Wente, F. U. Hartl, and J. C. Young**. 2002. Prediction of novel Bag-1 homologs based on structure/function analysis identifies Snl1p as an Hsp70 co-chaperone in Saccharomyces cerevisiae. J Biol Chem **277**:33220-33227.

140. **Sondermann, H., C. Scheufler, C. Schneider, J. Hohfeld, F. U. Hartl, and I. Moarefi**. 2001. Structure of a Bag/Hsc70 complex: convergent functional evolution of Hsp70 nucleotide exchange factors. Science **291**:1553-1557.

141. **Song, J., M. Takeda, and R. I. Morimoto**. 2001. Bag1-Hsp70 mediates a physiological stress signalling pathway that regulates Raf-1/ERK and cell growth. Nat Cell Biol **3**:276-282.

142. **Sorger, P. K., and H. R. Pelham**. 1987. Purification and characterization of a heat-shock element binding protein from yeast. EMBO J **6**:3035-3041.

143. **Steel, G. J., D. M. Fullerton, J. R. Tyson, and C. J. Stirling**. 2004. Coordinated Activation of Hsp70 Chaperones. Science **303**:98-101.

144. **Takayama, S., T. Sato, S. Krajewski, K. Kochel, S. Irie, J. A. Millan, and J. C. Reed**. 1995. Cloning and functional analysis of BAG-1: a novel Bcl-2-binding protein with anti-cell death activity. Cell **80**:279-284.

145. **Tanimura, S., A. I. Hirano, J. Hashizume, M. Yasunaga, T. Kawabata, K. Ozaki, and M. Kohno**. 2007. Anticancer drugs up-regulate HspBP1 and thereby antagonize the prosurvival function of Hsp70 in tumor cells. J Biol Chem **282**:35430-35439.

146. **Tong, A. H., G. Lesage, G. D. Bader, H. Ding, H. Xu, X. Xin, J. Young, G. F. Berriz, R. L. Brost, M. Chang, Y. Chen, X. Cheng, G. Chua, H. Friesen, D. S. Goldberg, J. Haynes, C. Humphries, G. He, S. Hussein, L. Ke, N. Krogan, Z. Li, J. N. Levinson, H. Lu, P. Menard, C. Munyana, A. B. Parsons, O. Ryan, R. Tonikian, T. Roberts, A. M. Sdicu, J. Shapiro, B. Sheikh, B. Suter, S. L. Wong, L. V. Zhang, H. Zhu, C. G. Burd, S. Munro, C. Sander, J. Rine, J. Greenblatt, M. Peter, A. Bretscher, G. Bell, F. P. Roth, G. W. Brown, B. Andrews, H. Bussey, and C. Boone**. 2004. Global mapping of the yeast genetic interaction network. Science **303**:808-813.

147. **Trott, A., and K. A. Morano**. 2003. The yeast response to heat shock, p. 71-119. *In* S. Hohmann, and P. W. H. Mager (eds.), Yeast Stress Responses, vol. 1. Springer-Verlag, Heidelberg.

148. **Tsai, J., and M. G. Douglas**. 1996. A conserved HPD sequence of the J-domain is necessary for YDJ1 stimulation of Hsp70 ATPase activity at a site distinct from substrate binding. J Biol Chem **271**:9347-9354.

149. **Tyson, J. R., and C. J. Stirling**. 2000. LHS1 and SIL1 provide a lumenal function that is essential for protein translocation into the endoplasmic reticulum. EMBO J **19**:6440-6452.

150. **Tzankov, S., M. J. Wong, K. Shi, C. Nassif, and J. C. Young**. 2008. Functional divergence between co-chaperones of Hsc70. J Biol Chem **283**:27100-27109.

151. **Unno, K., T. Kishido, M. Hosaka, and S. Okada**. 1997. Role of Hsp70 subfamily, Ssa, in protein folding in yeast cells, seen in luciferase-transformed ssa mutants. Biological & pharmaceutical bulletin **20**:1240-1244.

152. **Verghese, J., and K. A. Morano**. 2012. A lysine-rich region within fungal BAG domain-containing proteins mediates a novel association with ribosomes. Eukaryot Cell **11**:1003-1011.

153. **Vicart, P., A. Caron, P. Guicheney, Z. Li, M. C. Prevost, A. Faure, D. Chateau, F. Chapon, F. Tome, J. M. Dupret, D. Paulin, and M. Fardeau**. 1998. A missense mutation in the alphaB-crystallin chaperone gene causes a desmin-related myopathy. Nat Genet **20**:92-95.

154. **Vogel, M., M. P. Mayer, and B. Bukau**. 2006. Allosteric regulation of Hsp70 chaperones involves a conserved interdomain linker. J Biol Chem **281**:38705-38711.

155. **Walter, G. M., M. C. Smith, S. Wisen, V. Basrur, K. S. Elenitoba-Johnson, M. L. Duennwald, A. Kumar, and J. E. Gestwicki**. 2011. Ordered assembly of heat shock proteins, Hsp26, Hsp70, Hsp90, and Hsp104, on expanded polyglutamine fragments revealed by chemical probes. J Biol Chem **286**:40486-40493.

156. **Wang, Y., A. B. Meriin, N. Zaarur, N. V. Romanova, Y. O. Chernoff, C. E. Costello, and M. Y. Sherman**. 2009. Abnormal proteins can form aggresome in yeast: aggresome-targeting signals and components of the machinery. FASEB J **23**:451-463.

157. **Warrick, J. M., H. Y. Chan, G. L. Gray-Board, Y. Chai, H. L. Paulson, and N. M. Bonini**. 1999. Suppression of polyglutamine-mediated neurodegeneration in Drosophila by the molecular chaperone HSP70. Nat Genet **23**:425-428.

158. **Wegrzyn, R. D., D. Hofmann, F. Merz, R. Nikolay, T. Rauch, C. Graf, and E. Deuerling**. 2006. A conserved motif is prerequisite for the interaction of NAC with ribosomal protein L23 and nascent chains. J Biol Chem **281**:2847-2857.

159. **Weitzmann, A., J. Volkmer, and R. Zimmermann**. 2006. The nucleotide exchange factor activity of Grp170 may explain the non-lethal phenotype of loss of Sil1 function in man and mouse. FEBS Lett **580**:5237-5240.

160. **Werner-Washburne, M., D. E. Stone, and E. A. Craig**. 1987. Complex interactions among members of an essential subfamily of hsp70 genes in Saccharomyces cerevisiae. Mol Cell Biol **7**:2568-2577.

161. **Wotton, D., K. Freeman, and D. Shore**. 1996. Multimerization of Hsp42p, a novel heat shock protein of Saccharomyces cerevisiae, is dependent on a conserved carboxyl-terminal sequence. J Biol Chem **271**:2717-2723.

162. **Xu, Z., R. C. Page, M. M. Gomes, E. Kohli, J. C. Nix, A. B. Herr, C. Patterson, and S. Misra**. 2008. Structural basis of nucleotide exchange and client binding by the Hsp70 cochaperone Bag2. Nat Struct Mol Biol **15**:1309-1317.

163. **Yam, A. Y., V. Albanese, H. T. Lin, and J. Frydman**. 2005. Hsp110 cooperates with different cytosolic HSP70 systems in a pathway for de novo folding. J Biol Chem **280**:41252-41261.

164. **Yan, M., J. Li, and B. Sha**. 2011. Structural analysis of the Sil1-Bip complex reveals the mechanism for Sil1 to function as a nucleotide-exchange factor. Biochem J **438**:447-455.

165. **Yassour, M., T. Kaplan, H. B. Fraser, J. Z. Levin, J. Pfiffner, X. Adiconis, G. Schroth, S. Luo, I. Khrebtukova, A. Gnirke, C. Nusbaum, D. A. Thompson, N.**

Friedman, and A. Regev. 2009. Ab initio construction of a eukaryotic transcriptome by massively parallel mRNA sequencing. Proc Natl Acad Sci U S A **106**:3264-3269.

166. **Zhang, Y., G. Nijbroek, M. L. Sullivan, A. A. McCracken, S. C. Watkins, S. Michaelis, and J. L. Brodsky**. 2001. Hsp70 molecular chaperone facilitates endoplasmic reticulum-associated protein degradation of cystic fibrosis transmembrane conductance regulator in yeast. Mol Biol Cell **12**:1303-1314.

167. **Zhao, R., and W. A. Houry**. 2007. Molecular interaction network of the Hsp90 chaperone system. Adv Exp Med Biol **594**:27-36.

168. **Zhu, X., X. Zhao, W. F. Burkholder, A. Gragerov, C. M. Ogata, M. E. Gottesman, and W. A. Hendrickson**. 1996. Structural analysis of substrate binding by the molecular chaperone DnaK. Science **272**:1606-1614.

VITA

Jacob Verghese was born in Trivandrum, Kerala, India on October 14, 1980, the son of Jacob (Ashok) Verghese and Reena Verghese. After finishing at Union Christian Matriculation Higher Secondary School, Chennai, India in May 1998, he entered Loyola College, Chennai, India where he received the degree of Bachelor of Science in zoology in 2001. In May 2003, he received a Master of Science in zoology from Loyola College. In August 2003, he moved to Houston, Texas to pursue a Master of Science in biochemistry at the University of Houston-Central in the lab of Dr. William Widger. In August of 2006 he entered the University of Texas Health Science Center at Houston Graduate School of Biomedical Sciences. In spring 2007, he joined the laboratory of Dr. Kevin A. Morano.